Using Amines and Aldehydes as a Novel Crosslinking Method for Silicone Materials

Abstract

Silicones are a class of polymer possessing polysiloxane bonds, with broad industrial and commercial applications that are distinct from organic polymers. Functional silicones made by combining polysiloxanes with other materials, such as small molecules or other polymers, allow for tailoring the silicone's properties to a specific application. These materials are synthesized through well-established and specialized reactions specific to silicone polymers, and progress towards new crosslinking reactions is limited. The current methods of crosslinking silicones have several drawbacks, particularly: requiring harsh reaction conditions or poor tolerance towards many organic functional groups. The advent of novel crosslinking technologies is necessary for further innovation of silicones as materials such as functional coatings, polymers, and elastomers.

Functional organosilicone materials leverage the known chemistry of organic moieties and reactions to derivatize or synthesize silicones. These materials combine the properties and reactivity of organic functionality with polysiloxanes, augmenting reactions specific to silicones. This diversifies the library of synthetic routes for silicone materials while also producing unique properties and additional value. In addition, there is an opportunity to explore facile organic reactions as novel crosslinking chemistries.

The condensation between amines and aldehydes to form imines is an attractive synthetic scheme for crosslinking silicones that can solve many problems associated with traditional methods. These moieties are commonly employed for their relatively simple reaction conditions and high yields to assemble complex chemicals motifs. These features, along with the evolution of water as the only byproduct and tolerance to other organic functional

groups, make the synthesis of imines ideal for crosslinking silicones into functional materials.

This thesis explores the use of amine-functionalized silicone oils with various aliphatic and aromatic aldehydes as a novel method of crosslinking functional silicone materials via imines and the application of the resulting materials. These reactions overcome many of the drawbacks of traditional methods for crosslinking silicones and produces materials with novel properties that can enable their use in different applications. Furthermore, the differences in reactivity between the two types of aldehydes lead to two unique crosslinking motifs. Aromatic aldehydes produce conjugated Schiff-base crosslinks, while the crosslinking with aliphatic aldehydes undergoes various condensation reactions to give novel silicone materials.

The use of small aliphatic aldehydes such as formaldehyde, glutaraldehyde, and glyoxal was found to rapidly crosslink aminopropylsilicones into elastomeric materials. The high reactivity of the aldehyde towards the amine-moieties also allows for robust crosslinking into elastomers that can occur even in the presence of water, a remarkable feature for silicones that are normally water insoluble. These properties allowed for the application of the material as an ink for 3-D printing, where the rapid crosslinking allowed for the study of a novel free-space droplet merging printing method.

Silicone materials crosslinked with aromatic aldehydes produce conjugated Schiff-base bonds. These crosslinks can undergo dynamic exchange reactions in the presence of an amine catalyst to alter bonding in the material. These reactions gave the silicone chemoplastic and thermoplastic properties, allowing the material to be remoulded and reprocessed. Naturally-derived aromatic aldehydes can also be used as the crosslinker,

allowing for a multi-faceted approach to increasing the sustainability of silicone materials by increasing their utility, making them reprocessable, thus extending their lifespan while using sustainable materials as a filler.

Acknowledgements

Firstly, I want to thank my graduate supervisor, Dr. Michael A. Brook, for his guidance and the privilege of working in his research group. Mike offered me a position in his lab before I had any thoughts of pursuing a graduate degree; he saw my potential far before anyone else, including myself. His optimism and trust have been unwavering since giving me the freedom to explore ideas outside of convention and strive towards innovation. Mike has a remarkable ability to find the positive in any situation or result, which has helped me push through the most challenging times. I will always be grateful for all he has done; none of this would be possible without his support. I would also like to thank my graduate supervisory committee: Dr. Alex Adronov and Dr. Robert Pelton, for advising me throughout my graduate career. They challenged me to become a more thoughtful and thorough scientist. I would like to thank Dr. Yang 'Dan' Chen for always being someone I can ask for help with anything, in life or the lab and always steering me in the right direction.

To all my labmates that I've had the fortune of sharing the Brook lab with over the years, each of you has made this experience so memorable; I'll always cherish the time we spent together. Special thanks to Cody for being the person I tuned to for help, Harry for being so relaxed and the most honest person I've met in graduate school, Alyssa for your ability to always have fun no matter the situation, Nicole for always being my loudest supporter, Scarlet for being so kind to everyone, Mengchen for always being full of surprises and the many others I missed, thank you. I would also like to thank Dr. Ignacio Vargas-Baca and Dr. Peter Ho for their supervision during my undergraduate thesis. The lessons they taught me include to always try to have patience and integrity in all aspects of life.

My friends that I've met throughout my time at McMaster, I could never name you all, but each of you know what you mean to me. I spent the last five years not being as good of a friend as I wanted to be nor that you all deserved. You were all there to pick me up and remind me to always have fun.

I would like to thank my parents Dong Thi Bui and Ky Hung Nguyen. There are no words that can express how thankful I am to have you as my parents, and I could never begin to repay the sacrifices you have made for me. You worked tirelessly to give me the life you never had. Your lessons throughout my life shaped me into who I am today. Your love and support gave me the freedom I needed to find my own path. I could never repay you for everything that you two have done for me. Lastly, Ông Nội I kept my promise to you; this was for you.

Declaration of Academic Achievement

The work performed by the author is described in the footnote of each chapter contained in this document.

Published Journal Articles:

[1] R. Bui, and M.A. Brook, *Advanced Functional Materials*, 2020, 30, 2000737.

[2] M. Śliwiak, R. Bui, M. A. Brook, R. P. Selvaganapathy, *Additive Manufacturing*, 2021, 46, 102099.

[3] R. Bui, and M.A. Brook, *Polymer*, 2019, 160, 282-290.

[4] R. Bui, and M.A. Brook, *Green Chemistry*, 2021, 23, 5600-5608.

Table of Contents

Abstract i

Acknowledgements iv

Declaration of Academic Achievement vi

Table of Figures: xii

Chapter 1 : Introduction 1

1.1 Traditional Functional Silicone Elastomers 1

1.1.1 Properties of Silicones 1

1.1.2 Traditional Methods of Synthesizing Functional Silicones 2

1.2 Functional Silicones 2

1.2.1 Improving Traditional Silicones by Functionalization 2

1.2.2 How to Functionalize Silicone Polymers and Resins 3

1.2.3 Functional Silicone Composites and Blends 5

1.2.4 Functional Elastomers and Gels 5

1.3 Current Crosslinking Technologies and Their Limitations 6

1.3.1 Most Common Methods of Crosslinking 6

1.3.2 Radical-Initiated High-Temperature Vulcanization 7

1.3.3 Metal-Catalyzed Room Temperature Vulcanization 7

1.3.4 Limitations of Current Crosslinking Methods 8

1.4 New Chemistry as Crosslinking Methods for Silicone Elastomers 9

1.4.1 The Piers-Rubinsztajn Reaction 9

1.4.2 The Piers-Rubinsztajn Reaction for Functional Silicones 10

1.4.3 Crosslinking Chemistry from the Organic World 11

1.4.4 The Chemistry of Amines and Aldehydes for Crosslinking Silicones 12

1.5 Dynamic Silicone Materials 14

1.5.1 Applications of Dynamic Silicone Elastomers 14
1.5.2 Ionic interactions as Crosslinks in Silicone Elastomers 15
1.5.3 Non-covalent Interactions as Crosslinks in Silicone Elastomers 16
1.5.4 Dynamic Covalent Bonds in Silicones 17
1.6 Thesis Objectives 19
1.6.1 Overall Objectives 19
1.6.2 Aliphatic Aldehyde Crosslinkers 20
1.6.3 3-D Printing Silicones using Aliphatic Aldehydes 21
1.6.4 Aromatic Aldehyde Crosslinkers - Dynamic Crosslinking 23
1.6.5 Sustainable Dynamic Silicones Using Vanillin 24
1.7 References 26
Chapter 2 : Catalyst Free Silicone Sealants That Cure Underwater ** 35
2.1 Abstract 35
2.2 Introduction 36
2.3 Experimental 39
1.1.1 Materials 39
2.3.1 Methods 39
2.3.2 Synthesis of Formaldehyde Crosslinked Silicone Elastomers 40
2.3.3 Curing in Bulk Water: General Procedure 42
2.3.4 Rheological Measurements 42
2.3.5 Double Barrel Syringe Dispensing 43
2.3.6 Crosslinked Silicone Aldehydes as Sealants 44
2.3.7 Crosslinked Silicone Aldehydes as Adhesives 44
2.4 Results and Discussion 45
1.1.1 Spectroscopic Analysis of Aliphatic Aldehyde Crosslinking 45

2.4.1 Elastomer Preparation 46

1.1.1 Managing Issues of Toxicity 49

2.4.2 Curing in Air versus Under Water 49

2.4.3 Syringe Injectable Elastomers 51

2.4.4 Injectable Sealants Under Water 52

1.1.2 Adhesion to Different Materials 53

2.5 Conclusion 55

2.6 Acknowledgments 55

2.7 References 56

Chapter 3 : 3D Printing of Highly Reactive Silicones Using Inkjet Type Droplet Ejection and Free Space Droplet Merging and Reaction** 58

3.1 Abstract 58

3.2 Introduction 60

3.3 Experimental 62

3.3.1 Design of 3D printer 62

3.3.2 Materials 64

3.3.3 Method 65

3.3.4 Printable Liquids 66

3.4 Results and Discussion 68

3.4.1 Analysis of Ejected and Positioned Droplets 68

3.4.2 Fabricated Objects 72

3.4.3 Stability of the Printing 76

3.5 Conclusion 78

3.6 Acknowledgements 79

3.7 References 79

Chapter 4 : Dynamic Covalent Schiff-Base Silicone Polymers and Elastomers 82

4.1 Abstract 82

4.2 Introduction 84

4.3 Experimental 86

4.3.1 Materials 86

4.3.2 Methods 87

4.3.3 Synthesis of Polydimethylsiloxane-Schiff Base Polymers 88

4.3.5 Preparation and Physical Testing of Schiff-Base Elastomers 91

4.4 Results and Discussion 93

4.4.1 Formation of Schiff-Base Imine in a Silicone Environment 93

4.4.1 Schiff Bases as Links for Extended Linear Polymers 94

4.4.2 Formation and Physical Properties of Schiff-Base Silicone Elastomers 94

4.5 Discussion 105

4.6 Conclusions 108

4.7 Acknowledgments 108

4.8 References 109

Chapter 5 : Thermoplastic Silicone Elastomers from Divanillin Crosslinkers in a Catalyst-Free Process 112

5.1 Abstract 112

5.2 Introduction 113

5.3 Experimental 115

5.3.1 Materials 115

5.3.4 Synthesis of Divanillin for Vanillin - DiVan 118

5.3.5 Preparation of Divanillin Silicone Elastomers 118

5.3.6 Aqueous Preparation of DiVan-T Silicone Elastomers 120

5.3.7 Gel Fraction of Recycled Samples 120

5.3.8 Chemical Reprocessing of Divanillin Silicone Elastomers 121

5.4 Results and Discussion 121

5.4.1 Synthesis of DiVan 121

5.4.2 The Reactions of Divanillin with 3-aminopropylsilicones 122

5.4.3 Physical Properties of Divanillin-Silicone Elastomers 125

5.4.4 Remouldability/Thermal Properties of DiVan-P and DiVan-P Elastomers 129

5.5 Conclusions 135

5.6 Acknowledgments 135

5.7 References 136

Chapter 6 : General Conclusions 140

Appendix 144

Appendix: 1. Catalyst Free Silicone Sealants That Cure Underwater - Supplementary Information 148

Appendix 1.1. Spectroscopic Analysis of Aliphatic Aldehyde Crosslinking 148

Appendix 1.2. Spectroscopic Analysis of Aliphatic Aldehyde Crosslinking 150

Appendix 1.3. Determination of Elastomer Stoichiometery 152

Appendix 1.5. Aliphatic Aldehyde Elastomer Images 155

Appendix 1.6. Physical Properties of Elastomers Cured in Air and Water 159

Appendix 1.7. Hydrolytic and Thermal Elastomer Stability 160

Appendix 1.8. Thermogravimetric Analysis of Silicone Elastomers Crosslinked with Aliphatic aldehydes 162

Appendix 1.9. Equilibrium Swell Test - Flory-Rehner 163

Appendix: 2. 3-D Printing of Highly Reactive Silicones Using Inkjet Type Droplet Ejection and Free Space Droplet Merging and Reaction 165

Appendix: 3. Dynamic Covalent Schiff-Base Silicone Polymers and Elastomers 172

Appendix: 4. Thermoplastic Silicone Elastomers from Divanillin Crosslinkers in a Catalyst-Free Process 177

Table of Figures:

Figure 1.1: Traditional acid/base catalyzed synthesis of silicone 2

Figure 1.2: Synthesis of Si-H and Si-OH silicones using acid/base catalysis. 3

Figure 1.3: Structures of silicone units M (Me_3SiO), D ($Me_2SiO_{2/2}$), T ($MeSiO_{3/2}$), Q ($SiO_{4/2}$); and resins MQ-resin, DT-resin. 4

Figure 1.4: Different arrangements of functional groups (FG) on a silicone backbone. 5

Figure 1.5: Traditional methods of crosslinking silicone elastomers using peroxide or metal catalyst. A) Radical initiated vulcanization of silicone fluids using a peroxide catalyst at high temperatures, B) condensation cure of silanols and alkoxysilanes using a tin or titanium catalysts, C) addition cure between vinyl-functionalized silicones and hydride-functional silicones using a platinum-catalyst. 6

Figure 1.6: Peroxide-radical initiated vulcanization of a silicone elastomer at elevated temperatures. ROOR represents a peroxide initiator. 7

Figure 1.7: Metal-catalyzed room temperature vulcanization of silicone elastomers using A) Tin or titanium catalysts with alkoxysilane-silanol systems and B) Platinum-based Karstedt's (Platinum(0)-1,3-divinyl-1,1,3,3-tetramethyldisiloxane complex) with vinyl-hydride silicone systems. 8

Figure 1.8: Piers-Rubinsztajn reaction used to crosslink hydrosilanes and alkoxysilanes into silicone elastomer. 9

Figure 1.9: The Piers-Rubinsztajn reaction used to react hydrosilanes with functionalized alkoxysilanes to yield crosslinked functional silicone elastomers directly or from thiols, epoxides or phenols via new organosilicon bonds. 10

Figure 1.10: Model crosslinking scheme between two organo-functional silicones; one with pendent 'A' groups and one with telechelic 'B', that react to give crosslinks 'C' 12

Figure 1.11: Mechanisms for imine formation using acid-base through a zwitterionic transition or in organic solvents via a 4-membered ring transition. 13

Figure 1.12: Dynamic bond exchange reactions between imines and amines occur under equilibrium conditions. 14

Figure 1.13: Comparison between dissociative and associative dynamic bond exchange processes in a vitrimeric material. Dissociative bonds undergo bond breaking and forming reactions 15

Figure 1.14: Dynamic crosslinking using electrostatic interactions between two oppositely charged polymers or polymer with an oppositely charged ion. 16

Figure 1.15: Examples of dissociative and associative dynamic covalent bonds and their respective equilibria. 18

Figure 1.16: Model reactions between model aminoalkylsilicone 1 and A: formaldehyde 4 B: glyoxal 3, or C: glutaraldehyde 2. 21

Figure 1.17: Silicone-glutaraldehyde elastomers printed using the free-space droplet merging printer without the need of support material. [142] 22

Figure 1.18: Dynamic silicones synthesized by crosslinking aminopropylsilicones with terephthaldehyde. 24

Figure 2.1: Organic-cured silicones based on amine reactions. A: aza-Michael reactions, B: ureas from reaction with isocyanates, and C: Schiff-bases through reaction with arylaldehydes. 37

Figure 2.2: Model reactions between model aminoalkylsilicone 1 and A: formaldehyde 4 B: glyoxal 3, or C: glutaraldehyde 2. 38

Figure 2.3: Reactions of telechelic aminopropylsilicones with aldehydes A: glutaraldehyde. Glu-T, B: glyoxal Gly-T, and C: formaldehyde For-T. The processes operate in an analogous manner with pendant aminopropylsilicones (Table S 1). 47

Figure 2.4: Rheometry of cure in air (no added solvent) or in 50/50 wt. silicone-in-water emulsions of 3000 g mol^{-1} telechelic-aminopropylsilicone with A: formaldehyde, B: glyoxal, C: glutaraldehyde, and 50000 g mol^{-1} telechelic-aminopropylsilicone with D: formaldehyde, E: glyoxal, F: glutaraldehyde. The circles identify the G'/G" crossover points. Note: these charts do not reflect complete cure, which can take between 1-3 hours (see Figure S 7). 50

Figure 2.5: A: Two-barreled mixing syringe used to extrude curing mixtures of formaldehyde or glutaraldehyde with aminopropylsilicone. B: Elastomeric structures made by 3D printing by extrusion of glutaraldehyde- ("McMaster") or formaldehyde-based ("Chemistry") elastomers from the mixing syringe (3 passes x 0.1 cm film thickness) C: i) 5 x 1 cm diameter openings cut in polypropylene tub (42 cm w x 29 cm l x 14.5 cm h); ii) Extrusion of formaldehyde-based silicone elastomer during flow of water; iii) complete seal of opening; iv) plugs injected into the holes using the syringe in A (shown after 14 days withholding water) v) water leaking through the 5 holes; vi) injection of sealant under water; vii) no drips from the tub. 53

Figure 2.6: Stress-strain curves from elastomers cured using showing higher adhesion to polar substrates. A: **For-PDMS** and B: **Glu-PDMS**. The samples were pre-strained (0.002 N) to 100% prior to initiating the tensile measurements. 55

Figure 3.1: a) 3D inkjet printer with integrated a free space droplet mixing module. **b)** Schematic illustration of the inkjet 3D printer with an integrated free space droplet mixing module, where (i) two reactive droplets are ejected independently and simultaneously, (ii) droplets merge due to the intersection of their trajectories and mix supported by inertial effects in free space outside the nozzles, and (iii) the coalescent drop is deposited in patterned format on a moving substrate. **c)** Holder designed for the dispensing devices enables droplets mixing in free space (top), and the regulation spring-screw mechanism (bottom). 63

Figure 3.2:**a)** Collision and coalescence of droplets made of glutaraldehyde solution (left) and DMS-A11 (right) in free space (scale bar = 100 μm). **b)** Characterization of the method depending on the β parameter (scale bar = 50 μm). **c)** Top side and cross-section of a PDMS drop. The two pictures correspond to two different droplets (scale bar = 20 μm). 66

Figure 3.3: a) Formation of a continuous line. The consecutive snapshots were taken every 0.1ms (scale bar = 100 μm.) b) Printed line with different spacing between the deposited droplets on the glass surface. Deposition spacing of 167 μm which equals to 1.4 of contact diameter of the droplet (top). Deposition spacing of 73 μm (0.6 of contact diameter) (middle), Deposition spacing of 28 μm (0.2 of contact diameter) (bottom) (scale bar = 100 μm). 70

Figure 3.4: Printable shapes of PDMS. **a)** Image of high aspect ratio wall (~330 μm thick) consisting of 1560 layers (scale bar = 5 mm) (a, left), SEM image of a horizontal cross section of the wall (scale bar = 100 μm) (a, right). **b)** A frame (~290 μm thick) consisting of 200 layers (scale bar = 1 mm) (b, left). A vertical cross section of the frame (scale bar = 200 μm) (b, right). **c)** Cuboids with different heights (scale bar = 1 mm) (c, top). Cross section of the filled box with distinguished variable size of pores in different locations (scale bar = 200 μm) (c, bottom). **d)** Coil springs printed with different frequencies without a support material (scale bar = 2 mm). 73

Figure 4.1: Competing equilibria in these processes. A: imine formation which is controlled by the concentration of water. B: transimination which allows for redistribution of imine bonds with amines under equilibrium conditions. C: Exchanging aldehydes via an imine. D: Linear polymers created from α,ω-(3-aminopropyl)PDMS and terephthaldehyde. Two complementary schemes for crosslinking aminopropylPDMS through Schiff-base bonds; E: pendent-modified aminopropylPDMS with terephthaldehyde (**TPA-PDMS**), or F: α,ω-(3-aminopropyl)PDMS with 1,3,5-triformylbenzene (**TFB-PDMS**). 98

Figure 4.2: Changes in molecular weight distributions during the degradation of a Schiff-base polymer by A: benzaldehyde or B: allylamine. GPC data was taken 6 hours after addition of the reagent. 101

Figure 4.3: Comparative study on the binding rhodamine 123 to a **TPA-PDMS** elastomer and Sylgard 184 in water for 24 hours. After 24 h of submerging in 0.01 mM rhodamine 123, A) samples thoroughly rinsed with water, B) extracted with DCM. 102

Figure 4.4 Elastomers selective adhere to aminopropyl-functionalized glass slide by transimination, but no adhesion to unfunctionalized glass-slide. 102

Figure 4.5: Stress-strain graphs from tensile testing of 5% crosslinked **TPA-PDMS** elastomers held in contact with a 10 mm^2 contact surface area for various amounts of time to access the self-healing properties. 102

Figure 4.6: Elastomer recycling through imine exchange. A: Three mechanisms for recycling elastomers by promoting reactivity of imine crosslinks. B: Example of elastomer recycling from pulverized pieces of elastomer, during annealing process, and as single homogenous elastomer body by solvent annealing. C: Physical properties of recycled materials after 3 cycles of remolding. Left hand side - the original in orange followed by three repeat recycles using a solvent to reform the elastomer. Right hand side – the % changes in properties after repeat recycles using different methods. 104

Figure 4.7: Depolymerization of silicone-imines in the presence of benzaldehyde and allylamine (N-Sil-N = $N(CH_2)_3$Silicone polymer$(CH_2)_3N$). 107

Figure 5.1. A) Reaction of vanillin with 3-aminopropylpentamethyldisiloxane to produce a Schiff-base. B) Synthesis of **DiVan** by aqueous oxidative coupling of vanillin. 122

Figure 5.2. Crosslinking via with divanillin Schiff-base bonds of A) (3-aminopropyl)methylsiloxane-dimethylsiloxane copolymers to give **DiVan-T** and, B) α,ω-(3-aminopropyl)polydimethylsiloxanes to create **DiVan-P**, respectively. 124

Figure 5.3. A) Young's moduli for elastomers formed from pendent (3-aminopropyl)methylsiloxane-dimethylsiloxane copolymers with different amine densities and **DiVan-P**, terephthaldehyde **Tere-P**, and 4,4'-biphenyldialdehyde **DiPhen-P**, respectively. B) Young's modulus measurements for a series of **DiVan-T** formed from different molecular weights of α,ω-(3-aminopropyl)polydimethylsiloxanes. 127

Figure 5.4. Solvent interactions of **DiVan-T** and **DiVan-P** elastomers with toluene, and an excess of phenylhydrazine in toluene. 129

Figure 5.5. A) Thermal compression remolding of **DiVan-T-5**. B) Remolding of **DiVan-T-5** After heating at 180 °C for 5 min. C) **DiVan-P-7-3CL** elastomers over two cycles at 130 °C using 2 and 4 ToF, respectively. 130

Figure 5.6. Tensile testing of self-adhered **DiVan-PX-3CL** elastomers after heat pressing at 130 ˚C for A) 3h and B) 6h showing the efficiency of healing by the recovered tensile strength when compared to the initial break of a **DiVan-P-3** sample. 131

Figure 5.7. Dynamic mechanical analysis of A) **DiVan-T-19** and B) **DiVan-T-0.6** elastomers under constant strain (10%) from 120-150 °C and at 25 °C as a control.

Showing the relaxation of the material from initial stress, to E/E_0 = 1/e (~0.37), and Arrhenius plot modelling the Maxwell viscoelastic relaxation. ToF = tons of force. ___133

List of Tables:

*Table 2.1: Preparation of silicone elastomers using formaldehyde (See Table S 1 for **Glu** and **Gly**).* _____ *48*

Table 4.1: Characterization of Extended Linear Polymers Derived from α,ω-(3-aminopropyl)PDMS and Terephthaldehyde[a] _____ *95*

Table 4.2: Physical characterization of Schiff-base crosslinked elastomers _____ *95*

*Table 4.3: Changes in molecular weight (GPC) following the titration of **TPA-PDMS** polymers with allylamine or benzaldehyde, respectively.* _____ *100*

*Table 5.1 Mechanical properties of all **DiVan-T**, **DiVan-P** elastomers and control samples (prepared from pendent aminosilicones using 4,4'-biphenyldialdehyde **DiPhen-**P).* __ *126*

Chapter 1 : Introduction

1.1 Traditional Functional Silicone Elastomers

1.1.1 Properties of Silicones

Silicones are polymers that consist primarily of R_2Si-O repeat units. They represent an important class of polymeric materials.[1–4] Compared to traditional carbon-based organic polymers, silicones are unique for their thermal, biological, mechanical, chemical, and other properties that justify the relatively high energetic expense for their synthesis and commercial cost. Specifically, silicones are usually hydrophobic polymers with high thermal stability, biocompatibility, electrical insulating properties, optical clarity, and gas permeability while having low- toxicity, and a very low glass transition temperature (T_g).[5]

The desirable properties of silicones can be explained by differences between Si-O bonds and the conventional C-C or C-O bonds found in traditional organic polymers. The greater bond energy of Si-O bonds (1.62 Å) than those found in carbon-based polymers gives improved thermal stability, making them more challenging to degrade thermally.[6,7] Catenated Si-O bonds also have a lower barrier of rotation (i.e., SiO-SiO, 3.8 kJ/mol) and larger bond angle (i.e., Si-O-Si; 142.5º), resulting in greater flexibility and mobility, allowing for more efficient permeation of gases, reorientation of hydrophobic alkyl side chains, and segmental motion of the silicone-chain resulting in a low T_g (dimethylsilicones $T_g \approx$ -121 ºC).[3,8,9] These properties have led silicones to garner use in widespread applications as materials in adhesives, lubricants, sealants, cookware, electrical insulants, surfactants or implantable medical devices such as tubing, contact lenses, and breast implants.[2,10,11]

1.1.2 Traditional Methods of Synthesizing Functional Silicones

The traditional methods of preparing silicones on an industrial scale have remained essentially unchanged since the 1940s with the invention of the Direct Process independently by Müller and Rochow.[12,13] The synthesis of silicones begins with the reaction of an alkyl halide, commonly methyl chloride, with elemental silicon in the presence of copper to produce chlorosilanes. The chlorosilanes react with water or hydroxide through a nucleophilic substitution reaction to produce low molecular weight linear and cyclic silicone oligomers (Figure 1). These oligomers are converted into high molecular weight polymers by the reaction of siloxane (Si-O) or Si-OH groups with acid or base catalysts. This second chain extension reaction is an equilibrium process and is completely reversible; the reaction can be driven in either direction by controlling reaction conditions (Figure 1ii).[14] For example, it is critical to remove catalysts to suppress depolymerization once polymer growth is complete.[1]

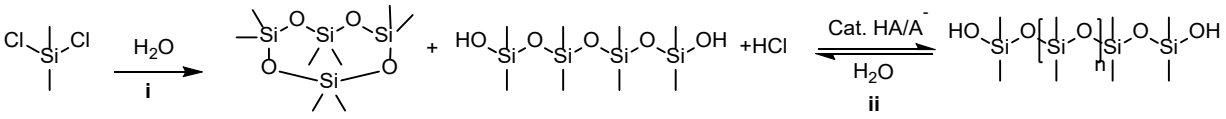

Figure 1.1: Traditional acid/base catalyzed synthesis of silicone

1.2 Functional Silicones

1.2.1 Improving Traditional Silicones by Functionalization

Non-functionalized polydimethylsilicones possess dimethyl groups that provide hydrophobicity to the silicone. While beneficial for application in sealants,[15] biomaterials,[2,16,17] etc.,[18] they do not always possess additional properties that are required for use of materials in different applications. In particular, there are no synthetic handles through which other entities may be added. The properties of the silicone must

be better adjusted to suit a specific purpose. Preparative methods similar to those for traditional silicones allow for the synthesis of end-capped polymers and/or block-copolymers by simply reacting chlorosilanes, cyclic silicones, or linear silanols containing a desired reactive functionality, then equilibrating under acidic or basic conditions (Figure 1.2).[19] Commercially, the reactive functionality is normally either hydride, hydroxyl-, or alkoxy- functionalizations.

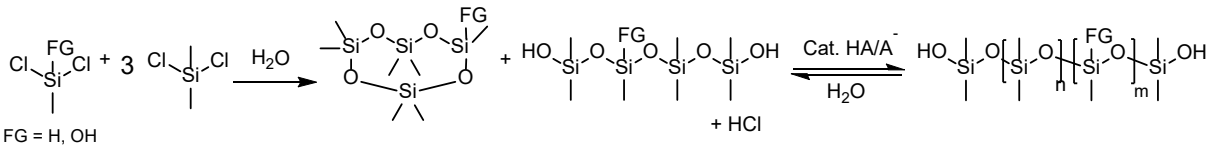

Figure 1.2: Synthesis of Si-H and Si-OH silicones using acid/base catalysis.

Functional silicone fluids, blends, and elastomers constitute an important class of commercial materials because they maintain many of the silicone's favourable physical and chemical properties after modification yet possess additional organic groups.[20] Modifying a typical dimethylsilicone structure with functional moieties improves their ability to be used in existing applications, and expands the range of silicones that can be adapted to new applications. Properties such as tack, viscosity, adhesion, gloss can all be changed according to the functionality of the silicone.[21]

1.2.2 How to Functionalize Silicone Polymers and Resins

Silicone resins are polysiloxane networks containing different degrees of siloxy- or alkyl-substitution by mixing the silicone monomers M (Me_3SiO), D ($Me_2SiO_{2/2}$), T ($MeSiO_{3/2}$), Q ($SiO_{4/2}$) (Figure 3).[22] The inclusion of T and/or Q groups produces a crosslinked polysiloxane with typical silicone viscoelastic properties but without the inclusion of organic moieties. MQ and DT networks are the most commonly used resins that serve as additives for dimethylsilicone polymers to improve their physical properties.[23,24] For example,

silicone resins are added to cosmetics to improve colour dispersion, to films to improve optical clarity,[25] or to elastomers to increase mechanical strength.[26]

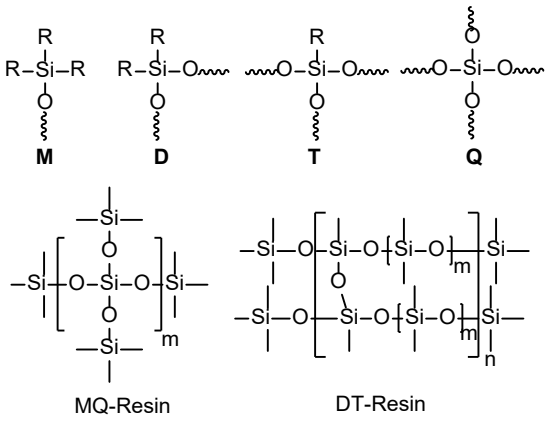

Figure 1.3: Structures of silicone units M (Me_3SiO), D ($Me_2SiO_{2/2}$), T ($MeSiO_{3/2}$), Q ($SiO_{4/2}$); and resins MQ-resin, DT-resin.

Organic functional silicone polymers and resins with vinyl, alkoxy, hydroxy, or hydride groups are commonly synthesized through equilibration of alkoxysilanes, silanols, and silicone fluids. The silicones are then normally reacted through hydrosilylation or condensation with organofunctional materials to install the desired functionality.[27,28] Further functionalization can be obtained by substitution or addition reactions once the organic moieties are installed.[29] The installed functionality can be organic,[30] ionic,[31] or supramolecular;[32,33] endowing the silicone with unique surface-,[34] thermal-,[35,36] and electrical chemistries.[37] Functionalization can be particularly useful in crosslinked materials.[28] For example, adding polar functional groups to a dimethylsilicone hydrophobic coating can increase the tackiness of a sealant for improved adhesion to surfaces.[22,38] The type of functional groups, as well as their arrangement along the silicone backbone, determines the properties adopted by the bulk silicone material. The

functional groups can be pendent to the silicone backbone, on the termini of the silicone, as blocks in an alternating polymer, or as crosslinks in a silicone elastomer (Figure 1.4).[39]

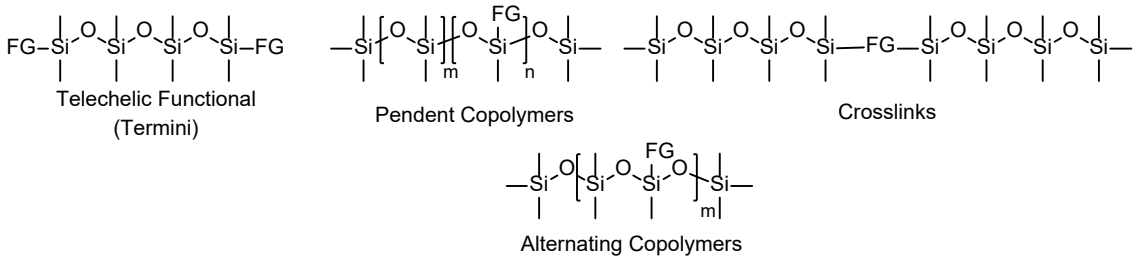

Figure 1.4: Different arrangements of functional groups (FG) on a silicone backbone.

1.2.3 Functional Silicone Composites and Blends

Silicone polymers can also be functionalized by using insoluble materials to create composite or blends. The combination of these materials with silicones typically leads to a product with properties in between the individual properties of the constituents of the mix.[40] However, the magnitude of the obtained properties is typically disproportionate to the amount of additive mixed with the polymer. Frequently, only a small amount of additive is required to increase the functionality of the silicone dramatically. For example, using polar functionalized polysiloxanes can aid the compatibility of the silicone with different hydrophilic materials such as polyethers or fumed silica to obtain more stable blends and composites.[41–44] However, in other cases, the incompatibility of silicones with many macromolecules, and hydrophilic compounds, in particular, limits their incorporation into materials, restricting their development.

1.2.4 Functional Elastomers and Gels

Elastomeric materials are of particular interest because their already desirable physical and chemical properties can be further tuned to a specific purpose, for example, in

dynamic materials,[45,46] pressure sensitive adhesives,[47–49] dielectric elastomers,[50,51] or renewable materials.[52] At the moment, many of these materials have limited commercial applications due to laborious preparations, harsh reaction conditions, the need to use organic solvents, incompatibility between reactants, or long reaction times for crosslinking. Therefore, there is currently interest in developing a crosslinking system for silicone materials that overcomes the limitations of current technologies and leads to high control over reaction times, using mild reaction conditions, and with a high tolerance to installed functional groups.

1.3 Current Crosslinking Technologies and Their Limitations

1.3.1 Most Common Methods of Crosslinking

Currently, the most common reactions used to crosslink silicone elastomers are platinum-catalyzed hydrosilylation, tin- or titanium- catalyzed condensation (RTV moisture cure), or radical-cure (Figure 1.5).[1]

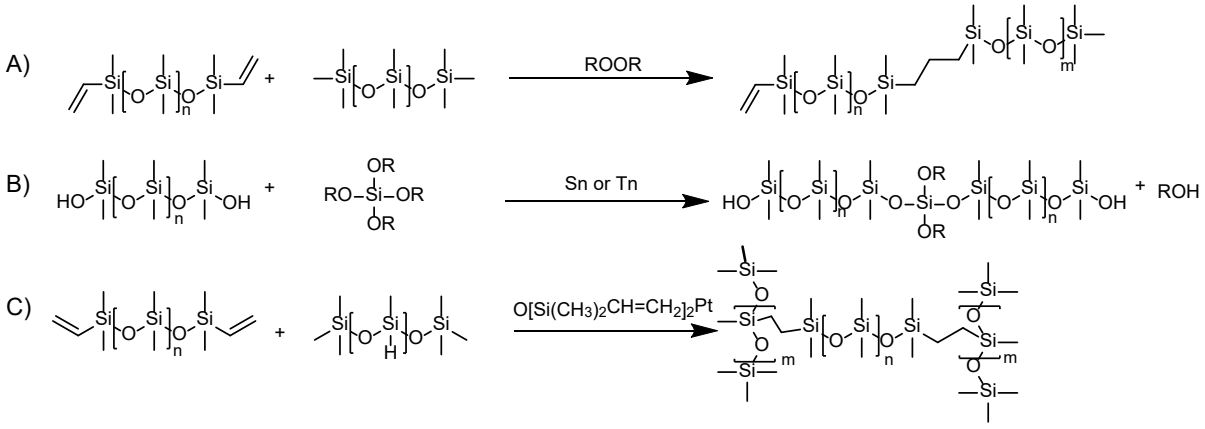

Figure 1.5: Traditional methods of crosslinking silicone elastomers using peroxide or metal catalyst. A) Radical initiated vulcanization of silicone fluids using a peroxide catalyst at high temperatures, B) condensation cure of silanols and alkoxysilanes using a tin or titanium catalysts, C) addition cure between vinyl-functionalized silicones and hydride-functional silicones using a platinum-catalyst.

These crosslinking methods are widely used in commercial preparations for silicone elastomers because the processes are robust, simple, use benign starting materials, and do not require sophisticated equipment or chemical knowledge.[39]

1.3.2 Radical-Initiated High-Temperature Vulcanization

Typical radical, high-temperature vulcanization uses heat to homolytically cleave a peroxide-initiator to form two radical initiators.[53] These radicals react with the methyl-groups on silicone to produce an $H_2C^{\bullet}Si$ radical. This newly formed radical can react with adjacent alkyl-chains to form alkyl bridges between two siloxanes (Figure 1.6). Recently, radical photoinitiators have replaced the use of high temperatures with UV-light for crosspolymerization with acrylates.[54] Regardless of the initiation process, the degradation products of the initiator must be removed from the silicone before use in applications, which has prevented its use in many applications, including medical applications and food-grade silicones.[55,56]

Figure 1.6: Peroxide-radical initiated vulcanization of a silicone elastomer at elevated temperatures. ROOR represents a peroxide initiator.

1.3.3 Metal-Catalyzed Room Temperature Vulcanization

Room-temperature vulcanization uses either titanium catalysts, such as tetraalkoxytitanates or chelated titanate compounds, or tin catalysts, typically dibutyltin dicarboxylates.[1,57] These catalysts hydrolyze to give Ti-OH or Sn-OH groups in the presence of water, which then act to facilitate crosslinking of silanol, alkoxysilanes, or acetoxysilanes, releasing an alcohol or acid as a byproduct (Figure 1.7A). The advantages

of this method are its low-cost, fast and robust cure, making it most commonly used as a crosslinking method for in sealants and as additives in composite materials such as concrete.[19] Platinum-catalyzed room temperature vulcanization involves the (mostly) anti-Markovnikov addition of a hydrosilane across the double bond of a vinyl-functional silicone (Figure 1.7B). This reaction produces no byproducts, allowing for transparent, medical grade silicone elastomers.[2,58]

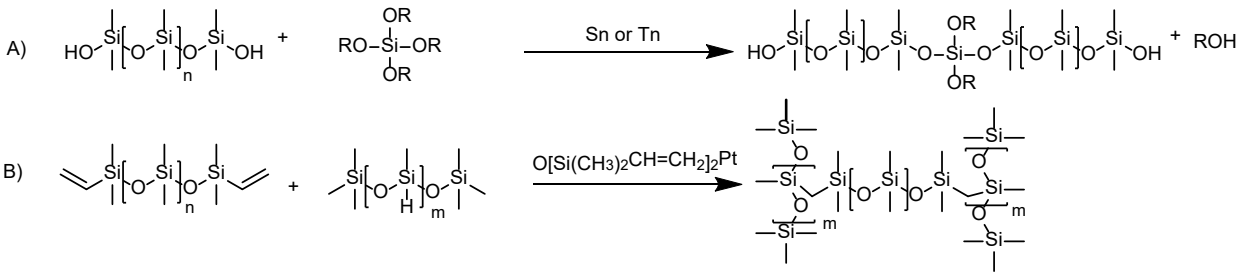

Figure 1.7: Metal-catalyzed room temperature vulcanization of silicone elastomers using A) Tin or titanium catalysts with alkoxysilane-silanol systems and B) Platinum-based Karstedt's (Platinum(0)-1,3-divinyl-1,1,3,3-tetramethyldisiloxane complex) with vinyl-hydride silicone systems.

1.3.4 Limitations of Current Crosslinking Methods

Despite the efficacy of these reactions for crosslinking silicone elastomers, each of these methods have limitations that constrain their wide application in functional silicone materials. Both metal-catalyzed reactions are incompatible with many Lewis acidic or basic functional groups because chelation will result in the deactivation of the metal center.[59,60] In addition, the tin and titanium catalysts can react with acidic functionalities on the silicone instead of crosslinking. Platinum catalyst cure is inhibited by the presence of many nucleophilic moieties that competitively act as metal ligands, such as mercapto- or amine- compounds. Both types of catalyst remain in the elastomeric material after curing, which may cause unwanted outcomes.[61–63] Radical-cure methods are restricted

by the elevated temperatures required to decompose the radical initiator and the high reactivity of the radical species towards some functional groups instead of the alkylsilicone required for crosslinking.[6,64] Note that it may be necessary for some applications to extract radical catalyst byproducts from the elastomer. Novel crosslinking methods must be developed to overcome the limitations of conventional crosslinking reactions.

1.4 New Chemistry as Crosslinking Methods for Silicone Elastomers

1.4.1 The Piers-Rubinsztajn Reaction

In a recent review, Piers describes the use of tris(pentafluorophenyl)borane ($B(C_6F_5)_3$) to catalyze the oxidation of hydrosilanes and the reduction of common organic functional groups.[65] Piers' works mentioned that complete reduction of the intermediate alkoxysilane, formed during reduction of some types of carbonyl group, by excess hydrosilane produces an alkane and a siloxane byproduct.[66,67] Rubinsztajn saw these works conversely; instead of an unanticipated problem, he viewed the second reduction as a novel method of synthesizing silicones.[68,69] It was demonstrated that siloxanes could be synthesized by the reduction of alkoxysilanes by hydrosilanes using small quantities (< 1 mol%) tris(pentafluorophenyl)borane as the catalyst, releasing an alkane byproduct from the reduction of the alkoxy-group (Figure 1.8).

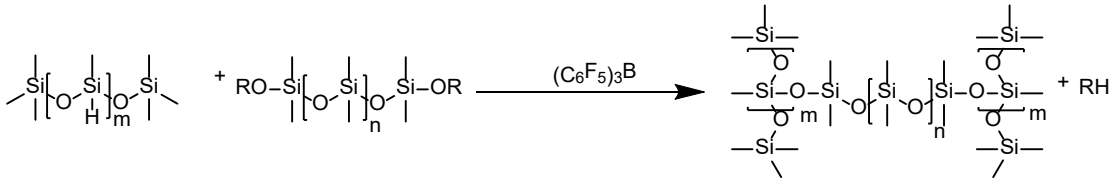

Figure 1.8: Piers-Rubinsztajn reaction used to crosslink hydrosilanes and alkoxysilanes into silicone elastomer releasing an alkane byproduct 'RH'.

This so-called Piers-Rubinsztajn reaction has been used to synthesize and crosslink novel silicone polymers.[70,71] This process gives greater synthetic control for preparing functional silicones when compared to traditional acid/base equilibration because the reaction is irreversible.

1.4.2 The Piers-Rubinsztajn Reaction for Functional Silicones

Grande and Fawcett separately demonstrated the utility of the Piers-Rubinsztajn reaction to crosslink silicone elastomers and foams.[70,72] It was also shown that the boron-catalyst has better tolerance towards several organic functional groups than catalysts used for metal-, or radical-catalyzed curing methods.[73,74] For example, the Piers-Rubinsztajn reaction was shown not to be affected by many common organic functional groups such as alcohols and alkyl halides. As a consequence, the first formed product can undergo nucleophilic substitution to install ionic groups,[75] azides,[76] triarylamines,[71] polysiloxazanes,[77] or supramolecular complexes to a silicone polymer (Figure 1.9).[78]

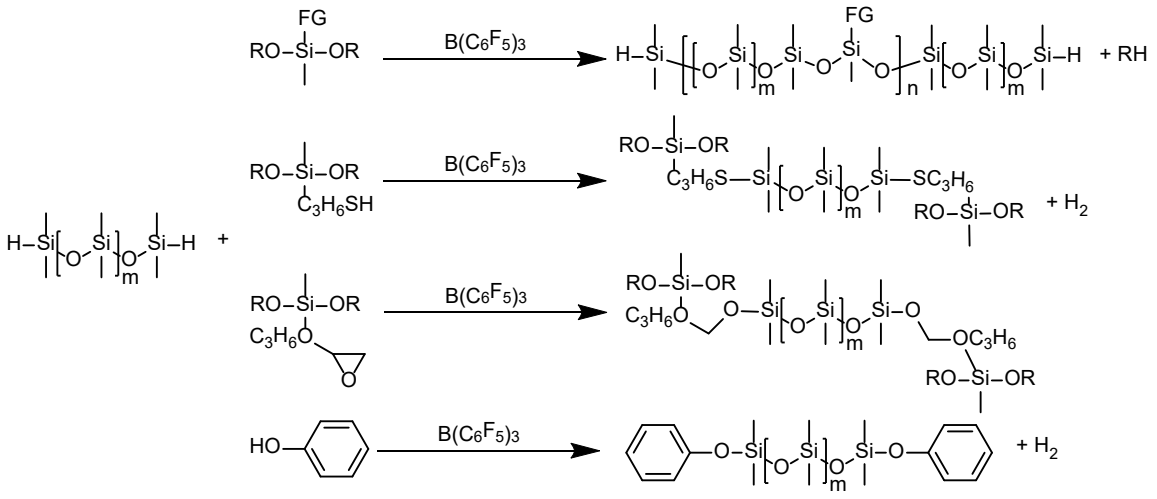

Figure 1.9: The Piers-Rubinsztajn reaction used to react hydrosilanes with functionalized alkoxysilanes to yield crosslinked functional silicone elastomers directly or from thiols, epoxides or phenols via new organosilicon bonds.

It is possible to create polymers with precise spacing between functional groups along the polysiloxane backbone; in this case, the resulting polymers have increased dielectric properties in silicone elastomers that are useful for electrical generation by wave action.[75] The Piers-Rubinsztajn can also be used to react hydrosilanes with many organic functional groups such as thiols,[79,80] phenolics,[81] or epoxides,[82] to produce organosilicones containing Si-X bonds that may be further exploited (Figure 1.9). When used as a method of crosslinking, the organosilicone bonds can introduce interesting physical or chemical properties to the elastomers and foams, allowing for a host of new applications and advancement of silicones in their specialized applications, including sustainable[83] or photosensitive materials.[84] Despite the improved tolerance of the Piers-Rubinszatjn reaction towards many organic functional groups over traditional cure methods, the use of a strong Lewis acid catalyst prevents its use in the presence of strong Lewis basic groups such as amines.

1.4.3 Crosslinking Chemistry from the Organic World

The availability of a greater variety of functional silicone polymers has allowed for novel crosslinking reactions based on traditional organic chemistry. Crosslinking through organic bonds uses the known chemistry of organic moieties, at least one of which is should be tethered to silicone via a non-hydrolyzable C-Si bond.[21,85] Typically, these organic groups will react through condensation or addition reactions with a small organic molecule or another silicone with the reactive partner as functionality to build a networked structure (Figure 1.10).

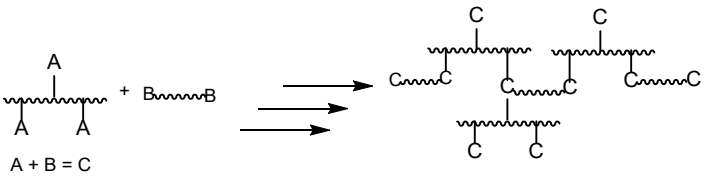

Figure 1.10: Model crosslinking scheme between two organo-functional silicones; one with pendent ‘A’ groups and one with telechelic ‘B’, that react to give crosslinks ‘C’

This approach is particularly useful because it employs well-established organic chemistry while the silicone serves as a hydrophobic medium for the reaction; solvents are not always required as, in some cases, the silicone can serve this function. This widens the scope of potential crosslinking reactions to many common organic moieties, except when reactions require strong Brønsted-Lowry acids or bases that may lead to decomposition of the silicone itself.[86] The resulting materials can convey a variety of interesting properties to the material that can be used for applications, such as amines for pressure-sensitive adhesives,[49,87] ureas for thermoplastic silicones,[88,89] or polyethylene oxide for surface activity on elastomer surfaces or as surfactants.[90]

1.4.4 The Chemistry of Amines and Aldehydes for Crosslinking Silicones

Amines react very efficiently and rapidly with aldehydes, a reaction that can be used for organic crosslinking. This reaction proceeds first through nucleophilic attack by the amine on the aldehyde to form a carbinolamine that decomposes, losing water as a byproduct to form an imine (Figure 9). Classical organic chemistry suggests that the imine forms through a zwitterionic carbinolamine intermediate that undergoes neutralization, then protonation, before degrading to form the imine. In a recent mechanistic review of such reactions in organic solvents, Di Stefano and Ciaccia found the zwitterionic species is not found in gas-phase calculations, there are slower reaction kinetics in protic solvents than

in aprotic solvents, and the reaction in toluene is strictly second-order involving only amine and aldehyde. Taking these data together, they proposed an alternative mechanism for imine formation in organic solvents (Figure 1.11).[91]

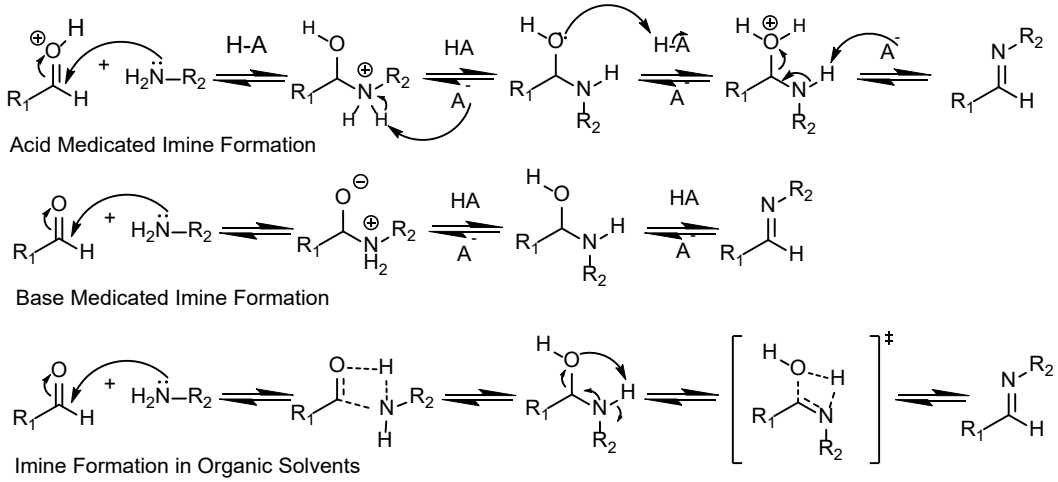

Figure 1.11: Mechanisms for imine formation using acid-base through a zwitterionic transition or in organic solvents via a 4-membered ring transition.

This mechanism involves simultaneous nucleophilic attack and proton transfers between the amine and aldehyde through a four-membered transition state to yield a carbinolamine. This carbinolamine then decomposes through a second four-membered transition state to yield the imine with accompanying loss of water.

The resulting imine constitutes a dynamic covalent bond with the ability to undergo dynamic exchange reactions.[92,93] The initial imine formation is reversible if exposed to water, reverting the imine to the initial aldehyde and amine. Furthermore, imines undergo exchange reactions with other amines or imines through transamination and transimination, respectively.[91] Transamination occurs through a similar mechanism as imine formation, except attack occurs by an amine on the imine to yield an aminal, which decomposes to form a new imine. The equilibrium of this exchange was found to be

approximately equal in both directions (K ≈ 1) when using primary, sterically unhindered amines for the formation and exchange of the imine.[94,95] Transimination or imine metathesis involves the scrambling of amines between two existing imines to yield two different imines; this process is catalyzed by an unbound amine. Imine metathesis is the apparent exchange of functional groups to produce the metathesis product of the two imines. In reality, this metathesis occurs through multiple transimination reactions catalyzed by a free amine (Figure 1.12).[95] Imines are attractive bonds for crosslinking materials because these dynamic exchange reactions can occur even after the material has cured; an elastomer is also a dynamic material.[96]

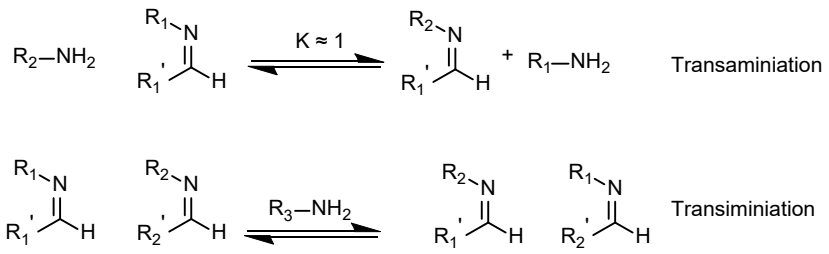

Figure 1.12: Dynamic bond exchange reactions between imines and amines occur under equilibrium conditions.

1.5 Dynamic Silicone Materials

1.5.1 Applications of Dynamic Silicone Elastomers

An emerging class of materials over the last couple of decades has been so-called stimulus-responsive or dynamic materials. [97–99] These materials possess labile bonds or undergo rearrangement when exposed to a specific stimulus or conditions. These bonds can autonomously self-assemble, dissociate, or alter crosslinking in a material at the molecular level, even after the material has been cured. Given the name ‘vitrimers’ by Ludwik Leibler, these materials manifest interesting properties such as self-healing,

thermoplasticity, chemical responsiveness, or photo-responsiveness, depending on the bonds used in the material.[100–102] The dynamic bonds can either be dissociative, where the external stimulus causes the bonds to break into two reactive moieties that can reform bonds, or associative, where the stimulus causes bond exchanges between dynamic functional groups (Figure 1.13).[103] Silicones lend themselves well for use in dynamic materials because their low T_g aids the kinetics of dynamic bond exchange by allowing for reactive handles to have greater mobility. Silicone materials possessing ionic, noncovalent, or dynamic covalent interactions as crosslinks are valuable because of their potential thermoplastic and dynamic properties. [104]

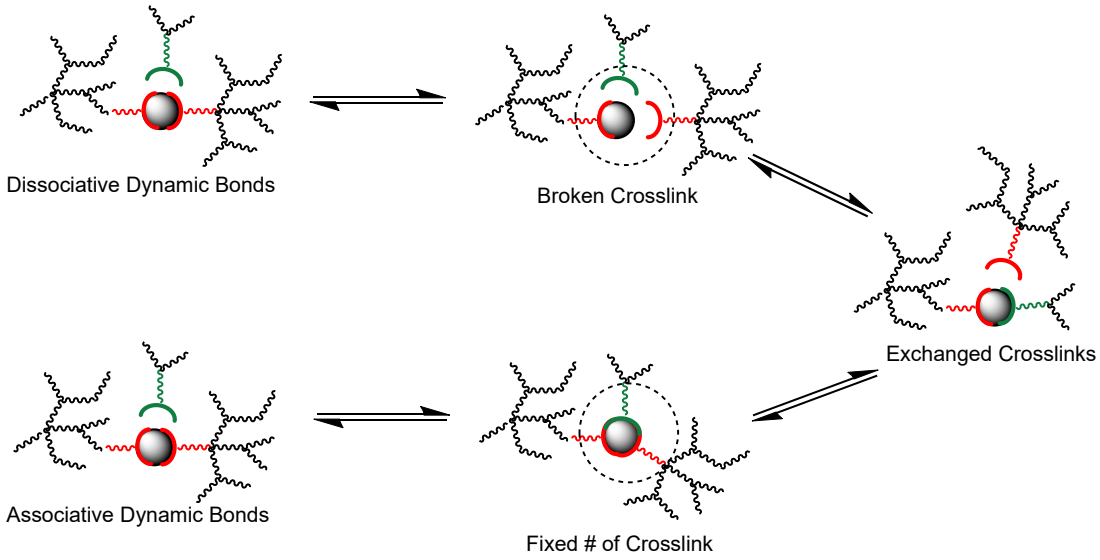

Figure 1.13: Comparison between dissociative and associative dynamic bond exchange processes in a vitrimeric material. Dissociative bonds undergo bond breaking and forming reactions

1.5.2 Ionic interactions as Crosslinks in Silicone Elastomers

Silicone materials crosslinked through ionic bonds depend on the electrostatic interaction between anionic and cationic groups to cause sufficient aggregation for crosslinking.[105] Typically, this is achieved by having at least one of the ions covalently bonded to the

polysiloxane backbone, while the counter ion can be bound to another polymer or exist as a free multi-valent ion (Figure 1.14). Skov et al. described an ionically crosslinked interpenetrating network produced by swelling carboxy- and ammonium- functionalized silicones into a traditional tin-catalyzed RTV-silicone, leading to the development of self-healing and improved dielectric properties.[50] Silicone elastomers crosslinked solely through ionic interactions have been synthesized using the interaction between maleic acid-functionalized silicones and a diaminosilicone,[106] or the interaction between a carboxylic acid functionalized silicone with free ZnO particles.[107] In both cases, the materials were imbued with self-healing and thermoplastic properties.

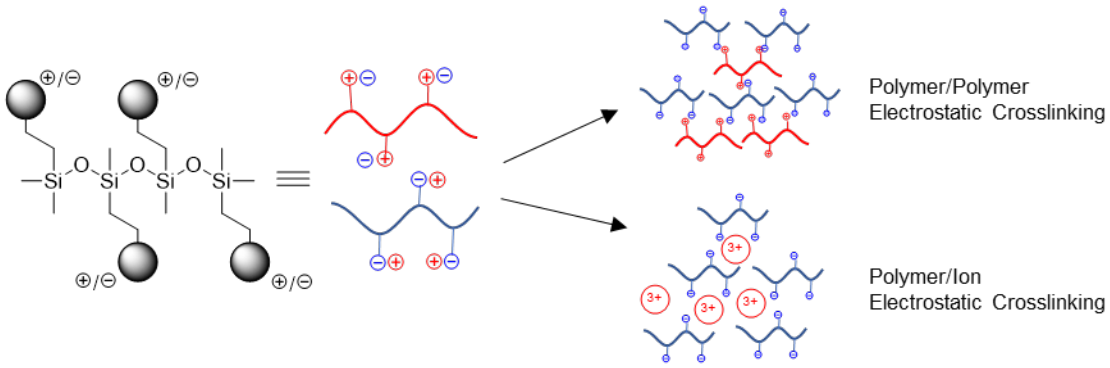

Figure 1.14: Dynamic crosslinking using electrostatic interactions between two oppositely charged polymers or polymer with an oppositely charged ion.

1.5.3 Non-covalent Interactions as Crosslinks in Silicone Elastomers

Silicones crosslinked through noncovalent interactions, typically hydrogen bonding,[108–113] metal-ligand interactions,[114–116] or π-interactions,[117] are a rapidly emerging class of materials in the literature. While individual noncovalent interactions are weaker than conventional covalent bonds, multiple noncovalent interactions can be combined to achieve similar bond strength.[33,118,119] The use of multiple noncovalent bonds is particularly interesting because of their ability to self-assemble into complex crosslinking

motifs that would be impossible to accomplish synthetically. The utilization of these bonds for crosslinking can be accomplished in various methods. For example, linear silicone-urea copolymers form dynamic elastomers via hydrogen bonding crosslinks between urea moieties to give dynamic properties depending on the Tg difference between the two monomers.[112,113,120] The silicone portion behaves as a fluid at all temperatures, while the hydrogen bonding between urea blocks can be disrupted at elevated temperatures, causing the elastomer to flow.

Individual noncovalent interactions tend to be weaker than conventional covalent bonds; larger molecules with multiple functionalities are required to achieve similar crosslinking strengths.[118] This is often paradoxical as these larger, more functional molecules tend to have poorer solubility and reactivity with the silicone. Incorporating these moieties into a silicone network as either covalently bound functional groups or physically mixed additives is frequently inefficient because of incompatibility with the hydrophobic polysiloxane backbone, even when functional polysiloxanes are employed to aid compatibility.[121] This has limited the quantity of functional entities that can be integrated into a silicone network, thereby limiting the magnitude of the dynamic properties bestowed.

1.5.4 Dynamic Covalent Bonds in Silicones

Dynamic covalent bonds are bonds under thermodynamic control with reversible equilibria between multiple reactive species.[96,99,122] They are commonly used in supramolecular chemistry to self-assemble complex macromolecules such as macrocycles,[123] organic frameworks,[124] or catalysts[125] from relatively simple molecular building blocks. Materials crosslinked through dynamic covalent bonds can distort the equilibria to change the bonding arrangement of the polymer network; however, as they are formal covalent bonds, they are significantly stronger than the previously mentioned dynamic noncovalent

bonds.[126–128] This increased strength allows for relatively simpler bonding motifs and smaller functional groups, allowing for better compatibility and a greater range of dynamic properties imbued to the silicone. There are a large variety of associative and dissociative dynamic bonds that each respond differently to various stimuli or conditions. Dissociative dynamic equilibria such as disulfide exchange,[129] Diels-Alder cycloaddition,[130] or ester exchange [131] undergo bond breaking and forming events when activated (Figure 1.15).

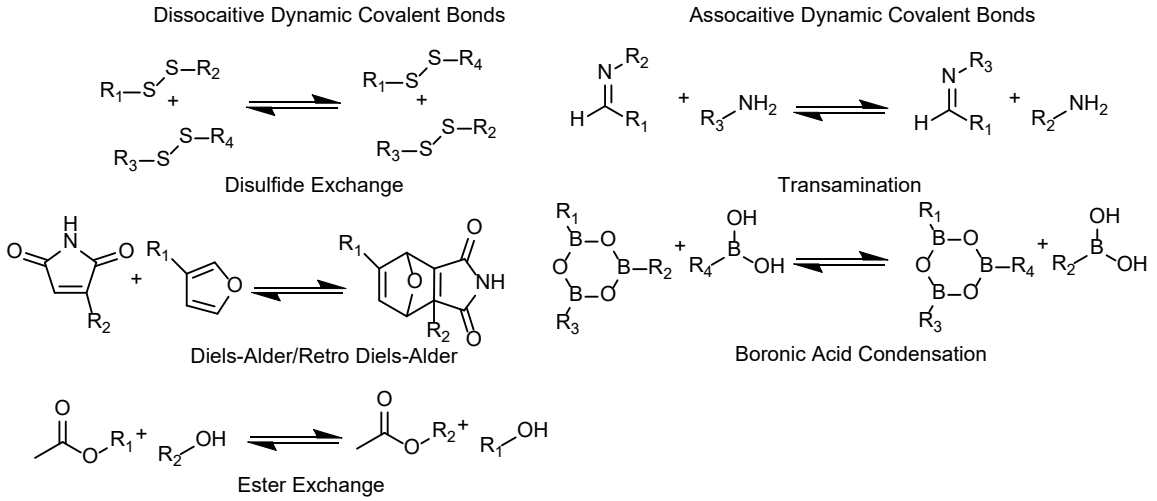

Figure 1.15: Examples of dissociative and associative dynamic covalent bonds and their respective equilibria.

Associative dynamic equilibria such as imine-aminal,[92] or boronic acid condensation,[132] in contrast, metathesize reactive group pairs allowing for an exchange of bonds without dissociation (Figure 1.15). This is attractive for crosslinking dynamic materials because the concentration of crosslinks in the material does not change, as is the case with dissociative processes, which can prevent potential errors in reactive partners. However, dynamic covalent bonding in silicone materials is currently limited and requires further investigation.

1.6 Thesis Objectives

1.6.1 Overall Objectives

Several organic functional groups are incompatible with traditional methods of crosslinking silicones, which has hindered progress towards new functional silicones. The objectives of this thesis are focused on developing an alternative crosslinking method for silicone materials. This method should involve high reactivity under mild reaction conditions and tolerances to organic moieties that would be inaccessible to traditional crosslinking methods. In addition, the use of organosilicones affords the ability to use organic functionalization on the polysiloxane backbone to crosslinking the silicones.

Amine-functionalized silicones are particularly interesting due to their use in many industrial applications, however, they are difficult to produce using traditional methods due to the amines poisoning the catalyst used in crosslinking. Although impressive progress has been made in creating silicone elastomers without catalysts, the use of many well-established organic reactions for this purpose have yet to be studied. The reaction between aldehydes and amines could potentially serve as a method of crosslinking silicones with bonds with high fidelity under mild conditions, without the need for neither solvent nor catalyst. Furthermore, the resulting materials would have attractive functionality that can imbue the silicone with unique properties that will be evaluated, then applied to an application. Therefore, this thesis aims to develop new crosslinking methods for amine-functionalized silicone materials by use of organic aldehydes as the crosslinkers, studying the properties of the crosslinked materials afforded by the crosslinks, and applying these materials to an application.

1.6.2 Aliphatic Aldehyde Crosslinkers

A starting point for aldehyde crosslinkers for silicone elastomers are aliphatic aldehydes, such as formaldehyde and glyoxal, as they constitute the simplest possible aldehydes. This reaction occurs through condensation with the aldehyde to form an imine that is subsequently attacked by a second amine to yield aminal (Figure 1.16). [133] The lack of resonance stabilization from the aliphatic alkyl-chain favours this aminal instead of further conversion into an imine. Although the reaction does not yield dynamic bonds, the renowned robustness of this reaction for a variety of biological matter in the presence of a complex matrix of different functional proteins was desirable. [134–137] There is an inherent incompatibility between the hydrophobic silicone backbone with the aqueous aldehyde solutions, which would be expected to reduce reactivity. Nonetheless, it was hypothesized that the high reactivity of these simple aldehydes towards aminopropyl silicones would overcome this hydrophobic barrier allowing crosslinking reactions to occur. The systematic study of crosslinking aminopropylsilicones using three different aliphatic aldehydes and characterization of the resulting materials is the basis of chapter 2.

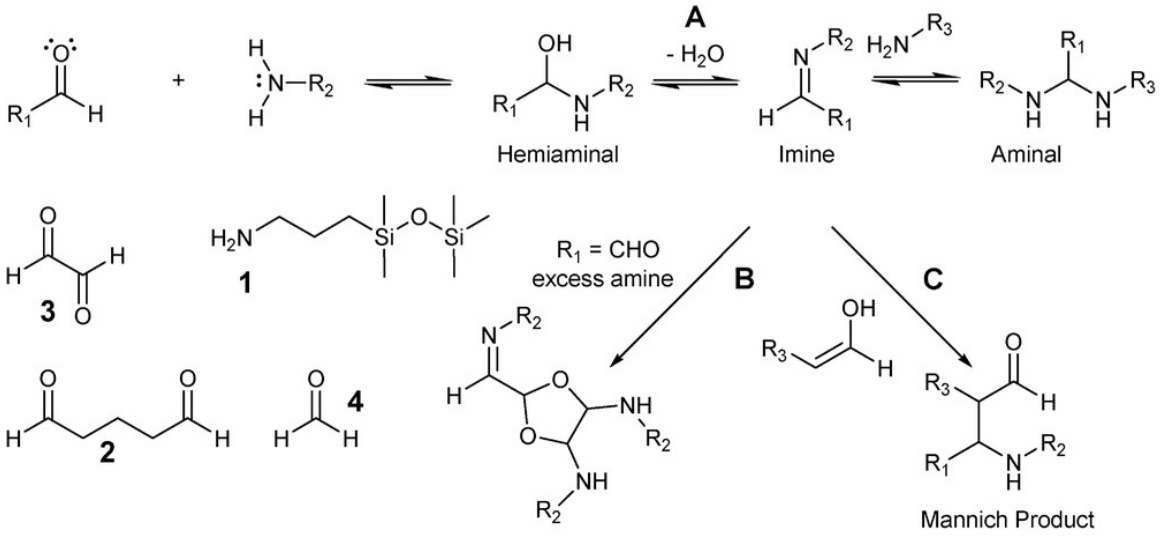

Figure 1.16: Model reactions between model aminoalkylsilicone 1 and A: formaldehyde 4 B: glyoxal 3, or C: glutaraldehyde 2.

1.6.3 3-D Printing Silicones using Aliphatic Aldehydes

While there are a variety of methods used for 3-D printing, it has proven difficult to 3D print silicone materials as they do not melt at 'normal' temperatures and flow at a rate competitive with crosslinking that is typically accomplished following extrusion onto a support structure of UV-initiated platinum- or radical-catalyzed cure system.[138] While this method has been established as the industry standard for 3-D printing silicone elastomers, several drawbacks have hindered its advancement. Using a UV-cure system means crosslinking can only be initiated after extrusion from the printer, which often necessitates the use of support structures and high viscosity silicones to provide structural strength to the product.[139] This greatly complicates the printing process by increasing cost, printing time, and decreasing printing resolution. The use of low viscosity silicones would facilitate delivery of reactive inks at low pressure, improving resolution by allowing for the deposition of smaller quantities of material that cure to greater structural rigidity. Achieving this

objective requires a high chemical reactivity such that the material cures to have sufficient structural rigidity to support subsequently deposited material. [138,140,141]

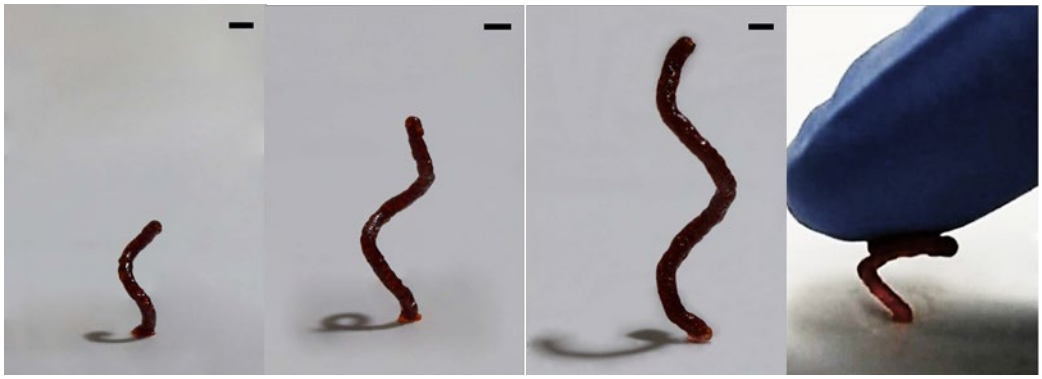

Figure 1.17: Silicone-glutaraldehyde elastomers printed using the free-space droplet merging printer without the need of support material. [142]

As discussed in chapter 2, the reaction between aminopropylsilicones and aliphatic aldehydes, formaldehyde and glutaraldehyde, leads to rapid crosslink into a free-standing elastomer gel.[142] This curing system showed promise when used in a 2-part mixing syringe for 3-D printing. The drawback of this cure-systems is that careful control over mixing the reactive components is required to prevent cure in the printer itself, leading to clogging in the printer components.[143] To combat this issue, a novel free-space droplet merging printer was designed by Monika Silwiak and Ravi Salvaganapathy. This printer ejects two congruent droplets from two nozzles on opposite sides of the print bed along the same trajectory, collide in the air, and mix before deposition. The combination of this printer with the aliphatic aldehyde-aminopropylsilicone cure system can be used to 3-D print unsupported silicone elastomer with unique morphologies (Figure 1.17). Chapter 3 discusses the design and use of the printer for 3-D printing glutaraldehyde-crosslinked aminopropyl silicone elastomers.

1.6.4 Aromatic Aldehyde Crosslinkers - Dynamic Crosslinking

The equilibrium reaction of amines with conjugated (particularly aromatic) aldehydes favours the formation of an imine, as opposed to the aminal, because of the thermodynamic benefit arising from the extension of the conjugated system.[91,94,95] Elimination of water from the system leads to nearly stoichiometric conversion of primary amines and aldehydes into imines in organic solvents. Crosslinking of organic carbon-based polymers through imine bonds yields dynamic materials that can undergo hydrolysis, transimination, and transamination reactions.[152,153] At room temperature, the imines are kinetically locked in the polymer with poor mobility, which leads to slow rates of these exchange reactions; the material behaves like a traditional thermoset. However, upon heating above the T_g, the material begins to flow as a viscoelastic fluid, giving the bonds sufficient kinetic energy for bond exchange between imine crosslinks. There have been several reports of imine-modified organic polymers, including polyesters,[154] polyurethanes,[155] polyalkylamines,[153] and polyethylene glycol,[152] all with impressive self-healing capabilities and reprocessability stemming from the imine crosslinks.

Despite the success of these dynamic materials, they are primarily based on hydrophilic polymers. As a result, over time, the imine crosslinks in the polymers undergo slow hydrolysis by atmospheric water. [152,153] This defect prevented a thorough investigation of the capabilities of all three bond exchange reactions and significantly reduced material lifetimes. Using a hydrophobic polymer such as polydimethylsiloxane would potentially protect the imine crosslinks by surrounding the bonds with hydrophobic groups creating a high kinetic energy barrier for hydrolysis. The synthesis of silicone elastomers crosslinked through dynamic Schiff-bases and the evaluation of their dynamic properties will be the subject of Chapter 4.

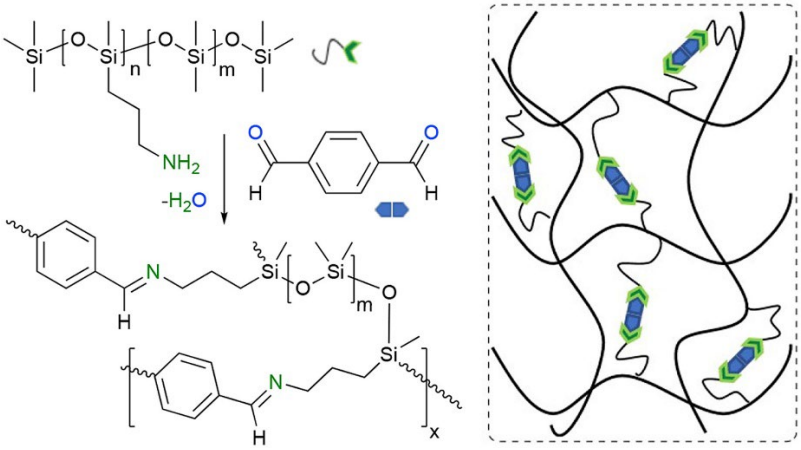

Figure 1.18: Dynamic silicones synthesized by crosslinking aminopropylsilicones with terephthaldehyde.

1.6.5 Sustainable Dynamic Silicones Using Vanillin

There is a trend in commercial materials towards renewable or sustainable products due to the alarming rates of environmental pollution, particularly of aquatic systems.[156] This trend has been accelerated by global government mandates to eliminate oxo-degradable plastics that degrade into harmful microplastics.[157] Alternative materials include bioplastics that are biodegradable materials made from renewable biomass.[145,149] Despite the raw materials for silicones, silicon (Si) and silica (SiO_2), being the second most abundant materials found in the earth's crust, they are not regarded as sustainable materials. This is mainly due in part to the high energy consumption during the conversion of sand to silicone, prior to the use of the Direct Process to create silicone precursors, the chlorosilanes.[158] This has necessitated the investigation of methods that permit the incorporation into silicones of renewable biomass, including lignin,[52] sugars,[109,110] and triglycerides.[159]

Lignin is an interesting source of biomass, as it is the second most abundant organic polymer on earth.[160,161] It is known for its complex polyphenylpropanoid structure that

contains functional groups that serve as reactive handles. To create bioplastics, lignin can be combined with other polymers, such as silicones.[162–164] Zhang synthesized silicone bioplastic foams and elastomers by copolymerizing hydrosilanes with phenols and phenolethers on lignin using the Piers-Rubinsztajn reaction.[52,165] While these materials predictably increase the sustainability through the inclusion of biomass, their additional functionality also granted novel properties to the bulk material. Surprisingly given the aromatic nature of lignin, foamed silicone lignin materials were better at flame tests than pure silicone foams.

An alternative route to lignin-based bioplastics is through its degradation products. The oxidative or reductive cleavage of lignin leads to various synthetically useful phenolic building blocks.[161,166,167] The processes used to convert lignin into these compounds are a different field of study. Vanillin is a particularly interesting product derived from lignin because of its reactive aldehyde functionality and its ready availability; vanillin is the only chemical currently derived from lignin on an industrial scale.[168–171] The aldehyde group allows for crosslinking of aminopropylsilicones through Schiff-base bonds that lead to dynamic materials which impart on their own to increase sustainability. These materials will be the topic of Chapter 5.

1.7 References

[1] Michael A. Brook, In *Silicon in Organic, Organometallic, and Polymer Chemistry*, John Wiley & Sons, Inc., New York, **2000**, ch.11.

[2] F. Abbasi, H. Mirzadeh, A. A. Katbab, *Polym. Int.,* **2001**, *50*, 1279.

[3] J. E. Mark, *Acc. Chem. Res.,* **2004**, *37*, 946.

[4] H. Sebag, G. Vanlerberghe, *Surface-active polysiloxanes*, Patent US 4490356A, **1982**.

[5] S. J. Clarson, J. A. Semlyen, *Siloxane Polymers*, Prentice Hall, Englewood Cliffs, NJ, **1993**.

[6] G. Camino, S. M. Lomakin, M. Lageard, *Polymer,* **2002**, *43*, 2011.

[7] G. Camino, S. M. Lomakin, M. Lazzari, *Polymer,* **2001**, *42*, 2395.

[8] M. A. Brook, In *Silicon in Organic, Organometallic and Polymer Chemistry*, Wiley, New York, **2000**, pp. 27–38.

[9] S. J. Clarson, J. J. Fitzgerald, M. J. Owen, S. D. Smith, M. E. Van Dyke, *Synthesis and Properties of Silicones and Silicone-Modified Materials*, Vol. 838, American Chemical Society, **2003**.

[10] N. A. Chekina, V. N. Pavlyuchenko, V. F. Danilichev, N. A. Ushakov, S. A. Novikov, S. S. Ivanchev, *Polym. Adv. Technol.* **2006**, *17*, 872.

[11] D. Jones, *Elastomerics,* **1988**, *120*, 12.

[12] L. Rösch, P. John, R. Reitmeier, In *Ullmann's Encyclopedia of Industrial Chemistry*, American Cancer Society, **2000**.

[13] H.-H. Moretto, M. Schultz, G. Wagner, In *Ullmann's 'Encyclopedia of Industrial Chemistry*, VCH, Wienheim, **1993**, pp. 57–93.

[14] S. J. Clarson, J. J. Fitzgerald, M. J. Owen, S. D. Smith, M. E. Van Dyke, *Synthesis and Properties of Silicones and Silicone-Modified Materials*, Vol. 964, American Chemical Society, **2007**.

[15] R. B. Malla, M. R. Shrestha, M. T. Shaw, S. B. Brijmohan, *J. Mater. Civ. Eng.* **2011**, *23*, 287.

[16] F. Abbasi, H. Mirzadeh, M. Simjoo, *J. Biomater. Sci. Polym. Ed.* **2006**, *17*, 341.

[17] A. B. Anderson, A. W. Dallmier, S. J. Chudzik, L. W. Duran, P. E. Guire, R. W. Hergenrother, M. A. Lodhi, A. E. Novak, R. F. Ofstead, K. Wormuth, In *Biomaterials in Orthopedics*, Dekker, New York, **2004**, pp. 93–148.

[18] R. R. McGregor, *Silicones and Their Uses*, **1954**.

[19] S. C. Shit, P. Shah, *Natl. Acad. Sci. Lett.,* **2013**, *36*, 355.

[20] K. M. Ryan, A. D. Drumm, C. E. Martin, A.-K. Krumpfer, J. W. Krumpfer, In *Reactive and Functional Polymers Volume One : Biopolymers, Polyesters, Polyurethanes, Resins and Silicones*, Springer International Publishing, Cham, **2020**, pp. 301–328.

[21] C. Racles, M. Dascalu, A. Bele, M. Cazacu, In *Reactive and Functional Polymers Volume One : Biopolymers, Polyesters, Polyurethanes, Resins and Silicones*, Springer International Publishing, Cham, **2020**, pp. 235–291.

[22] F. de Buyl, *Int. J. Adhes.,* **2001**, *21*, 411.

[23] W. Huang, Y. Huang, Y. Yu, *J. Appl. Polym. Sci.,* **1998**, *70*, 1753.

[24] M. D. Soucek, D. P. Dworak, R. Chakraborty, *J. Coat. Technol. Res.,* **2007**, *4*, 263.

[25] A. B. Pawar, B. Falk, In *Surface Science and Adhesion in Cosmetics*, John Wiley & Sons, Ltd; **2021**, pp. 151–182.

[26] C. Robeyns, L. Picard, F. Ganachaud, *Prog. Org. Coat.,* **2018**, *125*, 287.

[27] P. George, M. Prober, J. Elliott, *Chem. Rev.,* **1956**, *56*, 1065.

[28] J. M. Pujol, C. Prébet, *J. Adhes. Sci. Technol.,* **2003**, *17*, 261.

[29] W. Fortuniak, K. Rózga-Wijas, J. Chojnowski, F. Labadens, G. Sauvet, *React. Funct. Polym.,* **2004**, *61*, 315.

[30] T. Shimizu, K. Kanamori, K. Nakanishi, *Chem. – Eur. J.,* **2017**, *23*, 5176.

[31] J. H. Silver, J.-C. Lin, F. Lim, V. A. Tegoulia, M. K. Chaudhury, S. L. Cooper, *Biomaterials,* **1999**, *20*, 1533.

[32] A. H. Hofman, I. A. van Hees, J. Yang, M. Kamperman, *Adv. Mater.,* **2018**, *30*, 1704640.

[33] T. Christoff-Tempesta, A. J. Lew, J. H. Ortony, *Gels* **2018**, *4*, 40.

[34] J. H. L. Beal, A. Bubendorfer, T. Kemmitt, I. Hoek, W. M. Arnold, *Biomicrofluidics,* **2012**, *6*.

[35] D. W. Scott, *J. Am. Chem. Soc.* **1946**, *68*, 356.

[36] J. Cardoso, R. Manrique, M. Albores-Velasco, A. Huanosta, *J. Polym. Sci. Part B Polym. Phys.,* **1997**, *35*, 479.

[37] F. B. Madsen, A. E. Daugaard, S. Hvilsted, A. L. Skov, *Macromol. Rapid Commun.,* **2016**, *37*, 378.

[38] R. B. Malla, B. J. Swanson, M. T. Shaw, *Constr. Build. Mater.,* **2011**, *25*, 4132.

[39] W. Noll, *Chemistry and Technology of Silicones*, Elsevier, **2012**.

[40] L. Bokobza, *J. Appl. Polym. Sci.,* **2004**, *93*, 2095.

[41] I. Cifková, P. Lopour, P. Vondráček, F. Jelínek, *Biomaterials,* **1990**, *11*, 393.

[42] R. M. Hill, E. W. Kaler, L. D. Ryan, J. A. Silas, *Single phase silicone and water compositions*, Patent US 6013683, **2000**.

[43] Patrice Lucas, Jean-Jacques Robin, *Adv. Polym. Sci.,* **2007**, *209*, 111.

[44] J. H. Guo, X. R. Zeng, H. Q. Li, Q. K. Luo, *J. Elastomers Plast.,* **2010**, *42*, 539.

[45] J. S. A. Ishibashi, J. A. Kalow, *ACS Macro Lett.,* **2018**, *7*, 482.

[46] S. H. Cho, H. M. Andersson, S. R. White, N. R. Sottos, P. V. Braun, *Adv. Mater.,* **2006**, *18*, 997.

[47] H. Fakhraian, K. Anbaz, M. B. P. Riseh, M. Ghafouri, *Int. J. Adhes. Adhes.,* **2009**, *29*, 111.

[48] S. B. Lin, *Int. J. Adhes. Adhes.,* **1994**, *14*, 185.

[49] M. He, Q. Y. Zhang, J. Y. Guo, In *Emerging Focus on Advanced Materials, Pts 1 and 2*, **2011**, pp. 1773–1778.

[50] F. B. Madsen, L. Yu, A. E. Daugaard, S. Hvilsted, A. L. Skov, *RSC Adv.,* **2015**, *5*, 10254.

[51] J. Biggs, K. Danielmeier, J. Hitzbleck, J. Krause, T. Kridl, S. Nowak, E. Orselli, X. Quan, D. Schapeler, W. Sutherland, J. Wagner, *Angew. Chem. Int. Ed.,* **2013**, *52*, 9409.

[52] J. Zhang, Y. Chen, P. Sewell, M. A. Brook, *Green Chem.,* **2015**, *17*, 1811.

[53] M. L. Dunham, D. L. Bailey, R. Y. Mixer, *Ind. Eng. Chem.,* **1957**, *49*, 1373.

[54] V. Shukla, M. Bajpai, D. K. Singh, M. Singh, R. Shukla, *Pigment Resin Technol.,* **2004**, *33*, 272.

[55] A. Mashak, A. Rahimi, *Iran. Polym. J.,* **2009**, *18*, 279.

[56] K. Lund, J. Petersen, *Eur. Food Res. Technol.,* **2002**, *214*, 429.

[57] S. Balduzzi, M. A. Brook, *Tetrahedron,* **2000**, *56*, 1617.

[58] Y. H. An, R. J. Friedman, *J. Biomed. Mater. Res.,* **1998**, *43*, 338.

[59] S. Chen, J. Zhang, *Recent Pat. Mater. Sci.,* **2009**, *2*, 158.

[60] F. Faglioni, M. Blanco, W. A. Goddard, D. Saunders, *J. Phys. Chem. B,* **2002**, *106*, 1714.

[61] M. A. Brook, *Biomaterials,* **2006**, *27*, 3274.

[62] M. A. Brook, *Chem. Eng. News,* **2006**, *84*, 10.

[63] M. A. Brook, *Anal Chem,* **2006**, *78*, 5609.

[64] P. R. Dvornic, R. W. Lenz, In *High Temperature Siloxane Elastomers*, Huthig & Wepf, pp 20-65, **1990**.

[65] W. E. Piers, *Adv. Organomet. Chem.* **2005**, *52*, 1.

[66] J. M. Blackwell, E. R. Sonmor, T. Scoccitti, W. E. Piers, *Org. Lett.,* **2000**, *2*, 3921.

[67] J. M. Blackwell, K. L. Foster, V. H. Beck, W. E. Piers, *J. Org. Chem.,* **1999**, *64*, 4887.

[68] S. Rubinsztajn, J. A. Cella, *Macromolecules,* **2005**, *38*, 1061.

[69] S. Rubinsztajn, J. Cella, *Polym. Prepr.,* **2004**, *45*, 635.

[70] J. B. Grande, A. S. Fawcett, A. J. McLaughlin, F. Gonzaga, T. P. Bender, M. A. Brook, *Polymer,* **2012**, *53*, 3135.

[71] B. A. Kamino, J. B. Grande, M. A. Brook, T. P. Bender, *Org. Lett.,* **2011**, *13*, 154.

[72] A. S. Fawcett, J. B. Grande, M. A. Brook, *J. Polym. Sci. Part Polym. Chem.,* **2013**, *51*, 644.

[73] J. B. Grande, F. Gonzaga, M. A. Brook, *Dalton Trans.,* **2010**, *39*, 9369.

[74] J. B. Grande, F. Gonzaga, M. A. Brook, *Chem. Commun.,* **2010**, *46*, 4988.

[75] F. B. Madsen, I. Javakhishvili, R. E. Jensen, A. E. Daugaard, S. Hvilsted, A. L. Skov*, *Polym. Chem.,* **2013**, *00*, 1.

[76] T. Rambarran, F. Gonzaga, A. Fatona, M. Coulson, S. Saem, J. Moran-Mirabal, A. Brook Michael, *J. Polym. Sci. Part Polym. Chem.,* **2018**, *56*, 589.

[77] L. Ai, Y. Chen, L. He, Y. Luo, S. Li, C. Xu, *Chem. Commun.,* **2019**, *55*, 14019.

[78] R. C. Chadwick, J. B. Grande, M. A. Brook, A. Adronov, *Macromolecules,* **2014**, *47*, 6527.

[79] S. Zheng, M. A. Brook, *Macromol. Rapid Commun.,* **2021**, *42*, 2000375.

[80] S. Zheng, M. Liao, Y. Chen, M. A. Brook, *Green Chem.,* **2020**, *22*, 94.

[81] J. Cella, S. Rubinsztajn, *Macromolecules,* **2008**, *41*, 6965.

[82] S. Chandrasekhar, C. R. Reddy, B. N. Babu, G. Chandrashekar, *Tetrahedron Lett.,* **2002**, *43*, 3801.

[83] S. E. Laengert, A. F. Schneider, E. Lovinger, Y. Chen, M. A. Brook, *Chem. Asian J.,* **2017**, *12*, 1208.

[84] C. B. Gale, Z. B. Yan, M. Fefer, G. R. Goward, M. A. Brook, *Macromolecules,* **2021**, *54*, 4333.

[85] M. A. Brook, In *Silicon in Organic, Organometallic and Polymer Chemistry*, Wiley, New York, **2000**, pp. 381–458.

[86] E. Fritz-Langhals, In *Aldehyde and Carboxy Functional Polysiloxanes,* Springer Netherlands, **2008**, pp. 39–50.

[87] S. C. Mehta, P. Somasundaran, C. Maldarelli, R. Kulkarni, *Langmuir,* **2006**, *22*, 9566.

[88] D. B. Thompson, A. S. Fawcett, M. A. Brook, *Simple Strategies to Manipulate Hydrophilic Domains in Silicones*, Springer, **2008**.

[89] L. Simonin, G. Falco, S. Pensec, F. Dalmas, J.-M. Chenal, F. Ganachaud, A. Marcellan, L. Chazeau, L. Bouteiller, *Macromolecules,* **2021**, *54*, 888.

[90] G. E. ; P. LeGrow, In *Silicone Surfactants*, Marcel Dekker, Inc., New York, **1999**, pp. 49–64.

[91] M. Ciaccia, S. Di Stefano, *Org. Biomol. Chem.,* **2014**, *13*, 646.

[92] M. E. Belowich, J. F. Stoddart, *Chem. Soc. Rev.,* **2012**, *41*, 2003.

[93] P. T. Corbett, J. Leclaire, L. Vial, K. R. West, J.-L. Wietor, J. K. M. Sanders, S. Otto, *Chem. Rev.,* **2006**, *106*, 3652.

[94] M. Ciaccia, R. Cacciapaglia, P. Mencarelli, L. Mandolini, S. Di Stefano, *Chem. Sci.,* **2013**, *4*, 2253.

[95] M. Ciaccia, S. Pilati, R. Cacciapaglia, L. Mandolini, S. Di Stefano, *Org. Biomol. Chem.,* **2014**, *12*, 3282.

[96] Y. Jin, C. Yu, R. J. Denman, W. Zhang, *Chem. Soc. Rev.,* **2013**, *42*, 6634.

[97] L. Sun, W. M. Huang, Z. Ding, Y. Zhao, C. C. Wang, H. Purnawali, C. Tang, *Mater. Des.,* **2012**, *33*, 577.

[98] A. Wilson, G. Gasparini, S. Matile, *Chem. Soc. Rev.* **2014**, *43*, 1948.

[99] F. García, M. M. J. Smulders, *J. Polym. Sci. Part Polym. Chem.,* **2016**, *54*, 3551.

[100] L. Leibler, M. Rubinstein, R. H. Colby, *Macromolecules,* **1991**, *24*, 4701.

[101] M. Capelot, M. M. Unterlass, F. Tournilhac, L. Leibler, *ACS Macro Lett.,* **2012**, *1*, 789.

[102] F. Smallenburg, L. Leibler, F. Sciortino, *Phys. Rev. Lett.,* **2013**, *111*, 188002.

[103] B. R. Elling, W. R. Dichtel, *ACS Cent. Sci.,* **2020**, *6*, 1488.

[104] W. Denissen, J. M. Winne, F. E. Du Prez, *Chem. Sci.,* **2016**, *7*, 30.

[105] H. Yuan, G. Liu, *Soft Matter.,* **2020**, *16*, 4087.

[106] S. Zheng, Y. Chen, M. A. Brook, *Polym. Chem.,* **2020**, *11*, 7382.

[107] J. Shi, N. Zhao, D. Yan, J. Song, W. Fu, Z. Li, *J. Mater. Chem., A* **2020**, *8*, 5943.

[108] M. A. Brook, L. Dodge, Y. Chen, F. Gonzaga, H. Amarne, *Chem. Commun.,* **2013**, *49*, 1392.

[109] K. Faiczak, M. A. Brook, A. Feinle, *Macromol. Rapid Commun.,* **2020**, *41*, 2000161.

[110] A. Yepremyan, A. Osamudiamen, M. A. Brook, A. Feinle, *Chem. Commun.,* **2020**, *56*, 13555.

[111] C. L. Lewis, K. Stewart, M. Anthamatten, *Macromolecules,* **2014**, *47*, 729.

[112] I. Yilgor, T. Eynur, S. Bilgin, E. Yilgor, G. L. Wilkes, *Polymer,* **2011**, *52*, 266.

[113] I. Yilgor, T. Eynur, E. Yilgor, G. L. Wilkes, *Polymer,* **2009**, *50*, 4432.

[114] S. H. Cho, S. R. White, P. V. Braun, *Chem. Mater.,* **2012**, *24*, 4209.

[115] Y. Liu, J. Yuan, K. Zhang, K. Guo, L. Yuan, Y. Wu, C. Gao, *Prog. Org. Coat.,* **2020**, *144*, 105661.

[116] M. Tian, H. Zuo, J. Wang, N. Ning, B. Yu, L. Zhang, *Polym. Chem.,* **2020**, *11*, 4047.

[117] A. Fatona, J. Moran-Mirabal, M. A. Brook, *Polym. Chem.,* **2019**, *10*, 219.

[118] J.-F. Xu, L. Chen, X. Zhang, *Chem. Eur. J.,* **2015**, *21*, 11938.

[119] T. Kajita, A. Noro, Y. Matsushita, *Polymer,* **2017**, *128*, 297.

[120] A. M. Stricher, R. G. Rinaldi, C. Barrès, F. Ganachaud, L. Chazeau, *RSC Adv.,* **2015**, *5*, 53713.

[121] C. B. Gale, M. A. Brook, A. L. Skov, *RSC Adv.,* **2020**, *10*, 18477.

[122] R. A. R. Hunta, S. Otto, *Chem. Commun.,* **2011**, *47*, 847.

[123] Y. Jin, Q. Wang, P. Taynton, W. Zhang, *Acc. Chem. Res.,* **2014**, *47*, 1575.

[124] S. Y. Ding, W. Wang, *Chem. Soc. Rev.,* **2013**, *42*, 548.

[125] Y. Liu, X. Liu, R. Warmuth, *Chem. Eur. J.,* **2007**, *13*, 8953.

[126] J.-Y. Zhang, L.-H. Zeng, J. Feng, *Chin. Chem. Lett.,* **2017**, *28*, 168.

[127] W. Zou, J. Dong, Y. Luo, Q. Zhao, T. Xie, *Adv. Mater.,* **2017**, *29*, 1606100.

[128] P. Chakma, D. Konkolewicz, *Angew. Chem. Int. Ed,.* **2019**, *58*, 9682.

[129] E.-K. Bang, M. Lista, G. Sforazzini, N. Sakai, S. Matile, *Chem. Sci.,* **2012**, *3*, 1752.

[130] P. Reutenauer, P. J. Boul, J.-M. Lehn, *Eur. J. Org. Chem.,* **2009**, *2009*, 1691.

[131] Q. Ji, O. Š. Miljanić, *J. Org. Chem.,* **2013**, *78*, 12710.

[132] R. Nishiyabu, Y. Kubo, T. D. James, J. S. Fossey, *Chem. Commun.,* **2011**, *47*, 1124.

[133] A. Chao, D. Zhang, *Macromolecules*, **2019**, *52*, 495.

[134] F. Ch, J. Fb, W. J, R. Pp, *J. Histochem. Cytochem. Off. J. Histochem. Soc.,* **1985**, *33*, 845.

[135] N. H. R. Katharina N. Richter, *EMBO J.,* **2018**, *37*, 139.

[136] S. R. J. A. Jayakrishnan, *Biomaterials,* **1996**, *17*, 471.

[137] L. H. H. Olde Damink, P. J. Dijkstra, M. J. A. Van Luyn, P. B. Van Wachem, P. Nieuwenhuis, J. Feijen, *J. Mater. Sci. Mater. Med.,* **1995**, *6*, 460.

[138] F. Liravi, E. Toyserkani, *Addit. Manuf.,* **2018**, *24*, 232.

[139] L.-Y. Zhou, J. Fu, Y. He, *Adv. Funct. Mater.,* **2020**, *30*, 2000187.

[140] K. V. Wong, A. Hernandez, *ISRN Mech. Eng.,* **2012**, *2012*, 10.

[141] T. D. Ngo, A. Kashani, G. Imbalzano, K. T. Q. Nguyen, D. Hui, *Compos. Part B Eng.,* **2018**, *143*, 172.

[142] R. Bui, M. A. Brook, *Adv. Funct. Mater.,* **2020**, *30*, 2000737.

[143] Y. Tlegenov, G. S. Hong, W. F. Lu, *Robot. Comput.-Integr. Manuf.,* **2018**, *54*, 45.

[144] A. Tursi, *Biofuel Res. J.* **2019**, *6*, 962.

[145] Z. Wang, M. S. Ganewatta, C. Tang, *Prog. Polym. Sci.,* **2020**, *101*, 101197.

[146] D. Carpenter, T. L. Westover, S. Czernik, W. Jablonski, *Green Chem.,* **2014**, *16*, 384.

[147] A. J. J. E. Eerhart, W. J. J. Huijgen, R. J. H. Grisel, J. C. van der Waal, E. de Jong, A. de Sousa Dias, A. P. C. Faaij, M. K. Patel, *RSC Adv.,* **2014**, *4*, 3536.

[148] H. Pan, *Renew. Sustain. Energy Rev.,* **2011**, *15*, 3454.

[149] I. Spiridon, R. N. Darie-Nita, G. E. Hitruc, J. Ludwiczak, I. A. Cianga Spiridon, M. Niculaua, *J. Clean. Prod.,* **2016**, *133*, 235.

[150] W. Y. Chan, T. Bochenski, J. E. Schmidt, B. D. Olsen, *ACS Sustain. Chem. Eng.,* **2017**, *5*, 8568.

[151] H. Chen, L. Yuan, W. Song, Z. Wu, D. Li, *Prog. Polym. Sci.,* **2008**, *33*, 1059.

[152] A. Chao, I. Negulescu, D. Zhang, *Macromolecules,* **2016**, *49*, 6277.

[153] P. Taynton, C. Zhu, S. Loob, R. Shoemaker, J. Pritchard, Y. Jin, W. Zhang, *Polym. Chem.,* **2016**, *7*, 7052.

[154] K. Fukuda, M. Shimoda, M. Sukegawa, T. Nobori, J.-M. Lehn, *Green Chem.,* **2012**, *14*, 2907.

[155] J. Hu, R. Mo, X. Sheng, X. Zhang, *Polym. Chem.,* **2020**, *11*, 2585.

[156] G.-X. Wang, D. Huang, J.-H. Ji, C. Völker, F. R. Wurm, *Adv. Sci.,* **2021**, *8*, 2001121.

[157] W. Abdelmoez, I. Dahab, E. M. Ragab, O. A. Abdelsalam, A. Mustafa, *Polym. Adv. Technol.,* **2021**, *32*, 1981.

[158] R. Ninno Muniz, S. Frizzo Stefenon, W. Gouvêa Buratto, A. Nied, L. H. Meyer, E. C. Finardi, R. Marino Kühl, J. A. Silva de Sá, B. Ramati Pereira da Rocha, *Energies,* **2020**, *13*, 2366.

[159] C. B. Gale, B. Chin, C. Tambe, D. Graiver, M. A. Brook, *ACS Sustain. Chem. Eng.,* **2019**, *7*, 1347.

[160] E. Adler, *Wood Sci. Technol.,* **1977**, *11*, 169.

[161] P. Azadi, O. R. Inderwildi, R. Farnood, D. A. King, *Renew. Sustain. Energy Rev.,* **2013**, *21*, 506.

[162] M. R. Barzegari, A. Alemdar, Y. Zhang, D. Rodrigue, *Polym. Polym. Compos.,* **2013**, *21*, 357.

[163] Y.-L. Chung, J. V. Olsson, R. J. Li, C. W. Frank, R. M. Waymouth, S. L. Billington, E. S. Sattely, *ACS Sustain. Chem. Eng.,* **2013**, *1*, 1231.

[164] W. O. S. Doherty, P. Mousavioun, C. M. Fellows, *Ind. Crops Prod.,* **2011**, *33*, 259.

[165] J. Zhang, E. Fleury, M. A. Brook, *Green Chem.,* **2015**, *17*, 4647.

[166] G.-H. Delmas, B. Benjelloun-Mlayah, Y. L. Bigot, M. Delmas, *J. Appl. Polym. Sci.,* **2013**, *127*, 1863.

[167] A. K. Deepa, P. L. Dhepe, *ACS Catal.,* **2015**, *5*, 365.

[168] J. D. P. Araújo, C. A. Grande, A. E. Rodrigues, *Chem. Eng. Res. Des.,* **2010**, *88*, 1024.

[169] C. Fargues, Á. Mathias, A. Rodrigues, *Ind. Eng. Chem. Res.,* **1996**, *35*, 28.

[170] I. A. Pearl, *J. Am. Chem. Soc.,* **1942**, *64*, 1429.

[171] M. Fache, B. Boutevin, S. Caillol, *Eur. Polym. J.,* **2015**, *68*, 488.

Chapter 2 : Catalyst Free Silicone Sealants That Cure Underwater **

2.1 Abstract

Silicone sealants and adhesives are widely used to prevent the ingress of water. However, silicones must normally be cured in air, as excess water inhibits or prevents cure from occurring. We report that aqueous solutions of the aliphatic aldehydes glutaraldehyde, glyoxal or, particularly, formaldehyde rapidly react without catalysts with a variety of aminopropyl-modified silicone polymers to give silicone elastomers, even underwater. These products, whose properties are readily tailored by controlling the density of amino groups in the starting materials, may be 3D printed, or used both as adhesives and sealants in air or water.

** R. Bui, M. A. Brook, *Adv. Funct. Mater.,* **2020**, *30*, 2000737 - Reproduced with permission from Wiley-VCH. **Contributions** - Bui was responsible for all experimental work and subsequent write up of the work completed in this chapter.

2.2 Introduction

Silicone gels and elastomers are excellent sealants and adhesives because of their low T_g (~ -122 °C),[1] exceptional flexibility at both high and low temperatures, and ability to adapt/adhere to fine features, which leads to enhanced adhesive interactions with interfaces.[2] They adhere particularly well to mineral surfaces (aluminum oxide, silica/silicate, glass), while being essentially unwettable by water. The latter property is due to their low surface energy – which rests between those of hydrocarbons and fluorocarbons[3] – and their very high mobility. Even in the form of elastomers, the effective surface energy of silicones is arguably lower than either hydrocarbons or fluorocarbons because their chain mobility allows them to adapt structurally (e.g., creep) at interfaces.[3-4]

Given their resistance to water (the most water-soluble dimethylsilicone, a cyclic oligomer, D_4 $(Me_2SiO)_4$ has a solubility of only 56 parts per billion), [5] silicone elastomers are widely used in building joints, particularly windows (structural glazing)[6] and also for underwater applications and challenging environments, such as aquaria, pipe seals, water intake pipes, marine paints, etc. While silicones are ideal for underwater applications, silicone elastomers/sealants/adhesives must normally be applied and allowed to cure in air (a process that takes from minutes to days) prior to use as sealants/adhesives underwater; otherwise, sufficient cure and good adhesion to substrates is not observed.

In commerce, traditional silicone curing technologies involve radical cure, moisture cure (hydrolysis/condensation, room temperature vulcanization, RTV), and platinum-catalyzed hydrosilylation.[7] It is not possible to practice any of these processes underwater. In the case of tin-catalyzed RTV, too much water leads to hydrolysis of the crosslinker without cure and, with hydrosilylation, water can successfully complete with alkenes for the Pt/SiH

active catalyst leading to hydrolysis of the SiH groups and inefficient crosslinking. These issues are further complicated by the difficulties of processing insoluble silicones in an aqueous environment.

The Green Chemistry paradigm encourages the avoidance of compounds that may have an undesirable toxicological profile, including heavy metal catalysts.[8] An alternative strategy for crosslinking silicones, without requiring a catalyst, exploits organic chemistry. There is a myriad of applicable organic functional groups that have been used to form organic crosslinks in silicones (azide-alkyne cycloaddition,[9] boronic esters,[10] Diels-Alder,[11] etc.). Amine-functionalized silicones are particularly attractive as starting materials because of their high reactivity, and the commercial availability of polymers with different molecular weights and degrees of functionality. Some examples of organic crosslinks formed from amine-modified silicones include aza-Michael reactions,[12] ureas from reaction with isocyanates,[13] and Schiff-bases through reaction with arylaldehydes (Figure 2.1).[14] In the case of the latter two reactions, the elastomers form in minutes instead of hours, no catalyst is required, and water is the only by-product. However, in these reactions it is essential to moderate the concentration of water during cure; too much water can lead to hydrolysis of the starting material or the resulting crosslinks.

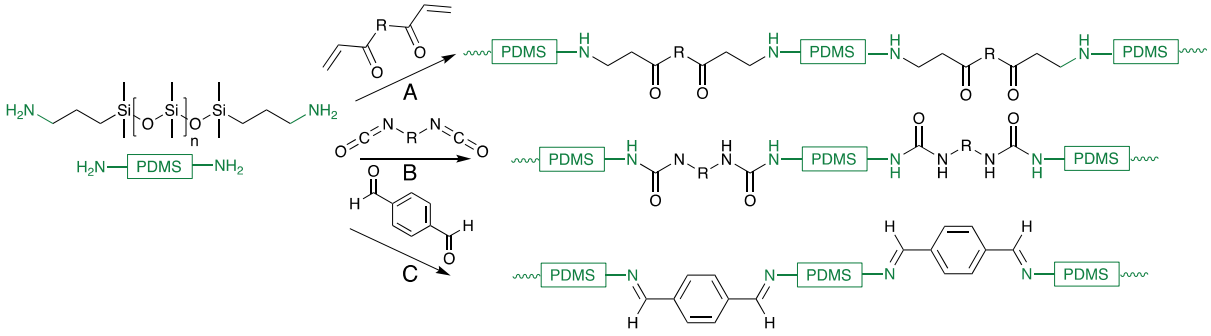

Figure 2.1: Organic-cured silicones based on amine reactions. A: aza-Michael reactions, B: ureas from reaction with isocyanates, and C: Schiff-bases through reaction with arylaldehydes.

The reaction of amines with aliphatic aldehydes or formaldehyde – in water – is extensively utilized in the characterization of biological entities and reaction products.[15] Historically, these processes have been used as fixatives for proteins, including in microscopy imaging, embalming of cadavers, sterilization of biological entities, etc.[16] Reaction begins with the formation of imine bonds, and loss of water as a byproduct. A cascade of reactions then occurs, the details of which depend on the presence or absence of enolizable protons on the aldehyde. In the absence of α-protons, the reaction occurs with a second amine to form an aminal linkage (methylene bridge, Figure 2.2A). Glyoxal, a highly reactive dialdehyde, may also form acetal bridges (Figure 2.2). The reactions of amines with aldehydes that also possess enolizable α-CH groups produce more a complex product mixture. While aminals can also form, amines can act as bases to catalyze aldol reactions with aldehydes or imines (Mannich reaction, Figure 2.2C), among others. Regardless of the specific reactions taking place with either enolizable or non-enolizable aldehydes, the net effect is to tether the organic components bearing aldehyde and amine group to each other if sufficient amines are present.

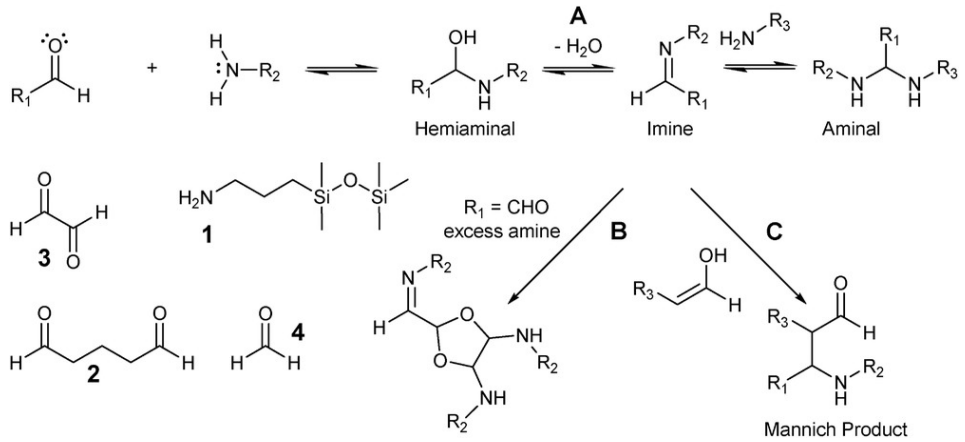

Figure 2.2: Model reactions between model aminoalkylsilicone 1 and A: formaldehyde 4 B: glyoxal 3, or C: glutaraldehyde 2.

We reasoned that it would be possible to make elastomers without the need for catalysts or organic solvents if silicones could rapidly react at an aqueous interface with appropriate functional groups. The ability to use water as a medium would significantly enhance the sustainability of the process. We report the formation of silicone elastomers from three structurally different, commonly used aldehydes dissolved in water: glutaraldehyde, glyoxal, and formaldehyde. The processes are rapid, efficient, and occur rapidly in air and slightly more slowly underwater.

2.3 Experimental

1.1.1 Materials

3-(Aminopropyl)methylsiloxane-dimethylsiloxane copolymers (in all cases, terminated with Me_3Si groups): AMS-132 (2-3% mol aminopropylmethylsiloxane, 4500-6000 g mol^{-1}), AMS-152 (4-5% mol amine 7000-9000 g mol^{-1}), AMS-162 (6-7% mol amine, 4000-5000 g mol^{-1}), AMS-191 (9-11% mol amine, 2000-3000 g mol^{-1}), AMS-1203 (20-25% mol amine, 2000 g mol^{-1}); and telechelic 3-(aminopropyl)-terminated polydimethylsiloxanes: DMS-A11 (850-900 g mol^{-1}), DMS-A12 (900-1000 g mol^{-1}), DMS-A15 (3000 g mol^{-1}), DMS-A21 (5000 g mol^{-1}), DMS-A31 (25000 g mol^{-1}), DMS-A35 (50000 g mol^{-1}); were purchased from Gelest. The formalin solution (37 wt% formaldehyde in water) was purchased from VWR. Glyoxal solution (40 wt% in water) and glutaraldehyde solution (50 wt% in water) were purchased from Sigma-Aldrich. All reagents were used as received.

2.3.1 Methods

Elastomers destined for physical testing were cured in a Teflon dog bone-mold (65 mm x 9.5 mm x 3.5 mm with a 3.5 mm x 15 mm inner central width and length) for tensile tests, or a Pyrex glass 9-well spot plate (22.2 mm x 7 mm wells) or a polypropylene flat-bottom 24-well plate for compression Young's modulus testing; samples cured in wells were 3-

3.5 mm thick. Young's moduli were measured using a MACH-1 micromechanical testing instrument (Biomomentum Instruments) equipped with a 17 N multi-axis load cell and 0.5 mm hemispherical indenter using a Poisson ratio of 0.5 and a constant indentation depth of 1.0 mm with a 1 s dwell time; all measurements were conducted at 22 °C and in triplicate; errors are reported as the standard deviation. Tensile strength experiments were performed on an Instron 5900 series Universal Mechanical Tester (ITW Company) equipped with a 50 N load cell. The bone-shaped elastomers were clamped at the (larger) ends and tested with an Instron. For all experiments, the samples were pre-strained (100%) with a force of 0.002 N, then pulled vertically at a constant rate of 5 mm min^{-1}; tests were done in triplicate with the standard deviation reported as error. A Shore OO durometer (Rex Gauge Company, Inc. U.S.) was used to characterize the hardness of the elastomer. For 2-part mixing applications, 1:1 or 10:1 dual-barrel syringes with a 10 mL large-barrel were equipped with a 74 mm ratio mixing nozzle (16 mixing elements) were purchased from McMaster-Carr. Infrared spectroscopy was conducted using a Thermo Scientific Nicolet 6700 FT-IR spectrometer equipped with a Smart iTX attenuated total reflectance (ATR) attachment. NMR spectra (at 600 Hz for ^{1}H) were obtained using a Bruker Avance 600 spectrometer. Thermal stability was determined using a TGA Q50 thermogravimetric analyzer (TA Instruments) in air. Rheology measurements were conducted on a TA Instruments HR-2 Rheometer with 40 mm parallel plate geometry and Peltier plate set to a 250 μm gap at 25 °C.

2.3.2 Synthesis of Formaldehyde Crosslinked Silicone Elastomers

For-P *(**For**maldehyde-Crosslinked **P**endent-Aminopropylsilicone Elastomers)* were prepared using 3-(aminopropyl)methylsiloxane-dimethylsiloxane copolymers (@ 3, 5, 7, 10 % mol 3-(aminopropyl)methylsiloxane, respectively) at room temperature (Table 2.1).

In a typical preparation, formalin solution (25.0 μL, 37wt% formaldehyde in water, 0.345 mmol H_2CO) was added to a vial containing AMS-152 (0.955 g, 5% mol aminopropylmethylsiloxane 8500 g mol^{-1}, 0.645 mmol NH_2) and stirred until the solution turned homogenous and opaque (~ 3 s). The mixture gelled rapidly (<30 s) into a soft white elastomer. The transparency slowly increased as water physically separated by moving from the interior to the external surface of the elastomer body. The elastomer was allowed to cure for 3 h at room temperature before being placed in a 45 °C vacuum oven at 0.3 torr for 3 h to further dehydrate the sample leaving a clear transparent elastomer. Physical tests on the elastomer were conducted after the latter dehydration step.

Alternatively, **For-T** elastomers were prepared using **t**elechelic 3-(aminopropyl)-terminated polydimethylsiloxanes (@ 900, 3000, 5000, 25000, 50000 g mol^{-1}) with formaldehyde in a 1:1 amine to aldehyde ratio. Longer reaction times were required; gelation occurred between 4 s - 25 min, decreasing as a function of functional group concentration (Table 2.1). For example, formalin solution (25.0 μL, 37wt% formaldehyde in water, 0.345 mmol H_2CO) was added to a vial containing 5000 g mol^{-1} telechelic aminopropylsilicone (0.910 g, 0.364 mmol NH_2) and stirred the mixture until was homogenous (but opaque, ~3 s). This mixture gradually crosslinked and then gelled after ~10 min. Crosslinking was completed after 1.5 h at room temperature giving an opaque, white elastomer. After slowly drying in a 45 °C vacuum oven at 0.3 torr for 12 h the elastomer became transparent.

Cure when using silicones with higher amine concentrations (e.g., telechelic 900 g mol^{-1} or pendent aminopropylmethyl-codimethylsiloxane, 2000 g mol^{-1}, 20-25% mol amine) was extremely rapid, impractically so in some cases. It was found that the addition of isopropanol could extend pot life. For example, formalin (88 μL, 37 wt% formaldehyde in

water, 1.12 mmol) was first combined with 30 μL of isopropanol. This solution was added to a vial containing 900 g mol^{-1} telechelic aminopropyl silicone (0.950 g, 2.23 mmol NH_2) and quickly stirred until homogenous (~ 3 s). Gelation occurred almost instantly after stirring, taking < 2 s. The elastomer was allowed to cure for 24 h at room temperature to allow the isopropanol to evaporate slowly, followed by the dehydration step at 45 °C in a vacuum oven at 0.3 torr for 12 h the elastomer became transparent. Analogous elastomers were made by combining telechelic and pendant aminopropylsilicones with formaldehyde to give **For-TP** (entries **31** & **32**, Table S1).

IR (ATR-IR): *v* = 2962, 2905, 1445, 1411, 1257, 1008, 862, 784, 698, 685, 661, 619, 605, 568, 560 cm^{-1}.

2.3.3 Curing in Bulk Water: General Procedure

The high reactivity of aldehydes with amines can allow for cure to occur even in the presence of excess water. Telechelic- or pendent- aminopropylsilicone oils could be emulsified with up to 50 wt% water and cured by adding aqueous aldehyde solution using the stoichiometry used to prepared elastomers outlined in section (2.2). For example, 3000 g mol^{-1} telechelic 3-aminopropylpolydimethylsiloxane, (4.85 g, 1.62 mmol) was combined with distilled water (5 mL) in a vial and shaken until it emulsified into a cloudy white liquid, 0.5 min. To this mixture, excess formalin solution (0.5 mL, 0.540 g, 6.66 mmol H_2CO) was added and the vial was shaken for 3 s. After <15 s the mixture gelled into a solid white elastomer that filled the shape of the vial. Note: this is distinct from curing “under water”, Figure 5B).

2.3.4 Rheological Measurements

Gelation times for reactions between each aldehyde with two molecular weights of telechelic 3-aminopropylpolydimethylsiloxanes (3000 g mol^{-1} and 50000 g mol^{-1}) were

measured using oscillatory rheology. The rheometer was set to a constant torque of 20.0 μN m and an angular frequency of 10.0 rad s^{-1}. In a typical experiment, 50000 g mol^{-1} telechelic 3-aminopropylpolydimethylsiloxane (1.25 g, 0.025 mmol) was first deposited on the Peltier plate, with a drop of formalin solution (3.70 μL, 37 wt% formaldehyde in water, 0.050 mmol) using an Eppendorf pipette; not allowing the formalin and silicone to mix. The gap between the Peltier plate and parallel plate was decreased from 1000 μm to 250 μm, the silicone and formalin rapidly mixed (<0.5 s), as the experiment began.

These experiments were repeated using the same two samples of telechelic 3-aminopropylpolydimethylsiloxanes but as 50 wt% emulsions with water. For example, 50000 g mol^{-1} telechelic 3-aminopropylpolydimethylsiloxane (0.625 g, 0.0125 mmol) was emulsified with water (0.625 g) in a vial by shaking. The emulsified silicone oil was deposited on the Peltier plate with formalin solution (1.85 μL, 37 wt% formaldehyde in water, 0.025 mmol), without mixing, using an Eppendorf pipette. The gap between the Peltier plate and parallel plate was lowered from 1000 μm to 250 μm and the silicone and formalin were rapidly mixed with a plastic spatula. The gelation point as a function of time was determined as the intercept of the storage (G') and loss (G") moduli.

2.3.5 Double Barrel Syringe Dispensing

A 10:1 or 1:1 double-barreled syringe with a 10 mL large barrel was equipped with a mixing nozzle with 16 mixing elements for convenient dispensing of formaldehyde or glutaraldehyde-crosslinked aminopropylsilicone pre-elastomers. The syringe was loaded with a pendent- or telechelic- aminopropylsilicone in one barrel, and formaldehyde or glutaraldehyde in the opposite barrel. When the components were mixed in an equal volume ratio, it may be necessary to dilute the aqueous aldehyde solution with water to

maintain ideal stoichiometry and prevent premature gelation inside the mixing nozzle. Using a 10:1 mixing syringe, 3000 g mol^{-1} telechelic 3-aminopropylpolydimethylsiloxane (6.78 g, 2.26 mmol) was added into the larger barrel and glutaraldehyde solution (0.8 mL, 0.885 g, 4.48 mmol) was added into the smaller barrel. The curing opaque-red elastomer mixture was extruded continuously from the mixing nozzle and gelled immediately after extrusion.

2.3.6 Crosslinked Silicone Aldehydes as Sealants

To test the abilities of **For-T** and **Glu-T** to act as sealants that can be deployed underwater, five circular voids (1 cm diameter) were made in a 1.5 L polypropylene container. The container was filled with 1.5 L of water, causing a flow-rate of approx. 0.5 L min^{-1}. A 10:1 mixing syringe was used to dispense the pre-sealant mixture of telechelic 3-(aminopropyl)-terminated polydimethylsiloxanes and either formaldehyde or glutaraldehyde. Using formaldehyde as the crosslinker, for example; the larger barrel was loaded with 900 g mol^{-1} telechelic 3-aminopropylpolydimethylsiloxane (6.55 g, 7.70 mmol) and the smaller barrel was loaded with formalin solution (0.756 g, 9.32 mmol H_2CO).The pre-sealant mixture was deployed mid-flow in a circular motion over the voids. It rapidly gelled immediately after dispensing into white-opaque elastomers (1.25 cm diameter) that adhered to the container, preventing further flow of water through the voids.

2.3.7 Crosslinked Silicone Aldehydes as Adhesives

The **For-P** and **Glu-P** elastomers were tested for their ability to act as adhesives by curing 1.5 mL (AMS-191 (9-11% mol aminopropylmethylsiloxane, 2000-3000 g mol^{-1}) with formaldehyde in a 1:1 amine to aldehyde ratio or with glutaraldehyde in a 1:2 amine to aldehyde ratio between two square (1.2 cm x 1.2 cm) dowels made from a variety of materials (methyl methacrylate, glass, polystyrene, and Teflon) to form a tensile butt

joint. The dowels were pulled apart using an Instron at a rate of 5 mm min^{-1} until adhesive failure between the cured elastomer and the substrate. The force applied by the Instron was normalized by the surface area of adhesion.

2.4 Results and Discussion

1.1.1 Spectroscopic Analysis of Aliphatic Aldehyde Crosslinking

Model reactions were undertaken with the model monofunctional silicone 3-aminopropylpentamethyldisiloxane **1** and glutaraldehyde **2**, glyoxal **3**, or formaldehyde **4**, respectively. The reagents were mixed in a small amount of (deutero)chloroform and heated for 2 hours at 60 °C, over a desiccant to help drive any equilibria involving water to the product side.

The products of all three aldehydes with **1** included imines, and water as a byproduct (Figure 2.2, for spectroscopic characterization of the products from these reactions, see Figure S1-S4).[15a, 17] These imines further reacted through condensation reactions that depending on the aldehyde used (Figure 2.2). Glyoxal and glutaraldehyde are dialdehyde crosslinkers that form oligomers through both acetal and aldol formation. The condensation products with glyoxal **3** were complex (yellow – red) mixtures of oligomers containing imines and various alkylamines.[18] The outcomes with glutaraldehyde **2** were yet more complex, due to the possibility of additional reaction outcomes, including the amine-catalyzed aldol autocondensation of glutaraldehyde, and Mannich reactions between imines and enols of glutaraldehyde, as a consequence of the presence of aldol oligomers that form.[19] With this aldehyde, even the reaction with monofunctional amine **1** led to organosoluble polymeric materials. The condensation with formaldehyde **4** first involves the formation of a methylene imine that can react with a second amine to form a

methylene bridge between the amines (Figure 2.2A). Thus, in organic solvents all three aldehydes reacted with silicone-modified amines react in a similar manner to organic amines.

2.4.1 Elastomer Preparation

Although silicones with very high densities of aminopropyl groups may be soluble in water (e.g., amine values[20] over 150), most aminopropylsilicones are only sparingly soluble in water, forming emulsions, including the silicones used here. Surprisingly, in the absence of a desiccator or other means of removing water, mixing was efficient, and reaction rates were extremely rapid in reactions between the neat aminopropylsilicones and aqueous solutions of aldehydes (37-50 wt% water, Figure 2.3A-C). The gelation time was dependent on the concentrations of amine, the aldehyde, and on the constitution of the aldehyde; gel times for glutaraldehyde and glyoxal were 10-15 s and up to 30 s, respectively. By contrast, with formaldehyde as the crosslinker, mixtures could gel in < 2 s. (Elastomer nomenclature: **Glu** (glutaraldehyde), **Gly** (glyoxal), **For** (formaldehyde), **T** (telechelic), **P** (pendant). Thus, **Glu-T** is the elastomer created by crosslinking a telechelic aminopropylsilicones with glutaraldehyde). Curing times were established by following the increase in Young's modulus until no further changes were observed; **Gl**y and **Glu** elastomers required ~3 hours for complete cure, while **For** elastomers only required ~1.5-2 hours in air, depending on crosslink density (Figure S7).

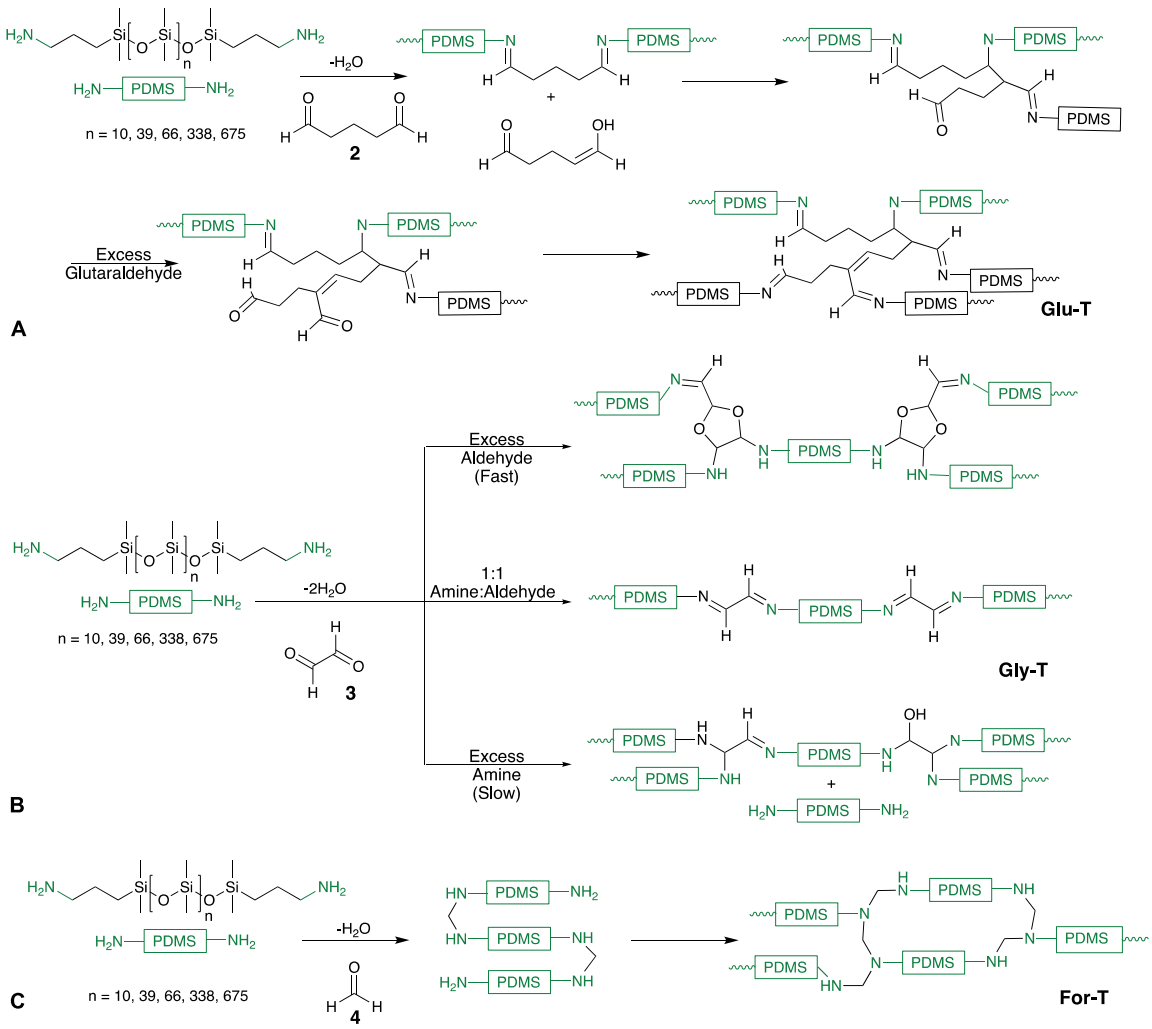

Figure 2.3: Reactions of telechelic aminopropylsilicones with aldehydes A: glutaraldehyde. Glu-T, B: glyoxal Gly-T, and C: formaldehyde For-T. The processes operate in an analogous manner with pendant aminopropylsilicones (Table S 1).

The physical properties of the elastomers were readily controlled by judicious use of the different aldehydes and telechelic and/or pendant aminopropylsilicones (Table S 1).

Libraries of elastomers were prepared from **2-4** and telechelic (MW from 900-50,000 g mol^{-1}) or pendant aminopropylsilicones (MW from 2000-8000 g mol^{-1} and amine densities ranging from 3-25% (((H$_2$N(CH$_2$)$_3$SiMeO)$_a$(Me$_2$SiO)$_b$)$_n$; a/b from 1/50 to 1/4, Table 2.1, Table S 1). Optimal reaction stoichiometries for crosslinking with the different aldehydes,

based on the highest Young's modulus achieved after complete curing and drying, were determined by titration of 3000 g mol^{-1} telechelic-aminopropylsilicones; optimal $[NH_2]$:[CHO] molar ratios were found to be 1:2 for glutaraldehyde, 3:4 for glyoxal and 1:1 for formaldehyde (Figure S 5). The crosslinking density of the resulting elastomers was determined by equilibrium swell test which are consistent with predicted values (Table S 4).[21] The **GLU** and **GLY** elastomers varied in appearance from yellow to red. The initially opaque white formaldehyde-crosslinked elastomers spontaneously lost water to form clear, transparent elastomers (Figure S 6). These elastomers exhibited hydrolytic and thermal stability similar to commercial silicone elastomers (Figure S 10). They were able to withstand boiling water for several hours and exhibited no change in physical properties after heating for several days at 250 °C (Table S 3).

Table 2.1: Preparation of silicone elastomers using formaldehyde (See Table S 1 for **Glu** and **Gly**).

Entry	% mol amino-propyl	M_n [g mol^{-1}][a]	[Amine] [mol L^{-1}]	Shore hardness [OO]	Young's modulus [MPa][b,c], [b,c]	Stress at break [MPa][b,c], [b,c]	Strain at break [%][c]
Telechelic-modified aminopropylsilicones and Formaldehyde (For-T)							
1		900	2.3	75	1.40 ± 0.01	0.32 ± 0.03	105
2		3000	0.653	64	0.880 ± 0.02	0.18 ± 0.01	133
3		5000	0.392	57	0.661 ± 0.002	0.10 ± 0.02	187
4		25 000	0.0784	38	0.0461 ± 0.001	0.088 ± 0.004	205
5		50 000	0.0392	22	0.0205 ± 0.003	0.065 ± 0.002	224
Pendent-modified aminopropylsilicones and Formaldehyde (For-P)							
6	3%	5500	0.258	12	0.0896 ± 0.0004	0.012 ± 0.01	185

Entry	% mol amino-propyl	M_n [g mol^{-1}][a]	[Amine] [mol L^{-1}]	Shore hardness [OO]	Young's modulus [MPa][b,c], [b,c]	Stress at break [MPa][b,c], [b,c]	Strain at break [%][c]
7	5%	8000	0.675	46	0.688 ± 0.001	0.37 ± 0.01	130
8	7%	4000	0.946	57	0.759 ± 0.003	0.42 ± 0.01	115
9	10%	2500	1.35	75	1.26 ± 0.02	0.66 ± 0.01	110
10	25%	2000	3.38	12 (A)	1.73 ± 0.03	0.95 ± 0.01	105

a) Manufacturer's specification, not measured. Since each amine can participate in 1 crosslink, this value constitutes the resulting crosslink density of the elastomer. For crosslink densities measured by swelling, see Table S4,

b) Mean value from triplicate measurements, with the standard deviation reported as error

c) Moduli were determined using compression measurements, while stress and strain at break were determined with dogbones in tensile measurements.

1.1.1Managing Issues of Toxicity

There are legitimate concerns about the toxicity of small aldehydes.[22] If a 1:1 stoichiometry was used [NH_2]:[CHO], the infrared spectra of the formaldehyde-crosslinked elastomers did not show any residual aldehyde groups even after only 1 hour (Figure S 8C), or after boiling in water. If excess aldehyde is used, it could be removed by heating in a vacuum oven. Nevertheless, an additional process was adopted to safeguard the elastomeric materials. Any excess aldehyde groups on the surface of the elastomers were consumed by rinsing/washing the elastomers in an aqueous solution of lysine (IR showed the process to operate on model solutions; and on surfaces of glutaraldehyde-derived elastomers) (Figure S 8). Note: running the crosslinking reactions slightly 'amine rich' avoids the presence of aldehydes in the product elastomers.

2.4.2 Curing in Air versus Under Water

In air, the cure rates of aqueous solutions of all three aldehydes were remarkably fast; gelation times were under 20 s with neat 3000 g mol^{-1} telechelic aminosilicone (Figure 2.4A-C). As expected, gelation times increased as the concentration of functional groups

was decreased by increasing the molecular weight from 3000 to 50000 g mol^{-1} telechelic aminopropylsilicone (Figure 2.4D-F). The gelation time for formaldehyde only increased slightly from 4 to 16s when as the concentration of amines was diluted 16-fold as a consequence of the longer telechelic silicone; the only solvent present in either case was the water in which the formaldehyde was dissolved (Figure 2.4A vs D). Reactions with glyoxal and glutaraldehyde had significantly longer gelation times at the same dilution. This difference in gelation time highlights the high reactivity of formaldehyde for amine groups when compared to glutaraldehyde or glyoxal.

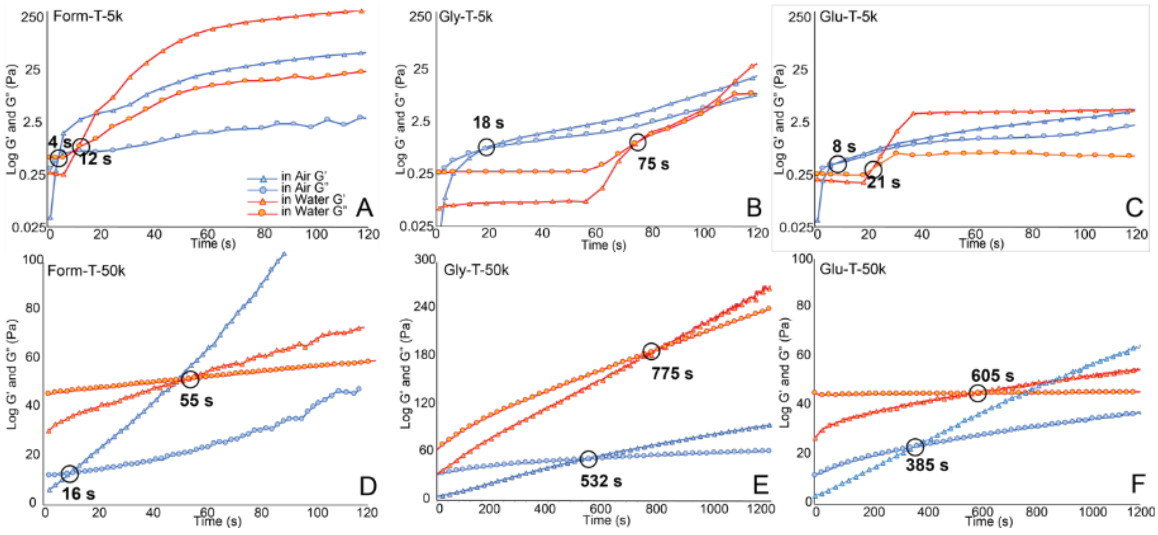

Figure 2.4: Rheometry of cure in air (no added solvent) or in 50/50 wt. silicone-in-water emulsions of 3000 g mol^{-1} telechelic-aminopropylsilicone with A: formaldehyde, B: glyoxal, C: glutaraldehyde, and 50000 g mol^{-1} telechelic-aminopropylsilicone with D: formaldehyde, E: glyoxal, F: glutaraldehyde. The circles identify the G'/G" crossover points. Note: these charts do not reflect complete cure, which can take between 1-3 hours (see Figure S 7).

We examined two other curing protocols: curing in air in the presence of additional water, or curing under water (see below). Additional water was expected to disrupt cure because of problems of miscibility and, since water is eliminated as a byproduct in the first step of the aldehyde reactions, by distorting any equilibria away from products. Oscillatory

rheology was used to probe the sol-to-gel transition during the crosslinking of 50 wt% aqueous dispersions of telechelic-aminopropylsilicone with aqueous solutions of each aldehyde (Figure 4A-C). The intercept of the storage (G') and loss (G") moduli determines the gelation time. A moderately long (3000 g mol^{-1}) telechelic-aminopropylsilicone was selected to ensure slow gel times could be measured rheologically at a convenient time scale (>2.5 s).

The use of additional water in the form of 50/50 dispersions of silicone/(distilled) water, prepared just prior to addition of the aqueous aldehyde solutions in air, did not prevent the crosslinking of aminopropylsilicones with any of three aldehydes but led to a significant increases in gelation time of the material; with a longer telechelic silicone 50000 g mol^{-1}, the gelation time for a glutaraldehyde-crosslinked materials increased from 385 s to 605 s, from 532 to 775 s for glyoxal, and 16 to 55 s for the formaldehyde-crosslinked elastomer (Figure 2.4D-F). Elastomers produced from these emulsions have lower Young's moduli than those cured neat. However, after drying and dehydrating the elastomers they had similar Young's moduli (>85%) to those produced neat (Table S 2). The differences in moduli can be attributed to voids formed in the material by the phase separation of water during cure (Figure S 9).

2.4.3 Syringe Injectable Elastomers

The rapid cure associated with combinations of neat or aqueous dispersions of silicone and formaldehyde, without the need for external stimuli such as heat or light, suggested the pre-elastomers could be practicably dispensed from syringes for various uses, for example, in 3D printing. The fast rate of cure causes a rapid increase in viscosity during mixing of the reagents such that the needs for high viscosity starting materials and/or high-pressure pumps used in traditional extrusion processes are obviated.[23] As a model

system, we loaded a dual-barrel syringe with either 5% mol pendent-aminopropylsilicone and glutaraldehyde, or 3000 g mol^{-1} telechelic aminopropylsilicone with formaldehyde (Figure 2.5A). Simple hand dispensing from the syringe allowed a layer-by-layer deposition of either material (3 x 1 mm layers → 3 mm thick letters, Figure 2.5B). The short gelation times – each extruded layer skinned over within ~15 s – relative to the complete cure times of these materials allowed the deposited material to hold its shape while curing was underway. The lag time between gelation and complete cure allows most of crosslinking to occur after each droplet was deposited, which left a significant concentration of functional groups in the evolving elastomer available to bond to subsequently dispensed material. For the formulations described, it was only necessary to apply subsequent layers within 2.5 h for glutaraldehyde, or 1 h for formaldehyde to avoid delamination between layers (i.e., a new pre-cured layer must be added to the elastomer layer before complete cure has taken place). One consequence of the high reactivity of the aldehydes was undesired gelation and crosslinking in the nozzle during mixing, which should be avoided to prevent a buildup of pressure over long periods of time due to clogging. It was necessary to replace the static mixing tips every few hours or so.

2.4.4 Injectable Sealants Under Water

To test if silicone elastomers could be formed entirely underwater, conditions under which traditional cure technologies are non-viable or too slow to be practical, five x 1 cm diameter holes were drilled into the base of a 1.5 L polypropylene container (Figure 2.5C); when filled, water rapidly (~ 0.5 L min^{-1}) drained through the five holes. While the vessel was filled with water, the formaldehyde/silicone pre-elastomer mixture was extruded under water from the dual barreled syringe, as described in the previous section, adjacent to the openings to create a white gel plug (Figure 2.5B) that quickly (5s) solidified into a ~1.25

cm diameter white elastomer that clogged the holes, preventing flow of water from the container (Note: The silicone and aqueous aldehyde will have a ~1 s mix time before extrusion into water, therefore the gelation times will lie between those of in air and in water conditions). Complete cure under water took ~6 hours but no leakage was observed for 14 days (at which point the experiment was stopped).

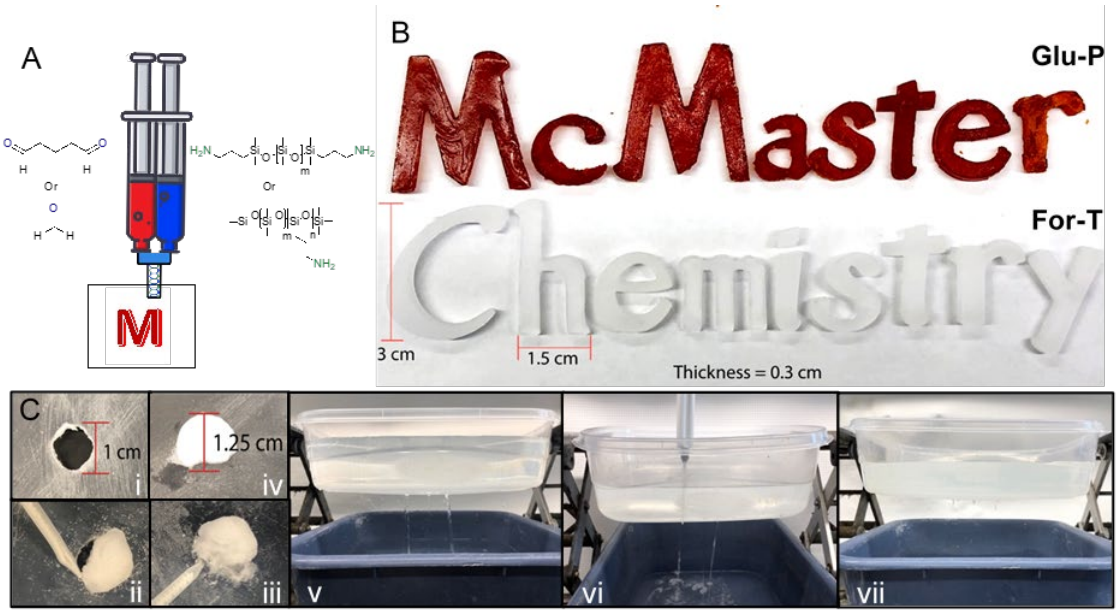

Figure 2.5: A: Two-barreled mixing syringe used to extrude curing mixtures of formaldehyde or glutaraldehyde with aminopropylsilicone. B: Elastomeric structures made by 3D printing by extrusion of glutaraldehyde- ("McMaster") or formaldehyde-based ("Chemistry") elastomers from the mixing syringe (3 passes x 0.1 cm film thickness) C: i) 5 x 1 cm diameter openings cut in polypropylene tub (42 cm w x 29 cm l x 14.5 cm h); ii) Extrusion of formaldehyde-based silicone elastomer during flow of water; iii) complete seal of opening; iv) plugs injected into the holes using the syringe in A (shown after 14 days withholding water) v) water leaking through the 5 holes; vi) injection of sealant under water; vii) no drips from the tub.

1.1.2 Adhesion to Different Materials

Silicone elastomers are frequently used as release coatings because of their mobility and their lower surface energies than other materials.[6] It was initially surprising to us that the adhesion, noted above, to the polypropylene container was so efficient. Amine groups are

commonly added to silicone elastomers to improve adhesive strength for applications in sealants and adhesives.[24] Elastomers derived from both glutaraldehyde and formaldehyde were found to efficiently bind to a variety of surface without modification of the formulations outlined in section 2.2. The adhesion to these surfaces was examined by making tensile butt joints with the elastomer holding two dowels of the substrate material together, then tested with an Instron (Figure 2.6 A,B). All elastomer joints broke adhesively, with only trace amounts of elastomer remaining on the dowels. One would normally expect to measure the strength of adhesion of a given elastomer to different substrates through different stress values. Essentially, no difference was observed in the stresses at break. However, very different strain at break values were observed. Since all four experiments measured the same batch and same type of silicone, these different strain values also represent the degree of adhesion to the substrate. Relatively small differences in the adhesion of the aldehyde/silicones to different substrates were observed, with the performance on more polar materials, such as glass, poly(methyl methacylate), and polystyrene, being better than on the lower surface energy fluoropolymer Teflon® surface. The glutaraldehyde-cured elastomers adhered more strongly than analogous formaldehyde elastomers.

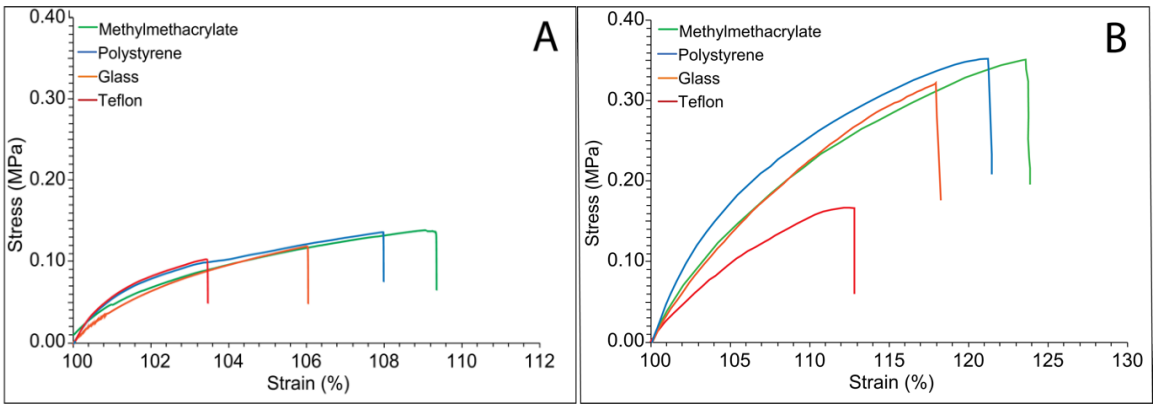

Figure 2.6: Stress-strain curves from elastomers cured using showing higher adhesion to polar substrates. A: **For-PDMS** and B: **Glu-PDMS**. The samples were pre-strained (0.002 N) to 100% prior to initiating the tensile measurements.

The broad utility of silicone elastomers, particularly in humid or wet environments, normally requires silicones to be first cured in air. Silicone elastomers derived from the efficient and rapid reaction of aqueous solutions of small aldehydes with aminoalkylsilicones readily form both in air or under water. The process is green insofar that no catalysts are required, the process is exceptionally mild, and water is the only solvent required. This process allows direct 3D printing without the needs for expensive pumping systems using static mixers, including as underwater sealants.

2.5 Conclusion

Silicone elastomers with controllable physical properties can be rapidly prepared from commercial aminopropylsilicones and aqueous solutions of aliphatic aldehydes; formaldehyde, glyoxal, and glutaraldehyde. The inherent incompatibility between the aqueous aldehyde and hydrophobic silicone is readily overcome by the high reactivity of the aldehydes and amines that allows cure at the oil-water interface. The reactions are tolerant of large quantities of water, including being performed underwater. Excess water slowed the rate of cure but, after drying, all elastomers had comparable physical properties to those cured in air. The rapid rate of cure allowed for convenient extrusion of curing elastomers via 2-part syringe for applications in 3-D printing and as an underwater sealant and adhesives.

2.6 Acknowledgments

We gratefully acknowledge the financial support of the Natural Sciences and Engineering Research Council of Canada.

2.7 References

[1] W. J. Noll, *Chemistry and Technology of Silicones*, Academic Press, New York **1968**.

[2] U. Eduok, O. Faye, J. Szpunar, *Prog. Org. Coat.* **2017**, *111*, 124.

[3] M. J. Owen, in *Siloxane Polymers* (Eds: S. J. Clarson, J. A. Semlyen), Prentice Hall, Englewood Cliffs **1993**, Ch. 7, p. 309.

[4] M. J. Owen, in *Silicon-Based Polymer Science: A Comprehensive Resource* (Eds: J. M. Zeigler, F. W. G. Fearon), American Chemical Society, Washington, D.C. **1990**, Ch. 40, p. 705.

[5] A. Franzen, T. Greene, C. Van Landingham, R. Gentry, *Toxicol. Lett.* **2017**, *279*, 2.

[6] F. de Buyl, *Int. J. Adhes. Adhes.* **2001**, *21*, 411.

[7] M. A. Brook, *Silicon in Organic, Organometallic, and Polymer Chemistry*, Wiley, New York, **2000**.

[8] P. T. Anastas, J. C. Warner, *Green Chemistry Theory and Practice*, Oxford University Press, Oxford **2000**.

[9] T. Rambarran, F. Gonzaga, M. A. Brook, *Macromolecules* **2012**, *45*, 2276.

[10] a) E. Mansuri, L. Zepeda-Velazquez, R. Schmidt, M. A. Brook, C. E. DeWolf, *Langmuir* **2015**, *31*, 9331; b) L. Zepeda-Velazquez, B. Macphail, M. A. Brook, *Polym. Chem.* **2016**, *7*, 4458.

[11] F. J. LaRonde, A. M. Ragheb, M. A. Brook, *Colloid Polym. Sci.* **2003**, *281*, 391.

[12] a) A. Genest, S. Binauld, E. Pouget, F. Ganachaud, E. Fleury, D. Portinha, *Polym. Chem.* **2017**, *8*, 624; b) A. Genest, D. Portinha, E. Fleury, F. Ganachaud, *Prog. Polym. Sci.* **2017**, *72*, 61.

[13] R. B. Bodkhe, S. J. Stafslien, J. Daniels, N. Cilz, A. J. Muelhberg, S. E. M. Thompson, M. E. Callow, J. A. Callow, D. C. Webster,*Prog. Org. Coat.* **2015**, *78*, 369.

[14] R. Bui, M. A. Brook, *Polymer* **2019**, *160*, 282.

[15] a) E. A. Hoffman, B. L. Frey, L. M. Smith, D. T. Auble, *J. Biol. Chem.* **2015**, *290*, 26404; b) B. W. Sutherland, J. Toews, J. Kast, *J. Mass Spectrom.* **2008**, *43*, 699.

[16] D. Hopwood, *Histochemical Journal* **1969**, *1*, 323.

[17] S. Srinivasan, X. Ding, J. Kast, *Methods* **2015**, *89*, 91.

[18] a) E. Avzianova, S. D. Brooks, *Spectrochim. Acta, Part A* **2013**, *101*, 40; b) V. P. Tuguldurova, A. V. Fateev, O. K. Poleshchuk, O. V. Vodyankina, *Phys. Chem. Chem. Phys.* **2019**, *21*, 9326.

[19] a) I. Migneault, C. Dartiguenave, M. J. Bertrand, K. C. Waldron, *BioTechniques* **2004**, *37*, 790; b) S. Margel, A. Rembaum, *Macromolecules* **1980**, *13*, 19; c) L. H. H. Olde Damink, P. J. Dijkstra, M. J. A. Van Luyn, P. B. Van Wachem, P. Nieuwenhuis, J. Feijen, *J. Mater. Sci.: Mater. Med.* **1995**, *6*, 460; d) E. B. Whipple, M. Ruta, *J. Org. Chem.* **1974**, *39*, 1666.

[20] *Encyclopedic Dictionary of Polymers* (Ed: J. W. Gooch), Springer New York, New York, NY **2007**, p. 49.

[21] E. Favre, *Eur. Polym. J.* **1996**, *32*, 1183.

[22] a) A. Ahmed Laskar, H. Younus, *Drug Metab. Rev.* **2019**, *51*, 42; b) R. M. LoPachin, T. Gavin, *Chem. Res. Toxicol.* **2014**, *27*, 1081; c) P. J. O'Brien, A. G. Siraki, N. Shangari, *Crit. Rev. Toxicol.* **2005**, *35*, 609.

[23] S. Zheng, M. Zlatin, P. R. Selvaganapathy, M. A. Brook, *Add. Manuf.* **2018**, *24*, 86.

[24] L. Jiesheng, W. Shaopeng, E. Dong, *J. Appl. Polym. Sci.* **2013**, *128*, 2337.

Chapter 3 : 3D Printing of Highly Reactive Silicones Using Inkjet Type Droplet Ejection and Free Space Droplet Merging and Reaction**

3.1 Abstract

Additive manufacturing and 3D printing technology using thermoplastics and metals have found mainstream use and acceptance. Nevertheless, these methods are not suitable for several industrially important materials, such as silicones and epoxies that are formed by mixing two or more reactive components and chemically inducing crosslinking. The reaction increases the viscosity of the material significantly, which greatly affects the printing process. Here, we develop an inkjet printer that generates droplets of the reactive components simultaneously, merges and mixes them in free space and deposits these curing droplets so that 3D structures can be formed. It uses low viscosity, highly reactive silicone inks that cannot be printed using conventional methods of additive manufacturing and expands the range of 3D printable materials. The method enables stable and uninterrupted printing and allows for multi and rapid start-stop cycles. The high reactivity of the ink used allows printing of high aspect ratio features, as well as structures that do not require supporting scaffolds. The capabilities of the new printer, such as non-contact printing, on-demand printing, and the ability to handle highly reactive materials make it suitable for a wide range of industrial and home use of 3D printing technology for non-thermoplastic polymeric materials.

** M. Sliwiak, R. Bui, M. A. Brook, P. Ravi Selvaganapathy, *Additive Manufactuing,* **2021**, 46, 102099. Reproduced with permission from Elsevier. **Contributions** - Bui was

responsible development of ink formulations. Sliwiak was responsible for design, fabrication, and operation of the printer; as well as the write up of the published chapter.

3.2 Introduction

3D printing technology has had a rapid growth during the last few decades and has enabled customized and rapid fabrication of complex shapes and structures in both the micro and macroscales.[1-9] Most of the methods developed have focused on thermoplastic polymers and metals due to the relative ease in handling these materials in the melt or in powder form. Nevertheless, they exclude a wide range of polymeric materials that are industrially important such as silicones and epoxies that come in two or more reactive components and are polymerized (cured) by initiating chemical reaction through mixing.[10,11] One example of such an industrially relevant polymer is the elastomer polydimethylsiloxane (PDMS), which is used in a wide variety of applications such as medical implants and devices,[12-15] flexible electronics,[16,17] and microfluidics[18] due to its versatile properties, such as biocompatibility, high permeability, stability in a widely range of temperatures, low toxicity and low thermal conductivity.[19]

Although the simplest method for polymerization is by chemically reacting reactive components by mixing, such mechanisms are unsuitable for 3D printing as these would clog the nozzles through which the prepolymers are spatially positioned. Therefore, alternate mechanisms including UV and thermally initiated cross-linking are used so that an independent external trigger to initiate the polymerization process can be used.[20-24] Nonetheless, the use of UV or thermal crosslinking causes additional instrumentation and processing complications. For instance, the distance of the printed layer from the heated print bed has a significant influence on the resolution achieved in the case of thermally cured systems.[25] Alternatively, modifying the ink to be thixotropic by adding wax microparticles[26] or using a scaffolding of thixotropic carbopol gel[27] to hold the extruded

PDMS in its spatial position for curing, have also been investigated. These approaches improve resolution, but are restrictive in the ink composition that can be used or require additional steps to remove the scaffold, which for some shapes can be difficult.

The properties of the ink used directly influence the resolution and finish of fabricated objects. Low viscosity would be ideal as it can provide smoother surface finish of the fabricated object due to the ability of the ink to flow easily. It also enables inkjet printing by which small droplets can be printed, which is widely described in the literature.[30, 32] Unfortunately, the same property causes the ink to spread rapidly once printed, reducing the resolution. The spreading can be minimized by almost instantaneous polymerization when two components are brought together. Such low viscosity highly reactive inks need to be ejected separately and mixed outside the dispensing system, as they could clog nozzles if mixed in-situ. Since they are highly reactive, they need to be mixed in extremely small volumes and deposited onto the substrate before complete polymerization to form well formed monolithic 3D printed structures. One can find a few inkjet printing methods which meet the above conditions. In one method, for example, droplet A is deposited on the top of droplet B,[33] while in the method proposed by[34] one reagent is injected into the bath with the second reagent. Another approach generates droplets in free space that deposit on the same location on the substrate and react with each other as demonstrated with hydrogel materials[28] or simple aqueous solution. Alternatively, droplets of one reactive species can be combined with a jet of the second one, and partially mixed ink can be deposited on the substrate creating a centimeter-scale object.[29]

A universal method that could combine and mix highly-reactive, low-viscosity silicone inks and 3D print them without the use of scaffolds or supporting structures and without the need for any post processing would be ideal for more widespread use of these chemically

reactive silicone polymers in small-scale 3D printing applications. Here, we describe such a method using ink-jet printing, in which the droplets containing individual components of the reactive ink merge in free space to initiate mixing and polymerization. After the deposition of the droplet on to the substrate, the polymerization is completed so that it adheres to the substrate. While we demonstrate this method using a reactive silicone ink composed of telechelic 3-(aminopropyl)polydimethylsiloxane and aqueous solution of glutaraldehyde, it could be applied to a broad range of other reactive materials. This method is versatile, does not require any post processing and can be used to form support free overhanging structures easily due to the fast reaction time of the ink.

3.3 Experimental

3.3.1 Design of 3D printer

The newly developed 3D inkjet printer, illustrated in Figure 3.1a consists of five main sub-assemblies, namely a printhead, 3D positioner, electronic control system for dispensers, chambers for the material, and, finally, a vacuum pressure system. The most critical part of our printer is the printhead, which is designed to eject two nanoliter droplets such that they collide with each other in free space, coalesce and mix initiating the polymerization reaction. The printhead (Figure 3.1b) consists of two piezoelectric dispensing devices (MJ-AB-80, MicroFab) that are positioned at a precise angle with each other and is firmly attached to the printhead to prevent any relative motion when the printer is in operation. The distance between the nozzle tips was optimized to 4 mm which was the minimum to prevent accidental accumulation of droplets at either tip and for clog free operation. The angle between the droplet dispensers was also optimized to be 60°, which ensured that the droplet coalesce rather than bounce off each other. The distance between the nozzle

tip and the point at which the two reactive droplets meet and merge was also optimized to 3.5 mm in order to minimize the effect of environmental parameters such as air movement around the printhead while it was in motion.

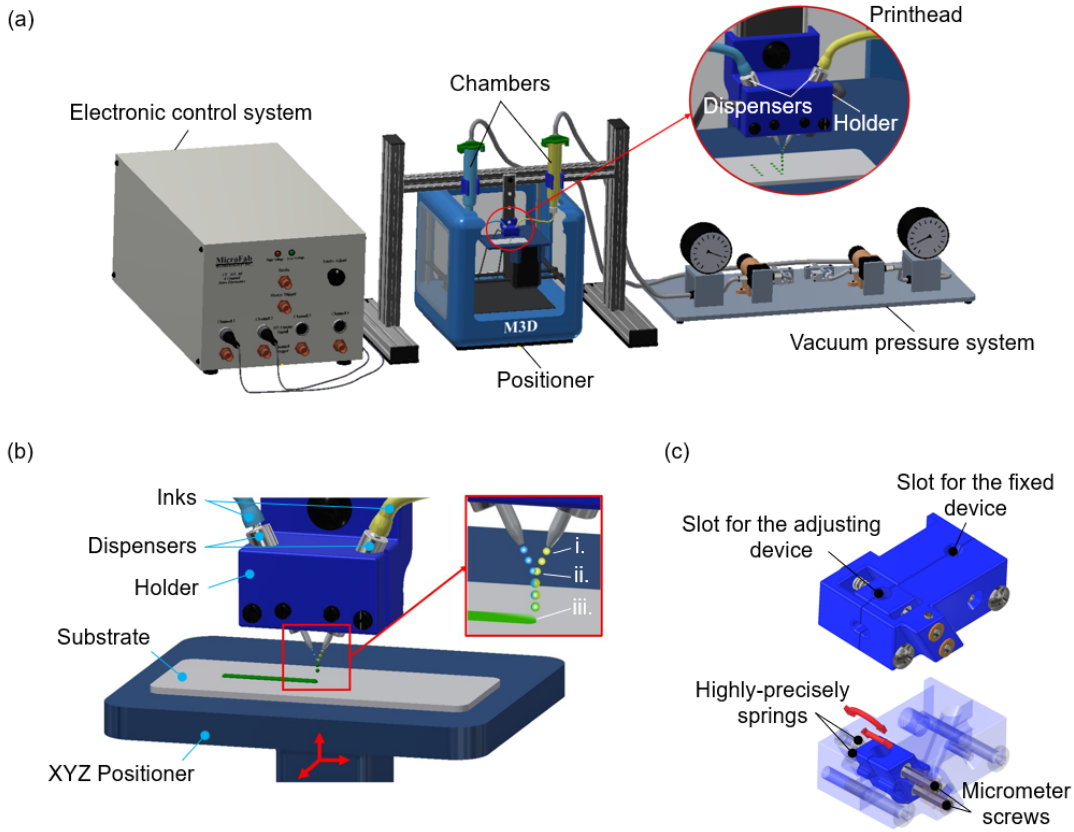

Figure 3.1: a) 3D inkjet printer with integrated a free space droplet mixing module. **b)** Schematic illustration of the inkjet 3D printer with an integrated free space droplet mixing module, where (i) two reactive droplets are ejected independently and simultaneously, (ii) droplets merge due to the intersection of their trajectories and mix supported by inertial effects in free space outside the nozzles, and (iii) the coalescent drop is deposited in patterned format on a moving substrate. **c)** Holder designed for the dispensing devices enables droplets mixing in free space (top), and the regulation spring-screw mechanism (bottom)**.**

To enable the collision of droplets in free space, both their trajectory and velocity must be precisely regulated. The position of inkjet nozzles can be controlled by a specialized holder mechanism that allows precise positioning of the nozzles with respect to each other to eliminate the influence of small variations in printing parameters and environmental factors

and to maintain trajectories of the droplets in the same plane (Figure 3.1c). In this holder, one dispensing device (nozzle) is fixed, while the second one has two degrees of freedom, which enables the control of its position rectilinearly in the plane parallel to the plane of the dispenser and to rotate it by up to two degrees in that plane (indicated by red arrows in Figure 3.1c). This manual adjusting mechanism consisted of two micrometer screws at the front and two high-precision springs at the rear and enabled robust and precise droplet contact and coalescence within a few minutes. The velocity of the dispensed droplets is controlled by electrical impulses, which are generated by an electronic control system and applied to the piezoelectric actuators in the dispensing devices. The vacuum system generates a negative pressure which is applied to the ink chambers to prevent free flow of the ink through the piezoelectric nozzle when it is not ejecting ink.

3.3.2 Materials

Telechelic 3-(aminopropyl)-terminated polydimethylsiloxanes, DMS-A11 (900 g mol^{-1}) was obtained from Gelest. The glutaraldehyde solution (5.6 M) was obtained from Sigma-Aldrich and diluted to 5.0 M using isopropanol (Caledon Laboratories Ltd).

Properties of PDMS inks: The viscosity of the inks were measured using a a StressTech HR high-resolution oscillatory rheometer equipped with a cone-plate attachment. The surface tension was determined using the pendent water drop method. Both commercial components, telechelic 3-(aminopropyl)polydimethylsiloxane (DMS-A11) and aqueous solution of glutaraldehyde (5.6 M), could be used undiluted, but better control was realized when the glutaraldehyde was slightly diluted with isopropanol. Their properties are following: density 935 [kg/m^3] and 1198 [kg/m^3], viscosity 17.86 [mPa s] and 17.42 [mPa s], surface tension 41.55 [mN/m] and 65.32 [mN/m], pH 10.5 and 4 for DMS-A11 and 50% wt. Glu, respectively.

DMS-A11: IR (ATR-IR): v = 2962, 2905, 1411, 1257, 1010, 862, 784, 698, 685, 617, 605, 572, 565 cm^{-1};

^1H NMR (600 MHz, CDCl3) δ 0.050 (s, 15H, Si-CH3), 0.50 (t, 2H, SiCH2, *J* = 8.64 Hz), 1.43 (p, 2H, CH2, J = 8.10 Hz), 2.65 (t, 2H, CH2, *J* = 7.12 Hz).

Glutaraldehyde: IR (ATR-IR): v = 3430, 2925, 1715, 1465, 1445, 1201, 1112, 875, 685.

^1H NMR (600 MHz, CDCl3) δ 9.57 (s, 2H, CHO), 1.45-1.85 (m, 6H, $(CH_2)_3$).

3.3.3 Method

The operation of the printer is shown in Figure 3.1b. The droplets of two highly reactive components are ejected simultaneously using two independent piezoelectric dispensing devices (ID = 80 μm) that are inclined towards each other (Figure 3.1b i.). When ejected with suitable velocities the trajectories of the droplets lay on the same plane and intersect with each other due to which the droplets collide and merge in free space during travel between the dispensing devices and the substrate (Figure 3.1b ii.). By matching the momentum of the two droplets they can be made to coalesce and significantly reduce the horizontal component of momentum of the merged droplet. Subsequently, the merged drop falls vertically down from the point of collision onto the substrate and is deposited in the patterned format (Figure 3.1b iii.) due to the movement of the substrate underneath.

Due to the sensitivity of the dispensing system and free space merging, the printhead is held immobile during the printing process, while the substrate attached to the XYZ

positioner moves in all three directions. Therefore, the shape and precision of a fabricated object is completely dependent on the movement of the positioner.

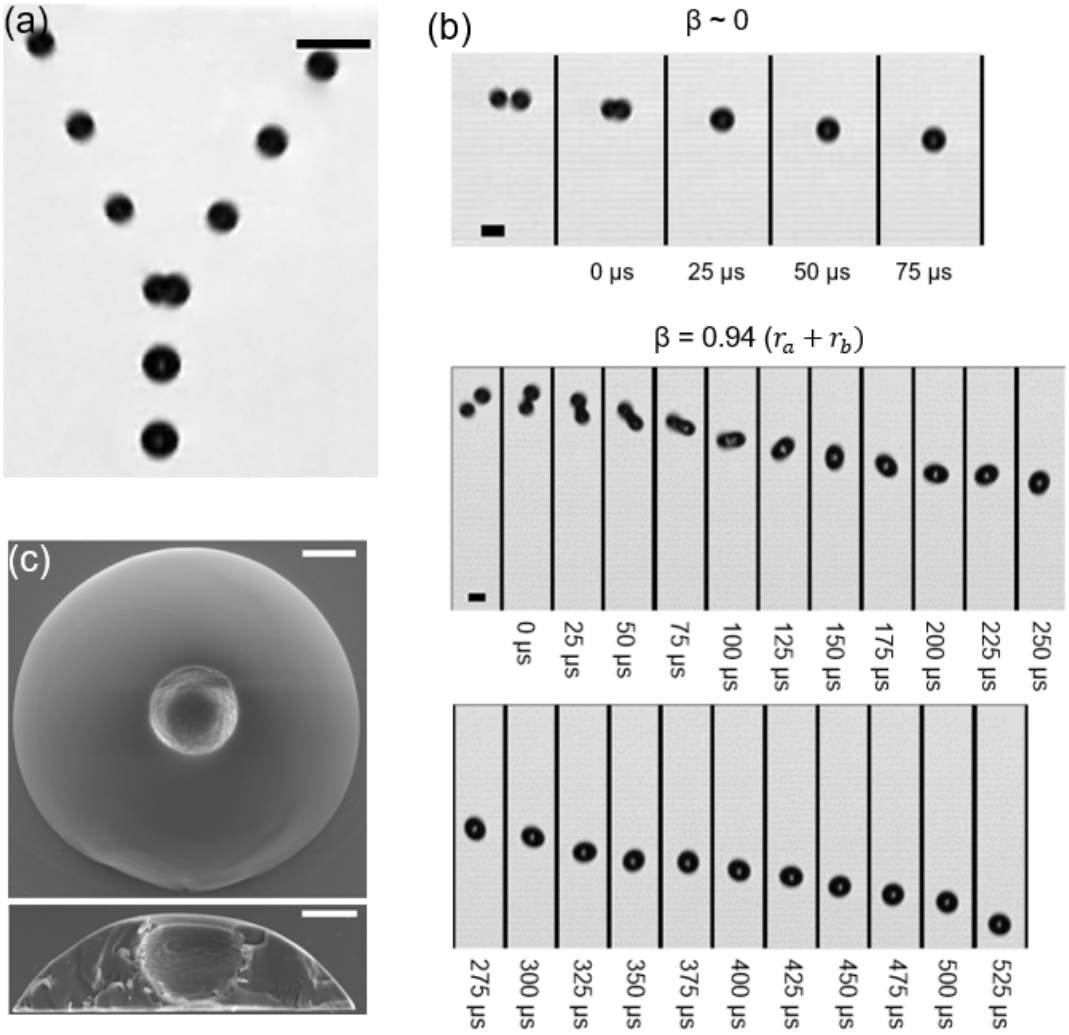

Figure 3.2:**a)** Collision and coalescence of droplets made of glutaraldehyde solution (left) and DMS-A11 (right) in free space (scale bar = 100 µm). **b)** Characterization of the method depending on the β parameter (scale bar = 50 µm). **c)** Top side and cross-section of a PDMS drop. The two pictures correspond to two different droplets (scale bar = 20 µm).

3.3.4 Printable Liquids

A fast reacting two-part ink, consisting of an amine-functionalized silicone base and glutaraldehyde crosslinking agent, was chosen for its rapid reaction time and suitability for inkjet printing [31]. In this system, cure is initiated simply on contact of the reagents (Figure

S 15). Rapid condensation of glutaraldehyde with an amine to form imine bonds leads to a rapid increase in viscosity, and then gelation. Additional, slower curing processes occur through aldol and Mannich condensations. The slower secondary reactions create a lag time between gelation and ultimate cure of the material. During this lag time, subsequently deposited material can cure homogenously with the existing substrate, that is, lead to adhesion between deposited droplets themselves and the underlying substrate.

The silicone base is a 900 g mol^{-1} telechelic dimethylsiloxane polymer terminated at each end with 3-aminopropyl groups. This compound was eventually selected from a library of telechelic and pendent aminosilicone polymers for all printing experiments because of its low viscosity and moderate reactivity ([aminopropyl] = 2.3 M) relative to pendent-modified analogues. The amine concentration was sufficient to initiate cure, but the lower reactivity of the ink allowed for a sufficient lag time between gelation and final cure. The low viscosity of the silicone is essential for stable ejection of droplets from the printing nozzle. The crosslinking agent contained an aqueous glutaraldehyde solution (5.6 M) diluted to 5 M with isopropanol, giving a 2.1/1 ratio of [glutaraldehyde]/[amine].

The glutaraldehyde-aminosilicone cure system requires a 1:1 ratio of amine to aldehyde to produce an elastomeric material. To provide some guidance about rates of reaction, simple mixing (e.g., static mixing head on a double barrel syringe) is not possible because gelation occurs within ~ 8 seconds, within the mixer, with full cure taking about 45s. The rate of cure can be further accelerated by increasing the concentration of glutaraldehyde. Using an excess of glutaraldehyde results in autocondensation of aldehyde groups to form polyglutaraldehyde groups. This feature is attractive for use in 3-D printing because the rate of reaction can be increased without producing, or leaving residual, unreactive materials in the deposited material droplet.

3.4 Results and Discussion

3.4.1 Analysis of Ejected and Positioned Droplets

The dynamics of printing process was observed by high speed imaging (Figure 3.2a) of the droplet movement and its coalescence. The piezoelectric dispensers containing the glutaraldehyde crosslinker (left) and the silicone base (right) were triggered by periodic pulses to produce droplets with near identical diameter (32 μm and 42 μm, respectively) and velocity (1.07 m/s and 0.93 m/s, respectively) in order to neutralize any resulting horizontal momentum in the merged droplet and to increase the robustness of the coalescence process. We noted that the robustness of the coalescence can be estimated by a simple measure of the distance between the center of mass of the droplet (β) when they are closest to each other. The droplets miss each other when $\beta > r_a + r_b$, which are the radius of the droplets. When $\beta < r_a + r_b < 0$, they make contact and some of the linear momentum of the droplets is converted into angular momentum (Figure 3.2b) rotating the droplets about their central axis of connection, which may result in the droplets not coalescing with each other. The larger the β, greater the momentum coupled to rotating the droplets. When $\beta \sim 0$, the collision is ideal and lost momentum in the horizontal direction is completely utilized in droplet coalescence and mixing. In this condition, the droplets mix well with each other and only have momentum in the vertical (downward) direction. The mixing initiates and accelerate the crosslinking reaction which proceeds to partially cure the droplet before it hits the substrate. Due to the fast reaction times, the shape of the droplet is retained upon deposition as shown in Figure 3.2c. One of the reactants (glutaraldehyde ink) contains water and so does the byproduct of the crosslinking reaction. This leads to formation of a small dimple in the deposited droplet due to phase seperation of water from the polymerized PDMS in the deposited structure.

Although the droplet streams ejecting from the printheads are captured here by high speed camera, they are quite visible to the naked eye (although not as individual droplets) and the condition when the droplet coalesce and form a single stream is quite distinct and can be clearly identified.

The appropriate mixing of both reactive components is crucial to provide a homogenous structure. In the generation process, the ejected droplets have a relatively large velocity, whose horizontal component is reduced at the moment of their collision. Therefore, the horizontal component of the net momentum could initiate the mixing of the droplets. Subsequently, the impact of the combined drop onto a substrate results in a dissipation of momentum that also supports the mixing. Finally, after the deposition, the diffusion of molecules further enhances the homogenization of the reactants in the combined drop. The image of a typical mixed and deposited droplet shown in Figure 3.2c demonstrates a uniform structure of a drop of PDMS. The material is deposited on a glass surface with a hydrophobic nanocoating (the substrate was dipped in a Drywired Textile Shield liquid) so as to preserve the shape of the deposited form. Its contact diameter (123 μm) determines the resolution of the method.

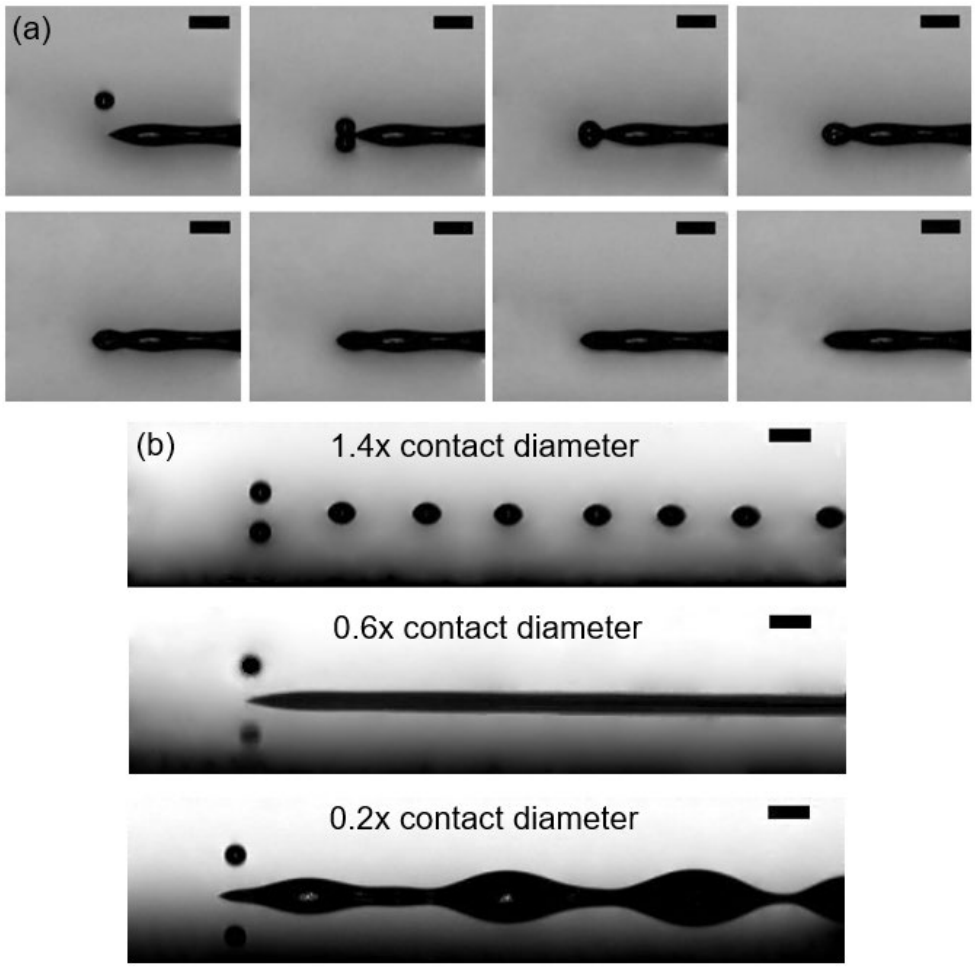

Figure 3.3: a) Formation of a continuous line. The consecutive snapshots were taken every 0.1ms (scale bar = 100 μm.) b) Printed line with different spacing between the deposited droplets on the glass surface. Deposition spacing of 167 μm which equals to 1.4 of contact diameter of the droplet (top). Deposition spacing of 73 μm (0.6 of contact diameter) (middle), Deposition spacing of 28 μm (0.2 of contact diameter) (bottom) (scale bar = 100 μm).

The reactive inks are designed to instantaneously start the polymerization reaction upon contact with each other. Nevertheless, the reaction time constant should be designed in such a way that the drop of PDMS remains in at least a semi-solid state until deposition to ensure appropriate adhesion to the previously deposited material and to produce smooth features. By adjusting the deposition parameters various 1D and 2D strucutures can be obtained.The shape and structure of a printed line is dependent on the surface

energy of the substrate, time and distance between consecutive droplets landing. When a hydrophobic surface is used, its low surface energy confines the deposited droplet and does not allow spreading. In this case, however, the shape of the printed pattern can be affected by the hydrodynamic instability. The coalescence of droplets on the substrate is presented in Figure 3.3a, in which mixed PDMS droplet with 47 μm of diameter (the contact diamerter is larger) is deposted within the distance of 47 μm from the previous one. One can observe that at the beginning, thanks to the slow capilary spreading, the droplet achieved a spherical shape on the substrate with the small necking connection with the previously printed line. Because on the line side the curvature of the liquid-air interface is smaller than on the side away of it, the Laplace pressure gradient occuring between both the sides pushes the liquid towards the line until the equilibrium state is achieved or polymerization prevents the movements.[32] The efect of droplets spacing on the line pattern in ilustrated in Figure 3.3b. The position on the substrate where the droplets are deposited can be controlled by fixing the droplet size (123 μm) and the ejection (deposition) frequency (50Hz) while varying the speed with which the print substrate is moved (feed rate) relative to the printhead between 500 mm/min and 80 mm/min. When the deposition spacing is much larger than the diameter of the deposited droplets, they are printed as hemispherical deposits on the substrates as shown in Figure 3.3b top. When the spacing is reduced to be slightly below that of the contact diameter, the droplets merge with each other forming a contiguous, smooth and uniform line and this condition represents the optimal print condition to obtain reproducible structures (Figure 3.**3b** middle). Interestingly, when the spacing is reduced to far below the contact diameter of the droplet, a periodic structure with a wavy pattern ensues (Figure 3.3b bottom) due to bulging instability[32] caused by competing flow paths when the impacting

droplets meets the leading edge of the previously drawn line. The flow physics of the formation of these lines are similar to inkjet printing despite the rapid polymerization occurring within these drops.

3.4.2 Fabricated Objects

This printing method also allows fabrication of complex 3D structures by additive manufacturing approaches where the shape is built by moving the printhead along a path that will fill the shape completely. An example of 3D printing is shown in Figure 3.4a where a thin wall was printed vertically without using any support materials. It consisted of 1560 layers and features the height 17 mm ±0.5 mm, width 9.5 mm ±0.2 mm and thickness 330 μm ±20 μm. The aspect ratio (AR) of this printed 3D structure was larger than 50 and was only limited by the vibration of the structure (due to its compliance) in response relative movement between the printhead and the substrate. The total printing time was about 40 minutes, which can be reduced by simultaneously increasing the frequency of the droplet generation and the feed rate of the positioner. The cross section of the wall (Figure 3.4a) cut off horizontally exhibits a slight wavy pattern due to vibrations introduced during the printing process.

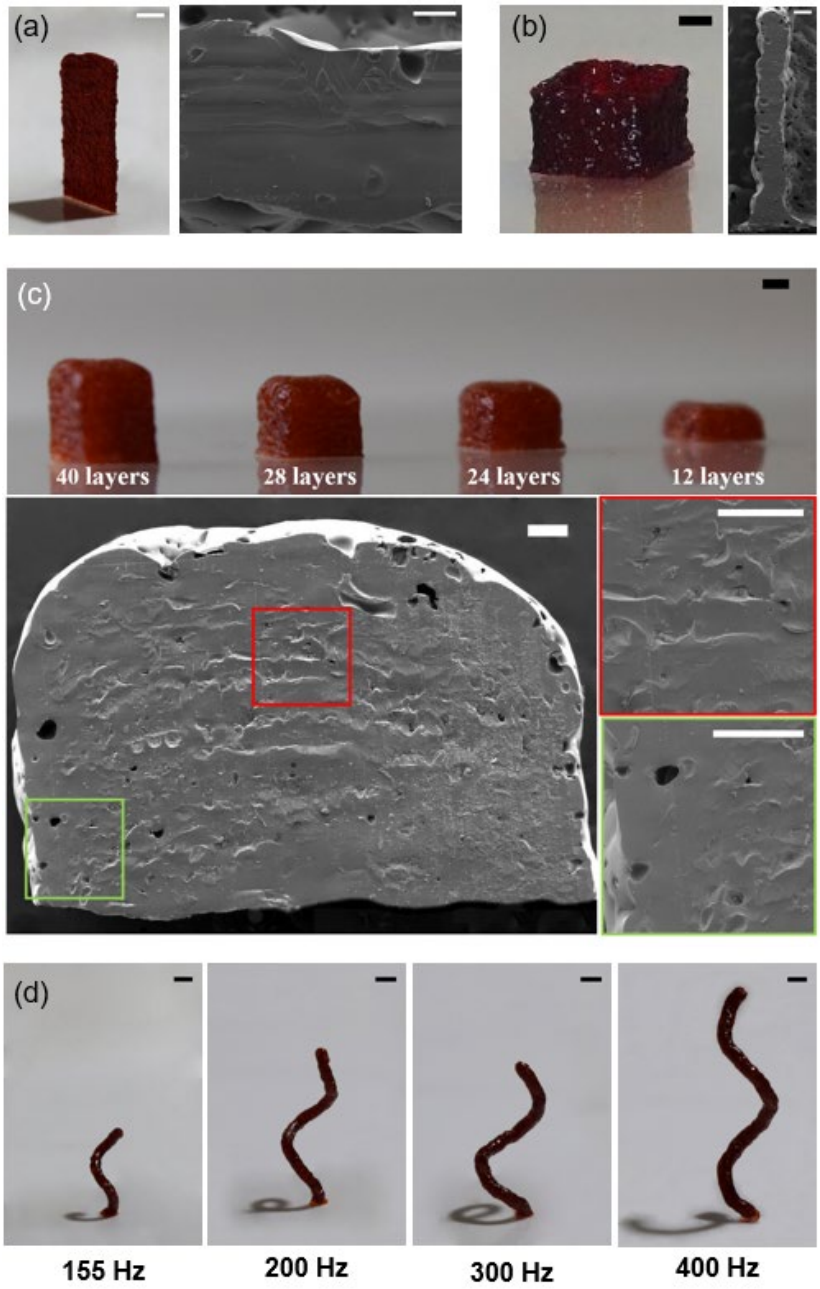

Figure 3.4: Printable shapes of PDMS. **a)** Image of high aspect ratio wall (~330 µm thick) consisting of 1560 layers (scale bar = 5 mm) (a, left), SEM image of a horizontal cross section of the wall (scale bar = 100 µm) (a, right). **b)** A frame (~290 µm thick) consisting of 200 layers (scale bar = 1 mm) (b, left). A vertical cross section of the frame (scale bar = 200 µm) (b, right). **c)** Cuboids with different heights (scale bar = 1 mm) (c, top). Cross section of the filled box with distinguished variable size of pores in different locations (scale bar = 200 µm) (c, bottom). **d)** Coil springs printed with different frequencies without a support material (scale bar = 2 mm).

Interestingly, cavities due to accumulation of water as the structure is printed are sparse and tend to appear on the surface rather than in the bulk indicating that it evaporates before the next layer is printed. Despite of the large AR, the thickness of the wall was quite uniform throughout its entire height. It suggests that the ejection frequency (50 Hz) was low enough to enable the polymerization and provide a stable base for the deposition of the subsequent layer of droplets. A similar characteristic was observed when a box was printed as shown in Figure 3.4b. The print consisted of 200 layers which was printed within 7 minutes. It produced a frame that was 4.14 x 4.0 x 2.43 mm in dimension along the X, Y and Z directions, respectively, with a dimensional error of 0.9%, 1.1%, and 2.8% along these axes. The cross-sectional section of the frame cut vertically as shown in Figure 3.4b indicates that its thickness is equal to 290 μm ±20 μm and it is very uniform in thickness throughout its entire height. These findings demonstrate that the printing process is robust for producing tall and uniform high aspect ratio 3D structures with smooth sidewalls.

Not only can frames be printed, but filled shapes such as a cube or a cuboid can also be 3D printed using the appropriate tool path as show in Figure 3.4c, where a series of cuboids with identical base dimensions 2.94 mm x 2.84 mm and different heights were printed. A cross-section of one of the printed cuboids shows that although the PDMS material is mixed homogeneously, the structure exhibits several cavities in the bulk that were unevenly distributed throughout the entire volume. The cavities located at the center have smaller sizes (Figure 3.4c red box) compared to those occuring close to the edge (green box). This cavity size distribution can be attributed to the migration and accumulation of water generated in the printing process to the surfaces where they are pooled and eventually evaporate. Moreover, it is expected the bulk will polymerize more

rapidly that the surface regions due to exposure to the atmosphere and hence the heterogeneity in the distribution of the cavities.

The simultaneous delivery, appropriate mixing of both components in free space, and short reaction times cause the fast polymerization of the deposited droplets on a substrate, allows this method to produce nearly free standing structures that are tenuously connected to the underlying printed feature. In order to demonstrate this feature of the printing method, a spiral microcoil shape (Figure 3.4d) was printed where each drop that is printed only partially overlaps to the underlying structure that was printed just before. Using this approach almost any free-standing structure can be printed without support materials. To ensure the structure is self-supporting, the minimum printing angle should be larger than 5 degrees, and in the case of a large-scale object, the support structure can be printed using the same material. In this printing process, the printhead was placed off center to a substrate rotated with the constant speed of 0.5 RPM, while its vertical position was changed step wise. The gap between the substrate and the printhead was changed by 1 mm after different time gaps: 28s, 25s, 20s, and 15s, respectively, in order to produce free standing microcoils as shown in Figure 3.4d. Due to the fast reaction rate the droplet solidifies immediately after impact and the structure to be formed grows from the substrate without the need for supports. The step change in the gap with time can dynamically change the pitch of the helical spring structure formed. Similarly, the ejection frequency of the droplet can determine the diameter of the winding coil wire generated with frequencies of 155 Hz, 200 Hz, 300 Hz, and 400 Hz producing wire diameters of 1.05 mm, 1.10 mm, 1.27 mm, and 1.43 mm, respectively. The length of the micro coil spring depends on both the capability of the printer to reduce vibration and the printing time, whereas the spring diameter can be set by changing the offset distance between the droplet point of collision

and the center of the rotating substrate. The compliance of the fabricated elastic coil spring subjected to compressive forces. Since the print material is elastomeric, the printed spring is elastically compressed upon application of the external vertical force and restores back to its original shape when the force is removed.

3.4.3 Stability of the Printing

Even though the process of droplet generation, free space merging and deposition may seem rather fragile, it is a surprisingly robust and stable process. To demonstrate its robustness, long term printing over several hours was performed. Parameters such as the velocity and diameter of the ejected reactant droplets, as well as the merged PDMS droplets, were measured every 5 minutes over one hour (Figure S 11). Once the nozzles were aligned and the conditions for the ejected droplet to merge was set, the process was very stable over the duration of time tested. The diameters and the velocities of all the droplets remained unchanged, which demonstrates the robust nature of the droplet generation and merging process, even when highly reactive materials are used. We also experimentally studied the influence of a nearby electrostatically charged surfaces such as a dielectric charged substrate on the droplet generation and merging process (Figure S 12). Polarizable droplets in free space can be influenced by electrostatic charges and electric fields and nearby charges on the substrate did have a significant effect on the velocity and trajectory of the reactant droplets containing water. This changed its trajectory and prevented effective merging. This issue can be mitigated by using a conducting substrate or neutralizing the effect of electrostatic charges by using a ground electrode underneath the printing substrate. We also show that this printing method does not require a close spacing between the printhead and the printbed. Therefore, printing can be performed on non-planar topographically defined substrate as well as non-planar surface

(Figure S 13). Finally, to demonstrate on demand printing, we performed multiple start and stop cycles for the printhead and show that after a brief unstable period (~ 94 msec and <300 pL of material loss), the droplet generation and merging process automatically stabilizes without need for any adjustment of the nozzle angles, position or the droplet generation voltages or pulse duration (Figure S 14). The instability time should be considered when 1D objects, such as dots, or high-precision 2D featurs, such as lines, are fabricated. In such cases, the injections should be turned on earlier to print the desired object when the steady state is achieved. However, printing of larger 3D structures does not require such treatments because the imprecisely deposited droplets during the unstable period do not affect the overall structure. All these findings demonstrate that the process is very robust and suitable for commercial applications.

Imaging and visualization: The ejection and collision phenomena were observed using a high-speed camera, Fastcam AS4 assembled with Monozoom-7 lens. The recording parameters were set to register every droplet in at least five snapshots. Therefore, the pictures were taken with the frame rate 10,000 fps and resolution 320 x 240 pix. However, the lens allows one to magnify the drops with the resolution of 4 μm/pix. The pictures were further analyzed using MATLAB software, which computed the diameter of drops and determined the locations of their centers, which was needed to calculate velocities. Because the pictures were not uniformly illuminated, the accuracy of the measurement could vary by +/- 4 μmin different places of the image.

In the analysis of samples, Scanning Electron Microscopy (TESCAN VP SEM) and a digital microscope camera (MicroDirect 1080p HDMI Handheld Digital Microscope, Calestron) with the maximal magnification 220 x were used.

Fabrication and assembly of the printhead

The four-part main body of the printhead was fabricated from VisiJet EX200 material using an Ultra High Definition 3DSystems ProJet HD3000 printer with the printing accuracy of 0.025-0.05 mm. The corpus parts were assembled together using screws, while the inner parts were positioned by tabs moved along the rails in the corpus, as well as by the precision screws and springs. Therefore, the assembly and disassembly of the printhead was effortless, which was advantageous in cleaning and mounting of dispensers.

Data processing and statistical analysis:

The MATLAB software was used to measure the diameter and compute the velocity of droplets. From at least five measurements for each droplet, the final value of each quantity was calculated based on the arithmetic average, supplemented with the corresponding standard deviation. To measure all relevant dimensions of printed structures, the ImageJ software was utilized. All dimensions were measured at least three times, while the number of measurement spots depended on the scale of the object. Again, the final value was determined based on the arithmetic average.

3.5 Conclusion

In summary, the newly developed 3D inkjet printing method allows the fabrication of complex shapes made of low viscosity and highly chemically-reactive components of PDMS consisting of the crosslinker and silicone base. Both droplets of two components are ejected simultaneously and mixed in free space outside the nozzle, which eliminates the clogging of the dispensing devices. Despite the complex integration of the free space mixing module with the traditional non-contact inkjet printer, the system works on demand and enables stable and continuous operation over several hours. Appropriate mixing of

the content of the droplets is essential to uniformly blend the combined drop and, consequently, to enable the formation of homogenous structures. Moreover, due to the possibility of depositing reactive materials in a form of a single drop, the printing of any programable shapes in high resolution is possible. For example, high aspect ratio structures can be fabricated with a remarkably small thickness without using support materials. In addition, the resolution might be improved by using a dispenser with a smaller diameter orifice. The new 3D printer is capable of printing in free space, which distinguishes it from all other well-known AM techniques. Due to the lack of precise knowledge on the reaction time, and the presence of pores and vibrations, however, the new printer requires further optimization, but provides new opportunities for fabricating objects from chemically reactive materials, such as silicones, epoxies as well as biomaterials.

3.6 Acknowledgements

The authors acknowledge support from the Natural Science and Engineering Research Council of Canada (NSERC) through their Strategic Grant program. PRS also acknowledges the Canada Research Chairs Program and the Discovery Accelerator Award.

3.7 References

[1] R. L. Truby, J. A. Lewis, *Nature*,**2016**, 540, 371-378.

[2] J. A. Lewis, G.M. Gratson, *Mater. Today*, **2004**, 7 ,32-39.

[3] A. D. Valentine, T. A. Busbee, J. W. Boley, J. R. Raney, A. Chortos, A. Kotikian, J. D. Berrigan, M. F. Durstock, J. A. Lewis, *Adv. Mater.*, **2017**, 29, 40.

[4] S. Hong, D. Sycks, H. F. Chan, S. Lin, G. P. Lopez, F. Guilak, K. W. Leong, X. Zhao, *Adv. Mater.*, **2015**, 27, 4035-4040.

[5] H. Yang, W. R. Leow, X. Chen, S*mall Methods, **2017***, 2, 1, (2017).

[6] X. Liu, H. Yuk, S. Lin, G. A. Parada, T.-C. Tang, E. Tham, C. de la Fuente-Nunez, T. K. Lu, X. Zhao, *Adv. Mater.*, **2017**, 30, 4.

[7] C. B. Highley, C. B. Rodell, J. A. Burdick, *Adv. Mater.*, **2015**, 27, 34, 5075-5079.

[8] D. P. Parekh, C. Ladd, L. Panich, K. Moussa, M. D. Dickey, *Lab Chip*, 2015, 10, 1812-1820.

[9] J. R. Tumbleston, D. Shirvanyants, N. Ermoshkin, R. Janusziewicz, A. R. Johnson, D. Kelly, K. Chen, R. Pinschmidt, J. P. Rolland, A. Ermoshkin, E. T. Samulski, J. M. DeSimone, *Science,* **2015**, 347, 6228, 1349-1351.

[10] Fan-Long Jin, Xiang Li, Soo-Jin Park,. *Ind. Eng. Chem.*, **2015**, 29,1-11.

[11] H. H. Moretto, M. Schulze, G. Wagner, *Silicones. Ullmann's Encyclopedia of Industrial Chemistry*, Wiley-VCH Verlag GmbH & Co. KGaA, **2000**

[12] A. Mata, A. J. Fleischman, S. Roy, *Biomed. Microdevices*, **2005**, 7, 4, 281-293.

[13] P. C. Nicolson, J. Vogt, Soft contact lens polymers: an evolution, *Biomaterials*, 22 24, (2001), pp. 3273-3283. https://doi.org/10.1016/S0142-9612(01)00165-X

[14] R. N. Palchesko, L. Zhang, Y. Sun, A. W. Feinberg, *PLoS One*, **2015**, 7, 51499,

[15] Byoung Yong Yoo, Byung Hwi Kim, Jae Sang Lee, Byung Ho Shin, Heeyeon Kwon, Won-Gun Koh, Chan Yeong Heo, *Acta Biomater.*, **2018**, 76, 56-70.

[16] C. Liu, Recent Developments in Polymer MEMS, *Adv. Mater.*, **2017**, 22, 3783-3790.

[17] H. Takaoa, K. Miyamurab, H. Ebib, M. Ashikia, et al, *Sensor Actuat. A-Phys.*, **2005**, 119, 2, 468-475.

[18] J. C. McDonald, D. C. Duffy, J. R. Anderson, D. T. Chiu, et al, *Electrophoresis*, **2000**, 21, 27-40.

[19] M. A. Brook, *Silicon in Organic, Organometallic, and Polymer Chemistry*, Wiley, New York, **2000**.

[20] Wacker Chemie, Q2 Interim Report January-June 2015, Germany, https:// www.wacker.com/cms/media/en/documents/investor-relations/quarterly report 1502.pdf accessed: 2015.

[21] S. Zheng, M. Zlatin, P. Selvaganapathy, M. A. Brook, Multiple modulus silicone elastomers using 3D extrusion printing of low viscosity inks, *Addit. Manuf.*, **2018**, 24, 86-92.

[22] S. Rekštytė, M. Malinauskas, S. Juodkazis, Three-dimensional laser micro-sculpturing of silicone: towards bio-compatible scaffolds, *Opt. Express*, **2013**, 21, 17028-17041.

[23] N. Bhattacharjee, C. Parra-Cabrera, Y. T. Kim, A. P. Kuo, A Folch, *Adv. Mater.*, 2018, 30, 22.

[24] F. Liravi, R. Darleux, E. Toyserkani, Nozzle dispensing additive manufacturing of polysiloxane: dimensional control, *Int. J. Rapid Manuf.*, **2015**, 5, 20-43.

[25] C. Sturgess, C.J. Tuck, I. A. Ashcroft, R. D. Wildman, *J. Mater. Chem. C*, **2015**, 5, 9733-9743

[26] S. Roh, D. P. Parekh, B. Bharti, S. D. Stoyanov, O. D. Velev., *Adv. Mater.,* 2017, 29.

[27] T. J. Hinton, A. Hudson, K. Pusch, A. Lee, A. W. Feinberg, *ACS Biomater-Sci. Eng.*, **2016**, 2, 1781−1786.

[28] K. Christensen, A. Compaan, W. Chai, G. Xia, and Y. Huang, *ACS Biomater-Sci. Eng.*, **2017**, 3, 3687−3694.

[29] C. W. Visser, T. Kamperman, L. P. Karbaat, D. Lohse, M. Karperien, Sci. Adv., **2018**, 4,

[30] B. Derby, Annu. Rev. Mater. Res., **2010**, 40, 395-414.

[31] R. Bui, M. A. Brook, *Adv. Funct. Mater., **2020**,* 30, 23.

[32] P.C.Duineveld, J. Fluid Mech., **2003**, 477, pp. 175–200,

[33] Rider, P., Zhang, Y., Tse, C. et al. J. Mater. Sci., **2016**, 51, 8625–8630 (2016).

[34] A. M. Compaan, K. Christensen, Y. Huang, ACS Biomater. Sci. Eng., **2017**, 3, 8, 1519–1526.

Chapter 4 : Dynamic Covalent Schiff-Base Silicone Polymers and Elastomers

4.1 Abstract

Polymers with dynamically exchanging crosslinks possess the ability to be repurposed, in whole or part, following a stimulus. The ability of imines to undergo dynamic exchange reactions under mild conditions was utilized to chain extend or crosslink silicone polymers. Schiff-base crosslinked polysiloxanes were prepared by reacting aminopropyl-functionalized polydimethylsiloxane with aromatic aldehydes. The reactions occur efficiently and the water byproduct spontaneously separates from the silicone if the weight fraction of silicone is sufficiently high. The physical properties of the products were readily tunable by crosslink density; the most practical reaction partners were commercial pendant aminopropylsilicones with terephthaldehyde, although telechelic silicones and triformylbenzene were also utilized. Complete breakdown of the polymers occurred with addition of excess amine. Silicone imine cleavage with excess aldehyde also occurred, but the two processes followed different pathways. The rate of the dynamic processes was increased with good solvents, or acid or amine catalysts. However, even in the absence of catalysts the dynamic transimination was efficient. Simply placing two strips of the elastomer in contact led to an adhesive bond that, depending on contact surface area, was stronger than the cohesive strength of the rubber. The process of self-healing was followed using rheology and was shown to be complete within an hour. Surface modification of elastomers with amines occurred in water, or at aminated solid surfaces.

** R. Bui, M. A. Brook, *Polymer*, **2019**, 160, 282-290 - Reproduced with permission from Elsevier Ltd. **Contributions** - Bui was responsible for all experimental work and subsequent write up of the work completed in this chapter.

4.2 Introduction

There is an evolving trend away from thermoset polymers. The utility of gels, rubbers and resins is self-evident, but there is increasing pressure to facilitate the recycling, reusing, and repurposing of polymers, particularly those derived from petrochemicals. Arguably, the most important example of this problem is automobile tires, which are commonly burned or used as landfill waste because of difficulties in reusing the materials [1].

An emerging class of polymers that can address this need possess chemical links which are susceptible to (bio)organic transformations that remove crosslinks to give linear chains and/or facilitate conversion back to monomers.[2] There is also strong interest in polymers designed to be repurposed. Thermoplastic elastomers, which possess weak links that can be overcome by heating to give processable fluids, fall into this category [3]. The nature of the crosslinks that are overcome with heating vary widely. Physical association, for example, the combination of hydrogen bonding, aromatic association (sometimes, but not always [4], noted as pi-stacking) can lead to dramatic increases in physical properties below the melt temperature; in the case of coumarin-modified silicones which possess both interactions, the viscosity was several orders of magnitude higher than the starting silicones [5]. Several covalent bond exchange reactions also lend themselves to the formation of thermoplastic elastomers, of which the Diels-Alder reaction [6, 7], alkene metathesis[8] and the Michael addition[9] are emblematic. A special class of these polymers are able to undergo dynamic changes in response to a stimulus other than heat [10, 11]. One particular benefit of such polymers can be the ability to undergo self-healing [12].

Silicone elastomers are used in a wide variety of applications because of their unusual properties including high oxygen permeability[13], thermal and electrical resistance,

biocompatibility, [14] and high surface activity.[15] Most silicone rubbers are thermosets cured using metal-catalyzed reactions (Sn, Ti, Pt),[16] although a few thermoplastic elastomers have been reported. [5, 17, 18] Some silicones are self-healing.[19, 20] While most dynamic processes used for self-healing are based on organic rather than silicon chemistry, one interesting example exploited simple acid catalysis of siloxane bonds with polycyclic silicone structures.[21]

Imines are covalent bonds that can undergo rapid bond exchange reactions with imines, or amines. They can form in high yields, at room temperature, without the need for a catalyst, and the only byproduct of the reaction is water. Ciaccia et al. demonstrated that transimination between an imine and an amine in organic solvent occurs through simultaneous proton-transfer from the amine to imine during the nucleophilic attack, and decomposition through intramolecular protonation in a non-polar 4-membered transition state. As a consequence, the formation of aromatic imines and their exchange reactions are relatively independent of the electronic behavior of the incoming amine/imine and more dependent on temperature, solvent effects, and sterics of the reactants.[22, 23]

Imine bond exchange is catalyzed by primary amines or Brønsted acids and allows for very precise control of the dynamic properties of the bonds. Zhang et al. showed several examples of materials with improved physical properties and dynamic functionality, including recyclability and self-healing, arising from imine linkages to polyethylene glycols. [24-26]

Yu et al. first demonstrated the potential for imine-modified silicones to operate as dynamic polymers.[27] The combination of a telechelic aminopropylsilicone of one molecular weight with triformylbenzene gave elastomers that proved to be able to self-heal. We wished to

better understand the degree to which the dynamic behavior of imines could be exploited both to depolymerize the materials and selectively functionalize elastomeric surfaces. We report the synthesis of a library of linear and elastomeric silicone imines and report their complete and partial depolymerization, functionalization at water and glass interfaces, and self-healing as a function of contact time.

4.3 Experimental

4.3.1 Materials

3-(Aminopropyl)methylsiloxane-dimethylsiloxane copolymers: AMS-132 (2-3% mol aminopropylmethylsiloxane, 4500-6000 g mol^{-1}), AMS-152 (4-5% mol aminopropylmethylsiloxane, 7000-9000 g mol^{-1}), AMS-162 (6-7% mol aminopropylmethylsiloxane, 4000-5000 g mol^{-1}), AMS-191 (9-11% mol aminopropylmethylsiloxane, 2000-3000 g mol^{-1}), AMS-1203 (20-25% mol aminopropylmethylsiloxane, 20000 g mol^{-1}); and telechelic 3-(aminopropyl)-terminated polydimethylsiloxanes: DMS-A11 (850-900 g mol^{-1}), DMS-A12 (900-1000 g mol^{-1}), DMS-A15 (3000 g mol^{-1}), DMS-A21 (5000 g mol^{-1}), DMS-A31 (25000 g mol^{-1}) were purchased from Gelest. Terephthaldehyde (99%), 3-(aminopropyl)triethoxysilane (99%), benzaldehyde (99.5%), 4-hydroxybenzaldehyde (98%), dodecylamine (≥99%), rhodamine 123, butylamine (99.5%) and allyl amine (99%) were purchased from Sigma Aldrich. Commercial solvents: dichloromethane, chloroform, toluene, dimethylformamide, methanol, and isopropanol were purchased from Caledon Laboratories and used as received. Cellulose filter papers were manufactured by Whatman, were purchased from VWR. Glass slides used in amine-functionalization were manufactured and purchased from VWR.

4.3.2 Methods

Polymer molecular weights were measured using gel permeation chromatography on a Viscotek GPC Max (VE 2001 GPC Solvent/Sample Module) equipped with a Viscotek VE 3580 RI Detector, a Viscotek 270 Dual Detector, and a PolyAnalytik SupeRes PAS-101 (8 mm x 30 cm) column with a single pore, styrene-divinylbenzene gel (6 nm particle size) with toluene as eluent at a rate of 1.0 mL/min. Vacuum stripping of volatiles from synthesized products was done using a Buchi Kugelrohr vacuum distillation apparatus at 0.3 Torr. Elastomers were cured in a Teflon dog bone-mold (30 mm x 10 mm x 5 mm with 5 mm inner central width) for tensile testing, and a Pyrex glass 9-well spot plate (22.2 mm x 7 mm wells) or a polypropylene flat-bottom 12-well plate for mechanical testing. Infrared spectroscopy was conducted using a Thermo Scientific Nicolet 6700 FT-IR spectrometer equipped with a Smart iTX attenuated total reflectance (ATR) attachment. Shore OO and Shore A durometers (Rex Gauge Company, Inc. U.S.) were used to characterize the hardness of the elastomer. Young's moduli were measured using a MACH-1 micromechanical testing instrument (Biomomentum Instruments) equipped with a 0.5 mm hemispherical indenter using a Poisson ratio of 0.3 and a constant indentation depth of 1.0 mm; all measurements were conducted at 22 °C and in triplicate. Tensile strength experiments were performed on an Instron 5900 series Universal Mechanical Tester (ITW company) equipped with a 50 N load cell, all experiments were conducted at a constant rate of 5 mm min^{-1}. Rheology measurements were conducted on a TA Instruments HR-2 Rheometer with 40 mm parallel plate geometry and Peltier plate set to a 500 μm gap at 25 °C. NMR spectra were obtained using a Bruker Avance 600 spectrometer. Thermal stability was determined using a TGA Q50 thermogravimetric analyzer (TA Instruments)

under an argon atmosphere. Fluorescence images of rhodamine binding to elastomers were taken using a Nikon Eclipse LV100N POL microscope.

4.3.3 Synthesis of Polydimethylsiloxane-Schiff Base Polymers

4.3.4 Reaction of Benzaldehyde with 3-(Aminopropyl)pentamethyldisiloxane

In a round-bottomed flask 3-aminopropyl-tris(trimethylsiloxy)silane (0.222 g, 1.08 mmol) and benzaldehyde (0.115 g, 1.08 mmol) were suspended in chloroform (10 mL); the solution was transparent and light yellow. The reaction was heated to 50 °C for 3 h over anhydrous sodium sulfate (0.125 g) to remove any water that formed. The reaction was cooled to room temperature and the product was obtained, after filtration, by evaporation of the solvent by rotary evaporation (0.304 g, 1.03 mmol, 96% recovered yield).

^{1}H NMR (600 MHz, CDCl3) δ 0.050 (s, 15H, Si-CH_3), 0.50 (t, 2H, Si-CH_2, *J* = 8.64 Hz), 1.76 (p, 2H, CH_2, *J* = 8.10 Hz), 3.59 (q, 2H, CH_2, *J* = 7.12 Hz), 7.73 (m, 5H, Ar-H), 8.16 (s, 1H, -CHN). IR (ATR-IR, cm^{-1}): 2954, 2924, 2869, 1645, 1595, 1581, 1450, 1441, 1410, 1342, 1310, 1251, 1176, 1030, 905, 888, 670.

4.4.3.1 Reaction of Benzaldehyde with α,ω-(3-Aminopropyl)dimethylsilylpolydimethylsiloxane

In a round-bottomed flask, DMS-A11 (0.114 g, 0.126 mmol, 850-900 g mol^{-1}, α,ω-(3-aminopropyl)dimethylsilylpoly-dimethylsiloxane)) was combined with benzaldehyde (0.0269 g, 0.253 mmol) in chloroform (25 mL), giving a pale-yellow solution. Anhydrous sodium sulfate (0.5 g) was added to the flask and the mixture was refluxed for 2 h. Reaction progress was monitored by IR spectroscopy using the disappearance of the aldehyde peak at 1685 cm^{-1}. The reaction mixture was cooled to room temperature, then filtered through cellulose filter paper to remove the hydrated sodium sulfate. The solvent

was removed under reduced pressure by rotary evaporation to give a pale-yellow oil. The product was purified by vacuum distillation using a kugelrohr distillation apparatus (110 °C, 3.0 Torr) to remove excess benzaldehyde and water. The residual viscous yellow oil, analyzed by NMR and IR, showed no aldehyde peaks, or water (0.128 g, 91% recovered yield).

^{1}H NMR (600 MHz, CDCl3) δ 0.050 (s, 36H, Si-CH_3), 0.51 (t, 4H, Si-CH_2, *J* = 8.47 Hz), 1.66 (p, 4H, CH_2, *J* = 8.97 Hz), 3.52 (q, 4H, CH_2, *J* = 7.04 Hz), 7.32 (m, 6H, Ar-H), 7.65 (m, 4H, Ar-H) 8.16 (s, 2H, -CHN). IR (ATR-IR, cm^{-1}): 2953, 2922, 2860, 1645, 1594, 1450, 1410, 1379, 1342, 1310, 1250, 1177, 1047, 836, 783, 734, 694.

4.4.3.2 Reaction of Terephthaldehyde with α,ω-(3-Aminopropyl)dimethylsilyl-polydimethylsiloxane

A 65000 g mol^{-1} Schiff-base silicone polymer **TPA-PDMS** was prepared by taking DMS-A12 (0.8750 g, 1000 g mol^{-1}, α,ω-(3-aminopropyl)dimethylsilylpolydimethylsiloxane), 0.8750 mmol) and mixing with terephthaldehyde (116 mg, 0.8677 mmol) dissolved in chloroform (1 mL). The solution quickly turned bright yellow and the viscosity of the mixture increased gradually over 2 h of stirring at room temperature. The solvent was removed by rotary evaporation, to yield a pale-yellow oil. The product was further purified with vacuum distillation using a Kugelrohr at 125 °C, 0.3 Torr. The product was isolated as a pale yellow/orange oil (0.955 g, 0.812 mmol, 93% yield).

^{1}H NMR (600 MHz, $CDCl_3$) δ 0.050 (s, Si-CH_3), 0.50 (t, 2H, Si-CH_2, *J* = 8.66 Hz), 1.76 (p, 2H, CH_2, *J* = 8.42 Hz), 3.59 (q, 2H, CH_2, *J* = 7.08 Hz), 7.73 (s, 4H, Ar-H), 8.25 (s, 2H, -CHN). IR (ATR-IR, cm^{-1}): 2959, 1645, 1463, 1257, 1059, 913, 844, 712. GPC: M_n= 51,990 Da M_w= 73,610 Da, $Đ_M$ = 1.416.

4.4.3.3 Hydrolysis of TPA-PDMS Polymers

To test hydrolytic stability of high silicone-containing polymers, a sample of terephthaldehyde-linked linear silicone polymer (12.3 mg, M_n= 51,678 g mol^{-1}, prepared from 1000 g mol^{-1} α,ω-(3-aminopropyl)dimethyl-silylpolydimethylsiloxane starting polymer) was suspended in D_2O (1 mL), then flame sealed in an NMR tube. The NMR tube was submerged in a 110 °C oil bath for 3 h and allowed to cool to room temperature before the NMR spectrum was collected to determine the composition of the hydrolysis product. The NMR spectrum in D_2O showed no resonances besides residual solvent peak. The polymer was extracted using chloroform (5 mL) and extracts were isolated by rotary evaporation of the solvent. An NMR of the extracted product in $CDCl_3$ also showed no resonances corresponding to the hydrolysis of the imine at (8.2 ppm), to the starting aldehyde (9.63 ppm) or to propylamine (2.56 ppm).

4.4.3.4 Degradation of TPA-PDMS Polymer by Amines and Aldehydes

A stock solution of the starting Schiff-base silicone polymer (0.910 g, M_n= 51,678 g mol^{-1}, prepared from 1000 g mol^{-1} α,ω-(3-aminopropyl)dimethylsilylpolydimethylsiloxane starting polymer)) was prepared in DCM (9.1 mL). From the stock polymer solution, 1000 µL aliquots were pipetted into separate vials then various quantities of 1.0 M allylamine or benzaldehyde, respectively, in DCM were added (1-10 µL, Table 4.3). The vials were stirred at room temperature for 4 h, then the solvent was removed by rotary evaporation. The polymers were purified by vacuum distillation using a Kugelrohr apparatus at 120 °C, 0.3 Torr and then analyzed by GPC.

4.3.5 Preparation and Physical Testing of Schiff-Base Elastomers

4.5.3.1 Preparation of Elastomers from α,ω-(3-Aminopropyl) dimethylsilylpoly-dimethylsiloxane and 1,3,5-Triformylbenzene (TFB-PDMS)

TFB-PDMS elastomers using 1,3,5-triformylbenzene as crosslinker were prepared from α,ω-(3-aminopropyl)PDMS (@ 850, 3000, and 5000 g mol^{-1}, respectively) at room temperature. In a typical preparation, 1,3,5-triformylbenzene (0.085 g, 0.524 mmol) was dissolved in chloroform (0.9 mL) then combined with telechelic 3-aminopropylpolydimethylsiloxane (3000 g mol^{-1}, 2.372 g, 0.790 mmol) in a vial such that $[amine]_0=[aldehyde]_0$; similar outcomes were obtained using DMF, or DCM as solvent instead of chloroform. The vial was stirred until homogenous, then poured into a Teflon dog bone-mold (3 cm x 1 cm x 0.5 cm with 0.5 cm inner central width) and allowed to crosslink for 10 h (gelation takes place within minutes and, using rheometry, full cure is complete after 3 h). The elastomers were then dried in a vacuum oven at a 60 °C at 0.3 Torr for 6 h to remove residual water. Stress-strain tests were conducted at a rate of 5 mm min^{-1} to determine the elongation at break (Table 4.2).

4.5.3.2 Binding of Rhodamine 123 to TPA-PDMS Elastomers

A solution of rhodamine 123 (0.01 mM) was prepared by first dissolving rhodamine 123 (0.010 g, 0.0262 mmol) in water (50 mL) and then diluting in a volumetric flask (100 mL) to give a 0.262 mM solution. In a second dilution, the prepared rhodamine 123 solution (3.82 mL) was diluted to 100 mL in a volumetric to yield a 0.01 mM solution of rhodamine 123.

In separate vials, 7% TPA-PDMS elastomer (0.956 g) and an equal sized piece (4 cm x 4 cm x 2 cm) of SylGard 184 (0.970 g) were submerged in the rhodamine solutions for 24

h. The samples were removed from the rhodamine solutions and subsequently washed thoroughly with distilled water to remove surface-bound dye. The elastomers were imaged using fluorescence microscopy to observe the dye bound to each elastomer sample. The dye was extracted from the elastomers by submerging the samples in DCM (50 mL) 24 h with stirring, replacing the solvent every 6 h (i.e., 4 x 6 h). The samples were imaged again under fluorescence microscopy.

4.5.3.3 Degradation of TPS-PDMS Elastomers by Dodecylamine

A 10% crosslinked **TPA-PDMS** elastomer (2.5 g) was placed in a vial containing dodecylamine (121 mg, 0.653 mmol) dissolved in chloroform (15 mL). The vial was gently stirred at room temperature for 12 h, causing the elastomer to slowly degrade and dissolve in solution. The degradation product was obtained by rotary evaporation of solvent to yield a viscous yellow oil. NMR analysis of the products revealed the superposition of the starting silicone elastomer, unreacted dodecylamine, and a mixture of the mono- and bis-dodecylimine.

^{1}H NMR (600 MHz, $CDCl_3$) δ 0.85 (t, 3H, CH_3, *J* = 10.8 Hz), 1.23 (m, 24H, $C_{10}H_{20}$), 3.59 (q, 2H, CH_2, *J* = 7.08 Hz), 7.73 (s, 4H, Ar-H), 8.25 (s, 2H, -CHN).

4.5.3.4 Remolding of Schiff-Base Silicone Elastomers by Dynamic Processes

The chemoplastic processing of elastomers was achieved under the conditions of solvent annealing with chloroform, acid catalysis, or amine-catalyzed mechanisms. Each remolding method employed different conditions. For a vial of pulverized elastomer (5.0 g): solvent annealing with chloroform (11 mL); acid catalyzed with acetic acid in chloroform (100 µL of 1.747 M); or using amine catalysis with butylamine in chloroform (100 µL of 1.514 M), respectively, was undertaken. After exposure of the elastomer for 1 h to the

conditions noted, the transparent elastomer had swollen to the shape of the vial. The vial was capped and allowed to react for an additional 5 h. The remolded elastomer was removed from the vial and allowed to dry in open atmosphere for 24 h before being placed in a 40 °C vacuum over for 3 h to remove residual solvent. The physical properties of the elastomers were measured using Shore hardness and Young's modulus. This procedure was repeated for 3 remolding cycles of the same elastomer, measuring the physical properties each time (Figure 4.6).

4.4 Results and Discussion

4.4.1 Formation of Schiff-Base Imine in a Silicone Environment

At the onset of this work, we sought to establish the facility with which aromatic imines form in a hydrophobic silicone environment. Initial NMR experiments probing the formation of imines using benzaldehyde demonstrated that Schiff-base bonds can form in nearly quantitative yield in the presence of PDMS using stoichiometric quantities of reagents, without producing any detectable byproducts besides water (Figure 4.1A). The water produced in the formation of imines has been shown to retard the rate of the reaction [22] and, therefore, a desiccant (molecular sieves or anhydrous sodium sulfate) to remove water is often used to drive the equilibrium towards the formation of imines. A desiccant was not required, however, to achieve full conversion of benzaldehyde to imines once the molecular weight of the α,ω-(3-aminopropyl)PDMS starting materials was above 3000 g mol^{-1} ([Me2SiO]:[ArC=N] = 20:1). In such reactions, the water spontaneously phase separated from the mixture to drive imine formation to completion, which highlights the benefits of the hydrophobic silicone environment in this process. The desired Schiff-base silicones could be obtained at room temperature in under 1 hour. 1H NMR analysis of the

products showed the full conversion of aldehyde resonances (9.6 ppm) to imines (8.2 ppm) and a shift of the protons adjacent to nitrogen from 2.5 to 3.58 ppm, and IR spectroscopy showed consumption of aldehyde at 1685 cm^{-1} and a new peak for imines at 1645 cm^{-1} (Supporting Information).

4.4.1 Schiff Bases as Links for Extended Linear Polymers

Linear alternating copolymers were prepared by linking various molecular weight α,ω-(3-aminopropyl)PDMS to terephthaldehyde through Schiff-base bonds; desiccants were not necessary when using α,ω-(3-aminopropyl)PDMS >3000 g mol^{-1}. The molecular weights of the product polymers depended both on the length of silicone used, and the care with which the stoichiometry of the starting reagents was managed (Figure 4.1C, Table 4.1). The molecular weights of the polymers were measured using GPC and confirmed by end-capping the polymers with 4-hydroxybenzaldehyde and comparing the integration of the resonances for the terephthaldehyde imine (8.21 ppm) vs the 4-hydroxybenzylimine (8.08 ppm) or aromatic protons (6.71 or 7.57 ppm) in the ^{1}H NMR. The product imine-linked polymers had dispersities ($Đ_M$ = 1.24-1.85) that were low, particularly for an AA+BB condensation copolymerization [28]. Unsurprisingly, viscosities depended on length of the silicone starting polymer (Table 4.1), since the silicone portion of the polymers is flexible while the organic portion is rigid.

4.4.2 Formation and Physical Properties of Schiff-Base Silicone Elastomers

Imine-silicone elastomers were readily prepared by the reactions of difunctional terephthaldehyde with pendant, polyfunctional aminopropylPDMS (**TPA-PDMS**), or from trifunctional 1,3,5-triformylbenzene with α,ω-(3-aminopropyl)PDMS (**TFB-PDMS**)[27] (Figure 4.1D,E). Infrared spectroscopy was used to monitor the progress of the reaction (Supporting Information), which had all reached high conversion in under 4 hours.

Table 4.1: Characterization of Extended Linear Polymers Derived from α,ω-(3-aminopropyl)PDMS and Terephthaldehyde[a]

Monomer MW (g mol^{-1})	M_n (kDa)	M_w (kDa)	$Đ_M$	RI	Number imine/ PDMS repeats (DP)
900	14.1	25.9	1.83	1.414	15
	31.8	41.3	1.29	1.462	35
3000	17.9	24.3	1.35	1.420	6
	26.8	38.6	1.44	1.448	9
	34.2	51.4	1.50	1.451	11
5000	21.8	27.2	1.24	1.411	4
	35.7	43.9	1.23	1.413	7
	73.6	52.0	1.42	1.423	15
25000	120.5	219.4	1.82	1.403	5

[a] All reactions were prepared using $[aldehyde]_0 = [amine]_0 = 0.18$ M in chloroform. Na_2SO_4 was added as a desiccant to polymers starting from 900 and 3000 g mol^{-1}, but was not required for the 5000 or 25000 g mol^{-1} silicone starting materials. Functional group conversion was assessed by ATR-FTIR. Note: the RI of the starting silicone is 1.408, and terephthaldehyde is 1.620, as measured before testing.

Table 4.2: Physical characterization of Schiff-base crosslinked elastomers

Entry	mol% aminopropyl	M_n (g mol^{-1})	$[Me_2SiO]_x$ /$[NH_2]_y$ (x/y)	Mass silicone (g)	[Amine] (mol L^{-1})	Shore hardness (OO)	Young's modulus (MPa)	Elongation at break (%)
Telechelic aminopropylPDMS and 1,3,5-triformylbenzene (**TFB-PDMS**)								
1		850		0.8781	2.066	86	3.667 ±0.022	122
2		3000		0.8610	0.574	52	0.762 ±0.045	173
3		5000		0.8782	0.351	42	0.304 ±0.021	180
Pendant-modified aminopropylPDMS and terephthaldehyde (**TPA-PDMS**)								
4	2	5500	33.6	0.8455	0.227	39	0.282 ± 0.01	185
5	5	8000	18.5	0.8668	0.585	50	0.740 ± 0.01	162
6	7	4500	14.3	0.8234	0.781	66	1.770 ± 0.02	145
7	10	2500	10.0	0.8772	1.335	87	3.224 ± 0.04	124
8	25	2000	4.0	0.8876	2.696	23[a]	4.367 ± 0.01	110

[a] Shore A.

A library of elastomers was prepared with crosslink densities varying from 2-25% pendent modified aminopropylPDMS for **TPA-PDMS**, or from 900-5000 g mol^{-1} telechelic aminopropylPDMS for **TFB-PDMS**; while keeping [aldehyde] = [amine]. As the crosslink density increased, there was a concomitant increase in Young's modulus and Shore hardness, but a lower elongation at break (Table 4.2).

Although the resulting network structures were different, the two types of elastomers exhibited comparable physical properties at comparable crosslink densities (Table 4.2). A

comparison of the two crosslinking methods was done by curing elastomers made from equal volumes of α,ω-(3-aminopropyl)PDMS 3000 g mol^{-1}), or 4-5% pendent-(3-aminopropyl)PDMS which have amine-concentrations of 0.574 M and 0.585 M, respectively. The **TFB-PDMS** elastomer had a Young's modulus of 0.762 MPa, while the analogous **TPA-PDMS** had a comparable modulus of 0.740 MPa; elongation at break and Shore hardness measurements followed a similar trend. The **TPA-PDMS** elastomers possessed slightly higher mechanical properties when compared to **TPA-PDMS**. However, the **TPA-PDMS** family of elastomers is perceived to be more practical because of the lower cost of the aldehyde (approximately 40 times less expensive) and, importantly, there is no need to use solvents; 1,3,5-triformylbenzene required a solvent and was prone to precipitation from PDMS during cure, leading to a reduction in cure efficiency at high crosslink densities. Note that combinations of these di- or trifunctional aldehydes, at appropriate stoichiometry, with pendant/telechelic aminopropyl-silicones led to networks with very tunable properties.

4.4.3 Dynamic Equilibrium of Schiff-Base Silicone Polymers

The produced Schiff-base bonds were resilient to hydrolysis, increasingly so with higher silicone content. There were no observable hydrolysis products by NMR from exposure to atmospheric moisture or room temperature water with any of the products. Small chain silicones with imines, such as the product of (3-aminopropyl)pentamethyldisiloxane and benzaldehyde, completely hydrolyzed after boiling for 30 minutes in water (Supporting Information). Linear **TPA-PDMS** polymers with a larger silicone fraction (α,ω-(3-aminopropyl)PDMS, >3000 g mol^{-1}) required 3 hours in boiling water for complete hydrolysis. For very silicone rich linear polymers derived from α,ω-(3-aminopropyl)PDMS

(52.0 kDa) and terephthaldehyde, even very vigorous conditions 120 °C in boiling water (in a sealed vessel) showed no hydrolysis products detectable by NMR.

The functional groups remain dynamic, undergoing rapid bond exchange with amines or aldehydes in the presence of adventitious water (Figure 4.1A).[29] Imines also directly exchange with amines through transimination, where the amine attacks, the imine to form an aminal intermediate that is rapidly converted into a new imine, even in the absence of water (Figure 4.1B).[22]

To explore the dynamic exchange of imine bonds in the presence of either aldehydes or amines, a linear 51.6 kDa (M_n) **TPA-PDMS** polymer (1000 g mol^{-1} silicone starting polymer, DP~50) was titrated with either benzaldehyde or allyl amine; changes in molecular weight were followed by gel permeation chromatography (Table 4.3, Figure 4.2). Either compound caused a decrease in molecular weight and an increase in dispersity, particularly as the concentration of aldehyde/amine was increased. This can be attributed to insertion of the monofunctional allylamine or benzaldehyde into the polymer through transimination or reversible bond exchange (Figure 4.1B), which leads to the formation of lower molecular weight polymers/oligomers terminated with the added molecules.

The two reagents seem to interact differently with the imine polymers, particularly at higher doses. The addition of benzaldehyde caused a shift of the entire distribution to lower molecular weights, consistent with random chain cleavage; at high doses a completely separate low molecular weight population was formed (Table 4.3, Figure 4.2A). By contrast, when the same polymer was challenged with allylamine, a second, lower MW

population immediately formed, while significant populations of original polymer remain (Figure 4.2B), suggesting a different decomposition mode.

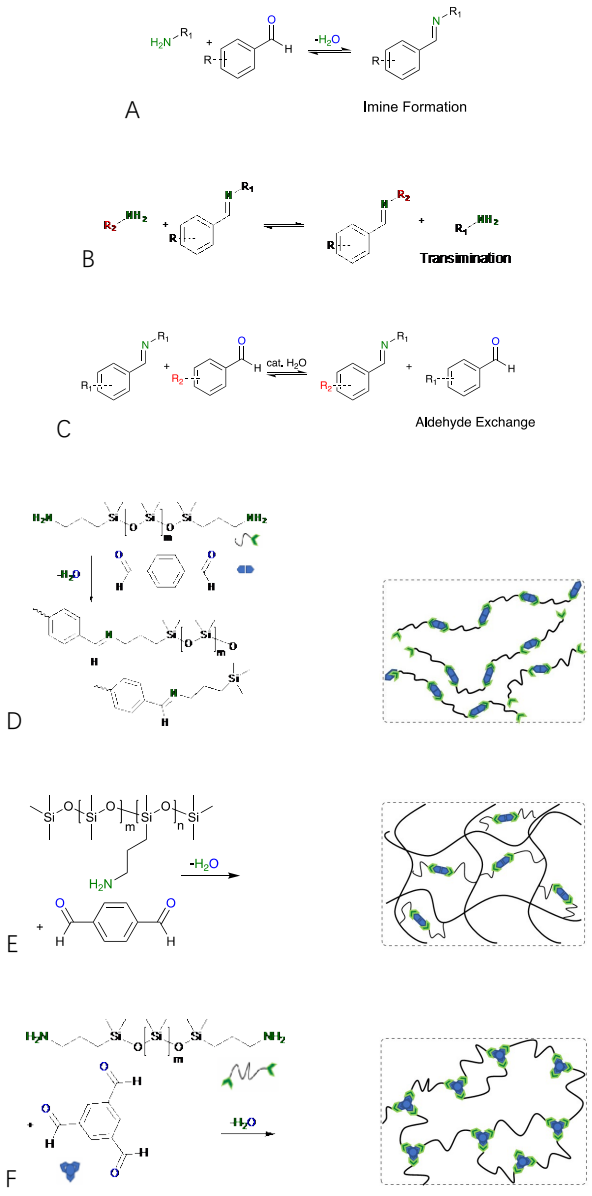

Figure 4.1: Competing equilibria in these processes. A: imine formation which is controlled by the concentration of water. B: transimination which allows for redistribution of imine bonds with amines under equilibrium conditions. C: Exchanging aldehydes via an imine. D: Linear polymers created from α,ω-(3-aminopropyl)PDMS and terephthaldehyde. Two complementary schemes for crosslinking aminopropylPDMS through Schiff-base bonds;

E: pendent-modified aminopropylPDMS with terephthaldehyde (**TPA-PDMS**), or F: α,ω-(3-aminopropyl)PDMS with 1,3,5-triformylbenzene (**TFB-PDMS**).

4.4.4 Self-Healing and Recyclable Silicone Elastomers

The dynamism of Schiff-base bonds can be exploited by reaction with a wide variety of amines. For example, a 5% **TPA-PDMS** elastomer was completely converted into a viscous oil 3 hours after exposure to an excess of dodecylamine. NMR analysis of the product showed the formation of the aryl bis(dodecylimine) and release of aminopropylPDMS (the original starting material, (Supporting Information). Thus, partial or complete loss of crosslinking, with concomitant incorporation of other imine functional groups, only requires exposure to appropriate amines. Such processes facilitate the reuse/recycling of these silicone polymers.

These dynamic exchange processes can be selectively used to modify only the surfaces of elastomers. A sample of 7% **TPA-PDMS** elastomer was submerged in a 0.01 mM solution of rhodamine 123 for 6 hours and rinsed with water. Fluorescence microscopy was used to qualitatively determine that the **TPA-PDMS** elastomers displayed much higher levels of adsorption, even after extraction with DCM, when compared to silicones that possess no organic functional groups, e.g., Sylgard 184, which only supports non-specific adsorption (Figure 4.3A,B); that is, chemisorption of amines occurred at the **TPA-PDMS** interface. The ability of amines to insert themselves into the elastomer, even in aqueous solution, highlights the utility of imine functional groups in a silicone environment. In this case, the aqueous solution almost certainly limited reactions to the interface; it is thermodynamically too expensive to hydrate the core of the silicone to enable reactions there.

Table 4.3: Changes in molecular weight (GPC) following the titration of **TPA-PDMS** polymers with allylamine or benzaldehyde, respectively.

	µL Added	mmol added	M_n (kDa)	M_w (kDa)	$Đ_M$
Starting polymer 5.4 mM Solution	500	2.7	51.6	92.8	1.79
Allylamine 1 M Solution	1	1.0	22.0	89.1	4.05
	2	2.0	13.6	86.2	6.30
	5	5.0	7.12	73.4	10.3
	10	10.0	1.89	40.3	21.5
PhCHO 1 M Solution	1	1.0	17.9	37.2	2.07
	2	2.0	12.8	30.1	2.35
	5	5.0	6.39	17.9	2.81
	10	10.0	2.34	13.6	5.82

An analogous process allowed the silicone to be bonded to an aminated surface. Glass slides were functionalized with aminopropyl groups using aminopropyltriethoxysilane (APTES). A Schiff-base crosslinked elastomer was pressed onto the aminated glass slide and, separately, an unfunctionalized piece of glass as a control (Figure 4.4). After 1 hour, the elastomer adhered to the aminated glass slide such that the elastomer could support the weight of the glass; little or no adhesion to the unfunctionalized glass was observed. The force of adhesion depended on the concentration of amine groups on the glass surface and the crosslink density of the elastomer. A 5% **TPA-PDMS** overlapped 1 cm^2 with the glass had a stress-at-failure of 0.180 MPa, and increasing the crosslink density to 10% causes the stress-at-break increased to 0.320 MPa. Note that the elastomer-glass samples failed cohesively, which indicates that adhesion is stronger than the crosslinks holding the material together. Furthermore, a significant quantity of residue was left on the aminated glass that could not be easily removed with either a scalpel or solvent. The absence of strong adhesion to normal glass shows that the process is selective for amines – hydroxyl groups were not active (Figure 4.4).

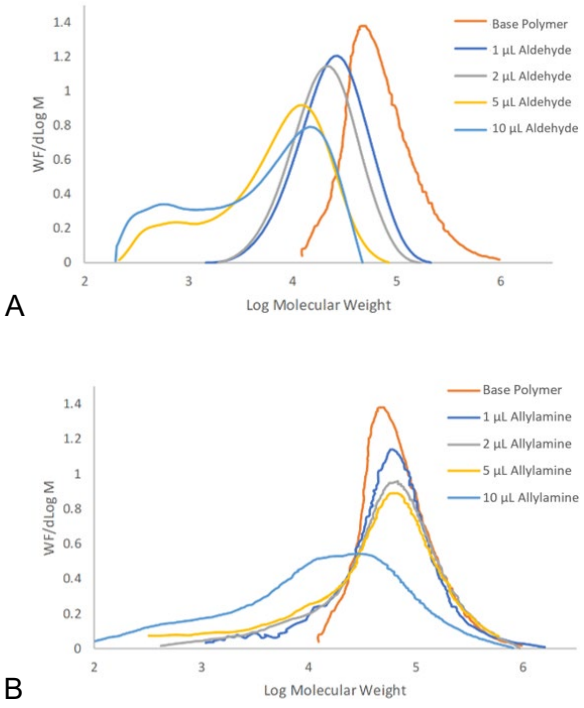

Figure 4.2: Changes in molecular weight distributions during the degradation of a Schiff-base polymer by A: benzaldehyde or B: allylamine. GPC data was taken 6 hours after addition of the reagent.

More interestingly, the dynamism of Schiff-base crosslinked elastomers provides self-healing properties. Rectangular strips of 5% **TPA-PDMS** elastomer were overlapped (10 mm^2) and held in contact to permit imine bond exchange between the two samples; the two layers bonded. The self-healed materials were evaluated with tensile measurements, which demonstrated that the strength of adhesion gradually increases with the contact time (Figure 4.5) with maximum adhesion reached after only 1 hour. After this time, the adhesive strength of the welded surface exceeded the cohesive strength of the material; the samples fractured at a different place other than the self-healed interface. The original elastomer had an elongation at break of 160% with a strain of 0.540 MPa, and after contact for twenty-four hours the strain and stress were 160% and 0.570 MPa, respectively.

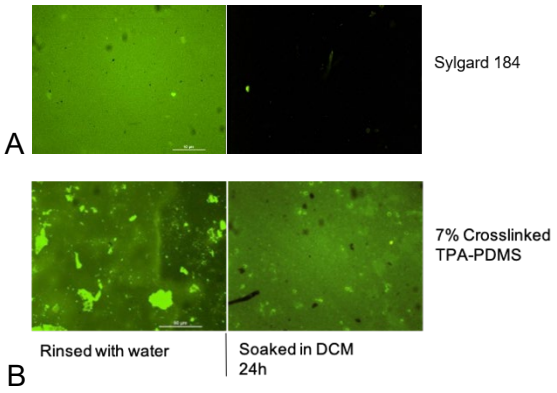

Figure 4.3: Comparative study on the binding rhodamine 123 to a **TPA-PDMS** elastomer and Sylgard 184 in water for 24 hours. After 24 h of submerging in 0.01 mM rhodamine 123, A) samples thoroughly rinsed with water, B) extracted with DCM.

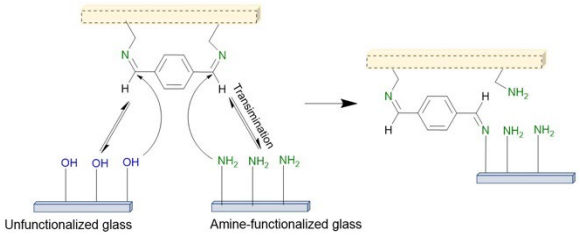

Figure 4.4 Elastomers selective adhere to aminopropyl-functionalized glass slide by transimination, but no adhesion to unfunctionalized glass-slide.

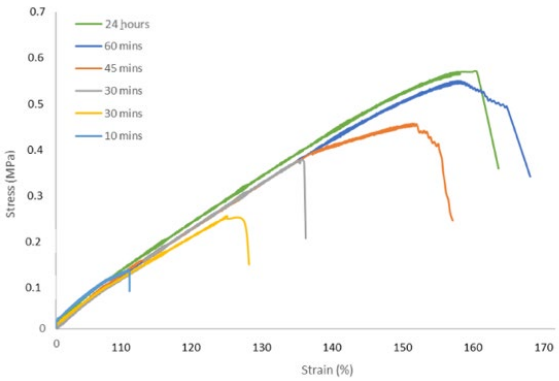

Figure 4.5: Stress-strain graphs from tensile testing of 5% crosslinked **TPA-PDMS** elastomers held in contact with a 10 mm^2 contact surface area for various amounts of time to access the self-healing properties.

The rate of bond exchange can be enhanced by increasing the chain mobility of the silicone or the addition of a catalyst (amine or proton). These techniques permit the reprocessing of the elastomers through a kind of chemoplasticity. The recyclability of the Schiff-base elastomers was tested using three methods; solvent annealing with chloroform, acetic acid-catalyzed metathesis, and butylamine-catalyzed transimination (Figure 4.6A). In each method, the intrinsic bond exchange is promoted increased mobility and/or concentration of reactive functional groups.

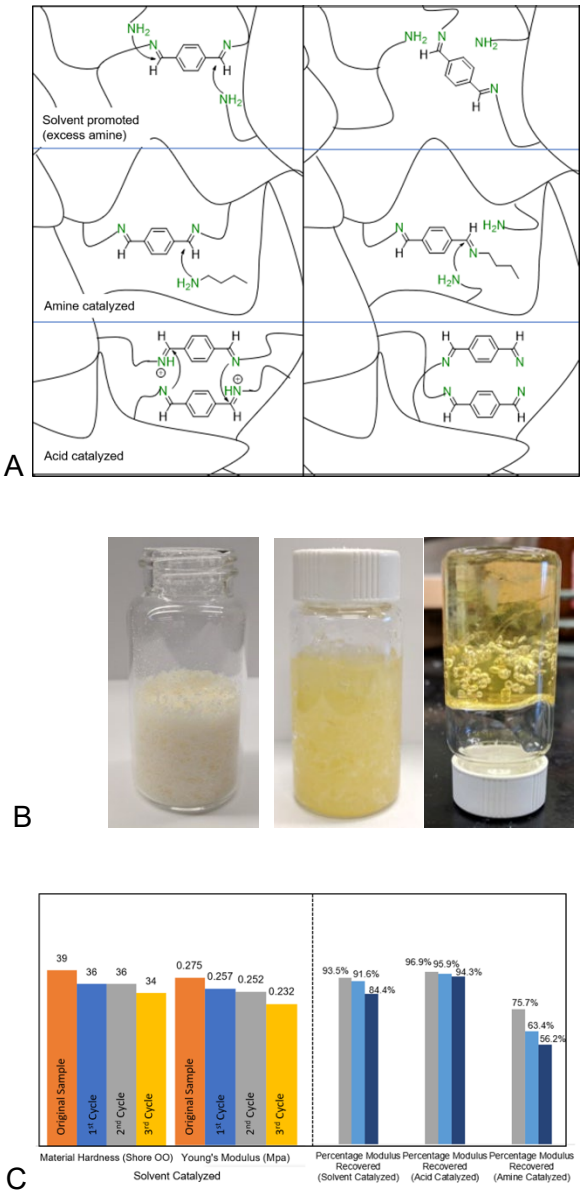

Figure 4.6: Elastomer recycling through imine exchange. A: Three mechanisms for recycling elastomers by promoting reactivity of imine crosslinks. B: Example of elastomer recycling from pulverized pieces of elastomer, during annealing process, and as single homogenous elastomer body by solvent annealing. C: Physical properties of recycled materials after 3 cycles of remolding. Left hand side - the original in orange followed by three repeat recycles using a solvent to reform the elastomer. Right hand side – the % changes in properties after repeat recycles using different methods.

The elastomers were pulverized into a fine powder and introduced into a vial to which the solvent and/or catalyst were added. After evaporation of the solvent and removal of the elastomer from the mold, Young's modulus and Shore hardness were measured and compared to the original elastomer. This procedure was repeated three times to evaluate the efficiency of the recycling (Figure 4.6).

The solvent annealing and acid-catalyzed methods recovered >90 % of the Young's modulus after one cycle, with only small decreases in the material's physical properties after subsequent cycles. For example, after three cycles of remolding, the chloroform annealed sample exhibited a Shore hardness and Young's modulus 34 and 0.230 MPa, respectively, a small decrease from the starting elastomer: 39 and 0.280 MPa, respectively. The butylamine-catalyzed recycling was less efficient and resulted in 76% recovery of the Young's modulus after only one cycle.

Measurements of crosslink density by swelling mirrored these results. After 4 cycles of remolding, the swelling ratio of a chloroform annealed, recycled elastomer was 600% compared to a piece of elastomer that had never been recycled/remolded, which swelled by 630 %. Thus, exposure to acid or solvent little changes the overall crosslinking. This experiment highlights a major advantage of using dynamic covalent bonds as opposed to non-covalent interactions, such as hydrogen bonding, that are often intolerant to solvents. [30-32]

4.5 Discussion

The mechanism of imine formation and transimination reactions has been comprehensively reviewed by Ciaccia and Di Stefano.[23] The chemistry of imine formation in silicone media fits well with their observations. One distinction between typical organic

reactions and those described here is the role played by the low surface energy of silicones. In the initial imine formation, the process is highly facilitated by the phase separation of water, which drives the equilibrium to product. This is the origin, in part, of the stability of the linear or crosslinked silicone imines. Reactions with water, even at elevated temperatures, were inefficient and slow in part because the water has breach the hydrophobic silicone barrier, or is limited to reactions at the silicone/water interface.

The mode of transimination when the silicone imine polymers were challenged by amines, was different than the effect shown by excess aldehydes (Figure 4.2). Decomposition of the chain in the latter case, followed classical random cleavage, leading to a gradual decrease of the average molecular weight, in an inverse condensation process. By contrast, in the presence of amines, the linear polymer degraded in a process that better mimics a chain depolymerization process (Figure 4.7). This suggests that, with amines, depolymerization is much faster from an active end than the initial chain cleavage. The origins of this effect need further investigation.

Unlike water, the reaction of silicone imine polymers with amines was facile. Complete degradation of the imine network was caused by reaction with excess amines; partial reactions facilitated changes in the type of imine, preferentially at the polymer surface (Figure 4.3, Figure 4.4). These processes are well known in the literature.[23] Thus, by judicious choice of reaction conditions, it is possible to decide the degree of erosion/functionalization of the silicone imine elastomer surface, or to choose complete depolymerization to reform the starting silicone.

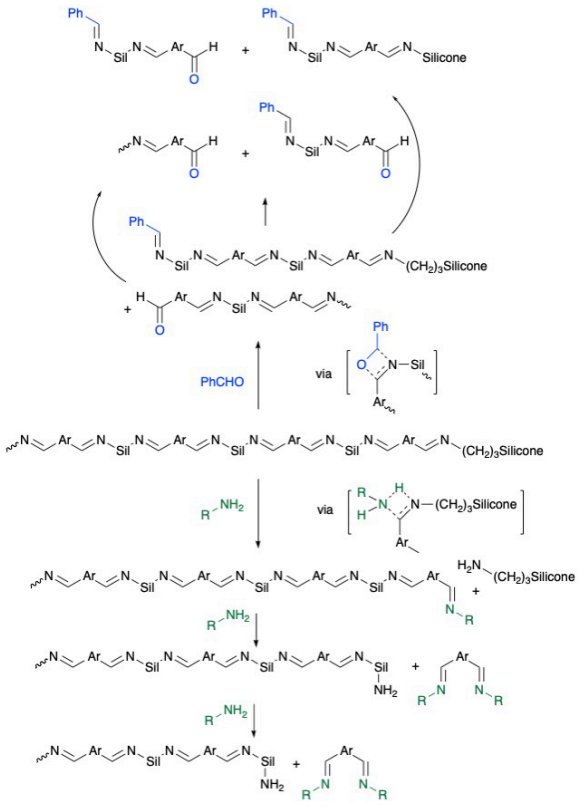

Figure 4.7: Depolymerization of silicone-imines in the presence of benzaldehyde and allylamine (N-Sil-N = $N(CH_2)_3$Silicone polymer$(CH_2)_3N$).

Yu et al. demonstrated that self-healing silicone imine networks could be formed from telechelic aminopropylsilicones and triformylbenzene, using process involving DMF.[27] We have expanded their work by showing that the use of terephthaldehyde obviates the need for organic solvents, making the process inherently greener. In addition, the combination of terephthaldehyde with commercial pendant aminopropylsilicones, which are available in both different molecular weights and fractions of aminopropyl groups, allows one to easily tune network structure and elastomer properties.

The main benefit provided by the silicone imine polymers is their dynamic nature. While transimination processes are accelerated with amine or acid catalysis,[33] or simply by swelling with solvents (increased rate due to increased mobility), the silicone imine

elastomers are dynamic as neat materials at room temperature. This was most clearly shown by their ability to undergo self-healing on contact to make bonds that were as strong as the original elastomer (Figure 4.5). In the sample tested, equilibrium at the interface was established after about an hour, a value that will depend on the specific silicone mobility, arylimine and crosslink density. We are currently examining ways to build both the magnitude of adhesion forces and rate at which they evolve.

4.6 Conclusions

Silicone imine polymers readily form from commercial aminopropylsilicones and aromatic amines; linear polymers and elastomers are both readily available using the method. In the latter case, either reaction partner can act as the crosslinker. The most attractive combination was pendant aminopropylsilicones and terephthaldehyde for both practical and cost reasons. The polymers are readily degraded at interfaces by amines or, with an excess of amines, completely back to the starting materials. While the dynamic transimination processes are accelerated by dilution with solvent, or acid or amine catalysis, they also operate spontaneously at room temperature. The dynamic nature of the imine bonds allows elastomers to efficiently self-heal, simply on contact for minutes to hours.

4.7 Acknowledgments

We gratefully acknowledge the financial assistance of the Natural Sciences and Engineering Research Council of Canada.

4.8 References

[1] K. Stevenson, B. Stallwood, A.G. Hart, *Bioremediation Journal*, **2008**, 12, 1-11.

[2] J.H. Song, R.J. Murphy, R. Narayan, G.B.H. Davies, Philos. Trans. R. Soc. B., 2009, 364, 2127.

[3] C.K. Das, In *Thermoplastic Elastomers - Synthesis and Applications*, IntechOpen, **2015**, 1-7.

[4] C.R. Martinez, B.L. Iverson, *Chem. Sci., **2012,*** 3, 2191-2201.

[5] A.S. Fawcett, M.A. Brook, *Macromolecules*, **2014**, 47, 1656-1663.

[6] R.C. Boutelle, B.H. Northrop, *J. Org. Chem.,* **2011**, 76, 7994-8002.

[7] P. Reutenauer, P.J. Boul, J.-M. Lehn, *Eur. J. Org. Chem.*, **2009**, 11, 1691-1697.

[8] Y. Jin, A.B. Zhang, Y.S. Huang, W. Zhang, *Chem. Commun.*, **2010**, 46, 8258.

[9] G. Joshi, E.V. Anslyn, *Org. Lett.*, **2012**, 14, 4714-4717.

[10] S.J. Rowan, S.J. Cantrill, G.R.L. Cousins, J.K.M. Sanders, J.F. Stoddart, *Angew. Chem. Int. Ed.,* **2002**, 41, 898-952.

[11] Y. Azuma, T. Terashima, M. Sawamoto, *Macromolecules*, **2017**, 50, 587-596.

[12] Y. Yang, M.W. Urban, *Chem. Soc. Rev.,* **2013**, 42, 7446-7467.

[13] N.A. Chekina, V.N. Pavlyuchenko, V.F. Danilichev, N.A. Ushakov, S.A. Novikov, S.S. Ivanchev, *Polym. Adv. Technol.,* **2006**, 17, 872-877.

[14] J.N. Lee, X. Jiang, D. Ryan, G.M. Whitesides, *Langmuir*, **2004**, 20, 11684-11691.

[15] M.J. Owen, J.I. Evans, Brit. Polym. J., **1975**, 7,(235-245.

[16] M. A. Brook, In *Silicon in Organic, Organometallic, and Polymer Chemistry*, John Wiley & Sons, Inc., New York, **2000**, ch.11.

[17] A.S. Fawcett, T.C. Hughes, L. Zepeda-Velazquez, M.A. Brook, *Macromolecules,* **2015**, 48, 6499-6507.

[18] C.-H. Lei, S.-L. Li, R.-J. Xu, Y.-Q. Xu, J. Elastomers Plast., **2012**, 44, 563-574.

[19] E. Ogliani, L. Yu, I. Javakhishvili, A.L. Skov, RSC Adv., **2018**, 8, 8285-8291.

[20] X. Wu, J. Li, G. Li, L. Ling, G. Zhang, R. Sun, C.P. Wong, J. Appl. Polym. Sci., **2018**,135, 534-539.

[21] P.S. Chang, M.A. Buese, *J. Am. Chem. Soc.,* **1993**, 115, 11475-11484.

[22] M. Ciaccia, R. Cacciapaglia, P. Mencarelli, L. Mandolini, S. Di Stefano, Chem. Sci., **2013**, 4, 2253-2261.

[23] M. Ciaccia, S. Di Stefano, *Org. Biomolec. Chem.*, **2015**, 13, 646-654.

[24] P. Taynton, C. Zhu, S. Loob, R. Shoemaker, J. Pritchard, Y. Jin, W. Zhang, *Polym. Chem.,* **2016**, 7, 7052-7056.

[25] P. Taynton, K. Yu, R.K. Shoemaker, Y. Jin, H.J. Qi, W. Zhang, *Adv. Mater.,* **2014**, 26, 3938-3942.

[26] Y. Jin, Q. Wang, P. Taynton, W. Zhang, *Acc. Chem. Res.,* **2014**, 47, 1575-1586.

[27] B. Zhang, P. Zhang, H. Zhang, C. Yan, Z. Zheng, B. Wu, Y. Yu, *Macromol. Rapid Comm.*, **2017**, 38, 1700110.

[28] A. Yokoyama, T. Yokozawa, *Macromolecules*, **2007**, 40, 4093-4101.

[29] M. Ciaccia, S. Di Stefano, *Org. Biomolec. Chem.,* **2014**, 13, 646-654.

[30] K. Imato, M. Nishihara, T. Kanehara, Y. Amamoto, A. Takahara, H. Otsuka, *Angew. Chem. Int. Ed.,* **2011**, 51, 1138-1142.

[31] P.J. Woodward, D. Hermida Merino, B.W. Greenland, I.W. Hamley, Z. Light, A.T. Slark, W. Hayes, *Macromolecules*, **2010**, 43, 2512-2517.

[32] C.-C. Liu, A.-Y Zhang, L. Ye, Z.-g. Feng, *Chin. J. Polym. Sci.,* **2013,** 31, 251-262.

[33] M. Ciaccia, S. Pilati, R. Cacciapaglia, L. Mandolini, S. Di Stefano, *Org. Biomolec. Chem.,* **2014**, 12, 3282-3287.

Chapter 5 : Thermoplastic Silicone Elastomers from Divanillin Crosslinkers in a Catalyst-Free Process

5.1 Abstract

Silicone elastomers are typically thermosets that are difficult to recycle or repurpose. Thermoplastic silicone elastomers formed from Schiff bases utilize crosslinkers based on petroleum. Vanillin is an aromatic phenolic aldehyde recovered from lignin. We demonstrate that its dimer, divanillin, formed by oxidative coupling using an Fe II/III catalytic process, serves as an effective crosslinker for telechelic and pendent aminopropylsilicones. Pendent-derived elastomers swell in solvents and exhibit dynamic adhesion at their interfaces, but are otherwise relatively intractable, essentially thermosets, due to the combination of Schiff base and H-bonding crosslinks. The elastomers derived from telechelic polymers, by contrast, are thermoplastic; chain extension through Schiff bases is accompanied by H-bonding crosslinking that is readily overcome by either solvents or heat. The silicone starting polymers are readily recovered

** R. Bui, M. A. Brook, *Green Chem., **2021,***23, 5600-5608 - Reproduced with permission from the Royal Society of Chemistry. **Contributions** - Bui was responsible for all experimental work and subsequent write up of the work completed in this chapter.

5.2 Introduction

Most elastomeric materials are thermosets that cannot be recycled or repurposed. Thermoplastic elastomers can exhibit both features, making them attractive as more sustainable alternatives. Silicone elastomers are widely used because of their unusual properties when compared to organic polymers. There are few examples of thermoplastic silicone elastomers, most of which are based on block copolymers that crosslink through noncovalent interactions (hydrogen bonding,[1–3] π-interactions[4]) or reversible covalent interactions (imine,[5] Diels–Alder,[6] borate-diol[7]) between organic building blocks. Both reversible bonding motifs have their advantages. Noncovalent interactions result from relatively simple structural motifs that allow for rapid assembly of multiple weak secondary bonds, while reversible covalent bonds provide relatively stronger interactions but may require more elaborate preparation of both precursor and elastomers.[8–10]

Dynamic thermoplastic polymers, which are remouldable below the melting point, usually offer the benefits of both reversible covalent and noncovalent interactions that allow one to further tune the properties of a material so it can be readily recycled or, better, repurposed.[11–15] The organic monomers required to install these dynamic properties are typically derived from petroleum, a nonrenewable resource.[16,17]

As part of a research program to enhance the sustainability of silicones, we are exploring strategies to increase the quantity of natural constituents carried within them, including saccharides for energy absorbing materials,[18] eugenol as a multifunctional crosslinker,[19] lignin as a functional flame retarding filler,[20] and cysteamine as a source of nitrogen in aminosilicones.[21] Silicone polymers have a high energy requirement for their synthesis. The inclusion of the natural materials dilutes that energy toll for a given

application and can beneficially modify the physical properties of the product elastomer. Could one create dynamic silicone elastomers using alternative abundant sources of sustainable biomass to make more sustainable silicones?

We previously demonstrated that aminosilicones can be used as the basis of dynamic elastomers based on Schiff-base linkages.[5] Vanillin constitutes a natural aromatic aldehyde commonly derived from lignin and is one of few biobased and aromatic compounds currently prepared on an industrial scale.[20,22–26] Polymers derived from vanillin have improved sustainability;[27,28] and/or may possess interesting properties such as chelation[29] and have been used in composites.[30] Dimers of vanillin have been combined with traditional polymers to create bio-based materials with dynamic properties.[31,32]

As with the conversion from petroleum-based to natural feedstocks in many arenas, the natural materials may initially be more expensive, as is the case with vanillin. However, the increasing uptake of lignin production and utilization, as a feedstock rather than simply a fuel,[33] is expected to change that situation. More exciting is the recent report that vanillin can be obtained from post-consumer poly(ethylene terephthalate), which could open it to many new applications.[34] We describe the use of the dimer of vanillin, produced by aqueous oxidation, in the production of dynamic silicone elastomers based on Schiff base crosslinks through divanillin, and examine the benefits in physical properties, including enhanced thermal stability, that result from the presence of phenolic hydrogen bonding.

5.3 Experimental

5.3.1 Materials

Pendent 3-(aminopropyl)methylsiloxane-dimethylsiloxane copolymers (in all cases, terminated with Me_3Si groups): **P-3** AMS-132 (2–3% mol aminopropylmethylsiloxane, **P-5** 4500–6000 g mol^{-1}), AMS-152 (4–5% mol amine 7000–9000 g mol^{-1}), **P-7** AMS-162 (6–7% mol amine, 4000–5000 g mol^{-1}), **P-10** AMS-191 (9–11% mol amine, 2000–3000 g mol^{-1}), AMS-1203 (20–25% mol amine, 20,000 g mol^{-1}); and telechelic 3-(aminopropyl)-terminated polydimethylsiloxanes: **T-19** DMS-A11 (850–900 g mol^{-1}), **T-5** DMS-A15 (3000 g mol^{-1}), **T-3** DMS-A21 (5000 g mol^{-1}), **T-0.6** DMS-A31 (25,000 g mol^{-1}), **T-0.3** DMS-A35 (50,000 g mol^{-1}); and 3-(aminopropyl)pentamethyldisiloxane were purchased from Gelest. Vanillin (≥ 97% purity), toluene, ferrous sulfate heptahydrate (>99 % purity), sodium persulfate (>99.5 % purity) and phenylhydrazine were purchased from Sigma-Aldrich. All reagents were used as received without further purification.

5.3.2 Spectroscopic Analysis of DiVan Silicone Elastomers

Infrared spectroscopy was conducted using a Thermo Scientific Nicolet 6700 FT-IR spectrometer equipped with a Smart iTX attenuated total reflectance (ATR) attachment on thin films of divanillin elastomers. ^{1}H NMR spectra (at 600 Hz) for **DiVan** and **DiVan-T** elastomers were obtained using a Bruker Avance 600 spectrometer.

5.3.3 Physical Testing of Elastomers

Compression Young's moduli of **DiVan-T** and **DiVan-P** elastomers were measured using a MACH-1 micromechanical testing instrument (Biomomentum Instruments) equipped with a 17 N multi-axis load cell and 0.5 mm hemispherical indenter using a Poisson ratio of 0.5 and a constant indentation depth of 1.0 mm with a 1 s dwell time; all measurements

were conducted at 22 °C and in triplicate; errors are reported as the standard deviation. Elastomers with different [divanillin] were cured in Pyrex glass 9-well spot plate (22.2 mm × 7 mm wells), then flat cylindrical disk (ca. *D* = 50 mm, *H* = 30 mm) were cut from the sample.

Thermal Elastomer Remolding Samples of **DiVan-T** elastomers were thermally (re)molded into films and sheets of identical thickness size, that could then be used for tensile testing, dynamic mechanical analysis, and mouldability tests. A heat press (CO-Z Industrial 5-in-1 Clamping heat press) equipped with a flat steel sheet for even pressure and heating was covered in a 0.1 mm Teflon sheet. Spacer of various lengths (1, 2, 5, 10, 50 mm) were used to ensure even thickness in the samples. The heat press was used to clamp samples of **DiVan-T** elastomers using 2 or 4 tons of ramp force between 130-160 °C for various periods of time (minimum 30 min).

Tensile Testing Bone-shaped elastomers **DiVan-T** and **DiVan-P** were clamped at the (larger) ends and tested with an Instron 5900 series Universal Mechanical Tester (ITW Company) equipped with a 25 N load cell. For all experiments, the samples were pre-strained (100%) with a force of 0.002 N, then pulled vertically at a constant rate of 60 mm min^{-1}; tests were done in triplicate with the standard deviation reported as error. Samples were prepared by curing film (thickness = 2.0 mm) with different [**DiVan**], then using a cutting die to cut bone mold samples according to ASTM-D412 Type-D (100 mm *Length* × 16 mm *Width* × 2.0 mm *Height* with a 3.0 mm × 33 mm inner central width and length) A Shore OO durometer (Rex Gauge Company, Inc. USA) was used to characterize the hardness of the elastomers.

Dynamic Mechanical Analysis Thermal creep experiments were conducted on a TA Instruments DMA-850, dynamic mechanical analyzer, equipped with a 5 mm parallel plate compression attachment; using cylindrical elastomer disks (ca. D = 5 mm, H = 3 mm). Creep experiments were conducted with constant strain (10%) and temperature (130-150 °C), allowing each sample to equilibrate at the determined temperature for 10 min, before zeroing the axial force to 0 N. The samples were compressed until the stress relaxation modulus relaxed to ~37% (1/e) of its initial value. This was performed three consecutive times for each sample. The activation energies of the elastomers (E_a) were determined using the methodology in the literature.

Tensile tests on the reprocessed elastomers were conducted to test the efficacy of the elastomeric recovery after thermal stress for **DiVan-T** and the remouldability of **DiVan-P** elastomers. **DiVan-T** elastomer samples of a given sample crosslink density were thermally reprocessed by first grinding the elastomer into a coarse powder using a mortar and pestle to give particles of approximate 0.5 mm diameter. The elastomeric powder was remolded into a monolithic sample using the procedure described for the heat press (see above, 4 tons ramp force, 150 °C) for 3 h. New tensile dog-bone samples were cut from this reprocessed elastomer, then subjected to tensile testing. For **DiVan-P** samples, the broken samples from a previous tensile test were used. The broken dog bone elastomer samples were placed in contact with each other such that the broken interfaces would be in complete contact. The elastomers were clamped in place, then placed in a 160 °C oven for various periods of time. The samples were tested using the previously described tensile testing procedure after 3-, 5-, 10-, and 15- cycles of remolding. Failure of the adhesive weld, or cohesive failure is reported.

5.3.4 Synthesis of Divanillin for Vanillin - DiVan

The divanillin crosslinker was synthesized at a multi-gram scale using a procedure adapted from Wang et al. with some minor modifications.[39] Vanillin (25.00 g, 0.164 mol) was stirred until dissolved in boiling distilled water. A mixture of ferrous sulfate heptahydrate (1.989 g, 6.57 mmol) as the catalytic oxidant and sodium persulfate (23.32 g, 0.970 mmol) as the stoichiometric oxidant; was added to the reaction, turning the initially clear colorless solution dark purple. The reaction was continued for an additional 10 min until a white precipitate formed and the solution turned light brown in color. The reaction was cooled to room temperature, then the precipitate was filtered by vacuum filtration. The collected precipitate was dissolved in 5 M NaOH (~50 mL), then reprecipitated by addition of 5 M HCl (~50 mL). The precipitate was filtered once again, then washed with copious boiling distilled water and boiling methanol. The solid **DiVan** was dried in a vacuum oven (110 °C, 0.3 torr) for 24 h, then ground into a fine powder before washing once again with boiling methanol and water to isolate the purified divanillin (23.97 g, 0.079 mol, 96 %yield) as a light brown solid.

m.p. 300 °C, IR (ATR-IR) ν = 3258, 1674, 1254, 1149, 775, 754 cm^{-1}; ^1H NMR (600 MHz, DMSO-d_6) δ 9.86 (s, 2H), 9.82 (s, 2H), 7.44 (d, 4H, J = 2.4 Hz), 3.93 (s, 6H).

5.3.5 Preparation of Divanillin Silicone Elastomers

Two types of divanillin crosslinked elastomers were prepared; **DiVan-T** elastomers made with telechelic 3-(aminopropyl)-terminated polydimethylsiloxanes of various lengths, and **DiVan-P** elastomers made with 3-(aminopropyl)methylsiloxane-dimethylsiloxane copolymers of various %amine functionality. The procedures for the initial crosslinking of the elastomer are similar, with the exception that **DiVan-P** elastomer must be cast into the

desired shape during the reaction because a thermoset results, while **DiVan-T** elastomer may be thermally remolded into the desired shape.

DiVan-T (DiVan-T-5 shown for DMS-A15): Telechelic 3-(aminopropyl)-terminated polydimethylsiloxanes (DMS-A15, 3000 g mol^{-1}; 10.05 g, 3.35 mmol, 6.70 mmol [amine]) was added to a round-bottomed flask (500 mL), containing toluene (150 mL), and divanillin (1.02 g, 3.35 mmol). The divanillin did not initially dissolve. The reaction was refluxed for 12 h, at which point the divanillin was completely dissolved and began reacting to form the Schiff-base giving the solution a deep wine-red color. The reaction, monitored by IR and NMR, continued at reflux for an additional 24 h, before removing the solvent by rotary evaporation, followed by distillation of excess solvent to yield a dark red elastomer.

For **DiVan-P** elastomers, the reaction mixture was cast into the required shape, for example, a flat sheet; and the reaction was completed in a vacuum oven (150 °C, 0.3 Torr, 24 h). The hardened elastomer was then placed in an oven equipped with a blower fan (160 °C, 72 h) to remove any residual solvent. The elastomer was then isolated as a dark red to black solid (yields > 95 %, for other examples, see Table S1).

Analogous elastomers were prepared from (3-aminopropyl)methylsiloxane-dimethylsiloxane fluids crosslinked using 4,4'-diphenyldialdehyde or terephthaldehyde were prepared using a similar procedure, using $[amine]_0$ = $[aldehyde]_0$. The higher solubility of these crosslinkers compared to **DiVan** decreased the quantity of solvent needed for the elastomer preparation.

Sylgard 184 controls were made by combining the base and curing agent in a 10:1 ratio (10 mL Sylgard 184 base, and 1 mL Sylgard 184 curing agent), then pouring into a Petri dish. The dish was cured in a vacuum oven for 12 h at 60 °C at 0.3 torr.

5.3.6 Aqueous Preparation of DiVan-T Silicone Elastomers

An alternative, more sustainable procedure was used to synthesize **DiVan-T** elastomers that obviates the need for solvent. In these reactions, **DiVan** was added in aliquots into neat telechelic 3-(aminopropyl)-terminated polydimethylsiloxanes. For example, telechelic 3-(aminopropyl)-terminated polydimethylsiloxanes (DMS-A15, 3000 g mol^{-1}; 5.12 g, 1.71 mmol, 3.41 mmol [amine]) was added to a ceramic flask containing divanillin (0.390 g, 0.128 mmol - a starting ratio of 1:0.75 for $[amine]_0 = [aldehyde]_0$. The mixture was heated (160 °C) and stirred until completely dissolved (72 h) to give a red viscous fluid. At that point, the final aliquot of **DiVan** (0.191 g, 0.0423 mmol) was added to the reaction, then the flask was heated in a vacuum oven (160 °C, 0.3 torr) without stirring for a further additional 72 h. The final divanillin elastomer was obtained after cooling to room temperature.

5.3.7 Gel Fraction of Recycled Samples

The gel fraction of **DiVan-T-AM** and **DiVan-P-B** elastomers were measured after multiple cycles of heat press remolding. For these experiments, ~ 2.00 g samples of **DiVan-T-5** (A15, 3000 g mol^{-1}) and **DiVan-P-5** (AMS-152, 4–5% mol amine 7000–9000 g mol^{-1}) were placed in vials containing 30 mL of toluene. The vials were heated to 60 °C for 24 h. The solvent was removed from the samples, which were then washed with toluene. The swollen elastomers were placed in a vacuum oven (110 °C, 0.3 torr) for 24 h. The gel fraction was measured as the ratio of the starting mass of the elastomer and the mass after distillation in the vacuum oven. To test the effect of heat remolding on the gel fraction; similar elastomer pieces were then ground into a powder using a mortar and pestle until a fine powder was obtained, that was then heat pressed (160 °C, 3 h) into a monolithic sample. The samples were reprocessed multiple times before being subjected to the same

gel fraction experiment as previously described, recording the Young's modulus of the sample and gel fraction after each cycle (Figure S3). This procedure was repeated for a maximum total of 15-cycles of heat pressing.

5.3.8 Chemical Reprocessing of Divanillin Silicone Elastomers

Samples of **DiVan-T-5** (A15, 3000 g mol^{-1} α,ω-(3-aminopropyl)polydimethylsiloxane, 0.653 M [amine]) or **DiVan-P** (A152, 5% mol aminopropyl, 8000 g mol^{-1} (3-aminopropyl)methylsiloxane-dimethylsiloxane copolymer, 0.675 [amine]) with similar [**DiVan**] were cut into identical sized strips (10 mm x 100 mm x 0.10 mm thickness), that were partially submerged in toluene (25 °C) and observed over 7 d. The experiment was repeated with new pieces of the same elastomer but with the addition of an excess of phenylhydrazine (72.2 mg, 0.70 mmol) to capture any exposed aldehydes. This experiment proceeded for 48 h at room temperature, at which time NMR was used to determine the composition of the liquid phase of both experiments.

5.4 Results and Discussion

5.4.1 Synthesis of DiVan

Control studies were undertaken to ensure that the natural aldehyde vanillin would react with 3-aminopropylpentamethyldisiloxane (Figure 5.1A) to give imines in a similar fashion to terephthaldehyde, which we previously examined.[5] A Schiff-base, **1**, formed in nearly quantitative yields in under 1 hour, as determined by NMR (Figure S 22). The only byproduct of this reaction was water, which spontaneously phase separated from the hydrophobic silicone and then evaporated; the presence of water was not observed to be detrimental to the yield of the reaction.

A difunctional analogue of vanillin was required to act as a chain extender to form copolymers and/or crosslink linear polymers into elastomers. Vanillin was therefore dimerized using an aqueous radical coupling reaction with ferrous sulfate as the radical initiator, and sodium persulfate, formed cleanly using the electrolysis of sulfate, as the stoichiometric oxidant to form divanillin **DiVan** (Figure 5.1B).[35] The reaction was rapidly and easily accomplished on a multi-gram scale in good yield, ~95%, with water as the only solvent and a simple workup; two batches (2 x ~25 g) of **DiVan** were synthesized and purified within 3 hours. The low solubility of **DiVan** in common solvents, relative to vanillin and the sulfonated organic salt impurities, facilitated its isolation.

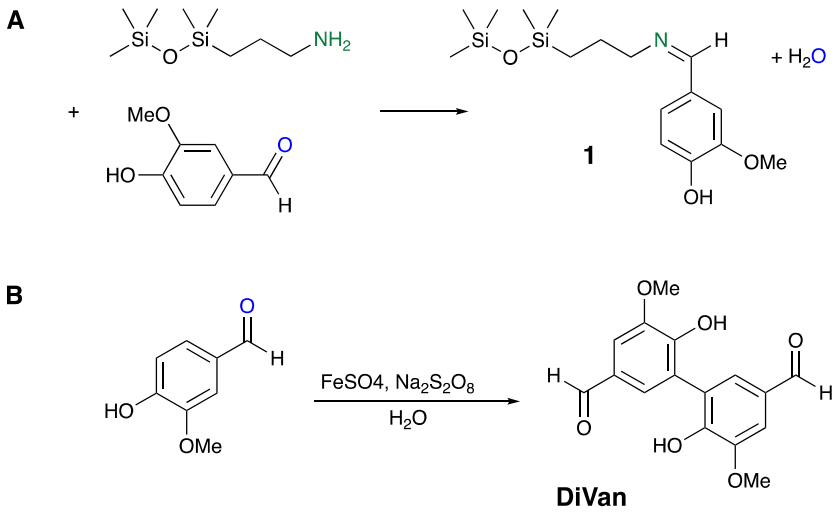

Figure 5.1. A) Reaction of vanillin with 3-aminopropylpentamethyldisiloxane to produce a Schiff-base. B) Synthesis of **DiVan** by aqueous oxidative coupling of vanillin.

5.4.2 The Reactions of Divanillin with 3-aminopropylsilicones

The synthesized **DiVan** was used as a chain extender with telechelic α,ω-(3-aminopropyl)polydimethylsiloxanes to give **DiVan-T** elastomers or as a crosslinker with different pendent (3-aminopropyl)methylsiloxane-dimethylsiloxane copolymers, in which the mol% aminopropyl mole groups varied, to give **DiVan-P** elastomers (Table S 5, Figure

5.2). The amines condense with the aldehydes to yield Schiff bases that serve as crosslinks between silicone backbones.

DiVan has low solubility in all organic solvents except DMSO, which was advantageous with respect to synthesis and purification but was detrimental when trying to react it with 3-aminopropylsilicones. The reactions of aminopropylsilicones with **DiVan** were relatively slow when compared to more soluble aromatic aldehydes.[5] Both pendent and telechelic-derived elastomers required synthesis at reflux in toluene of a

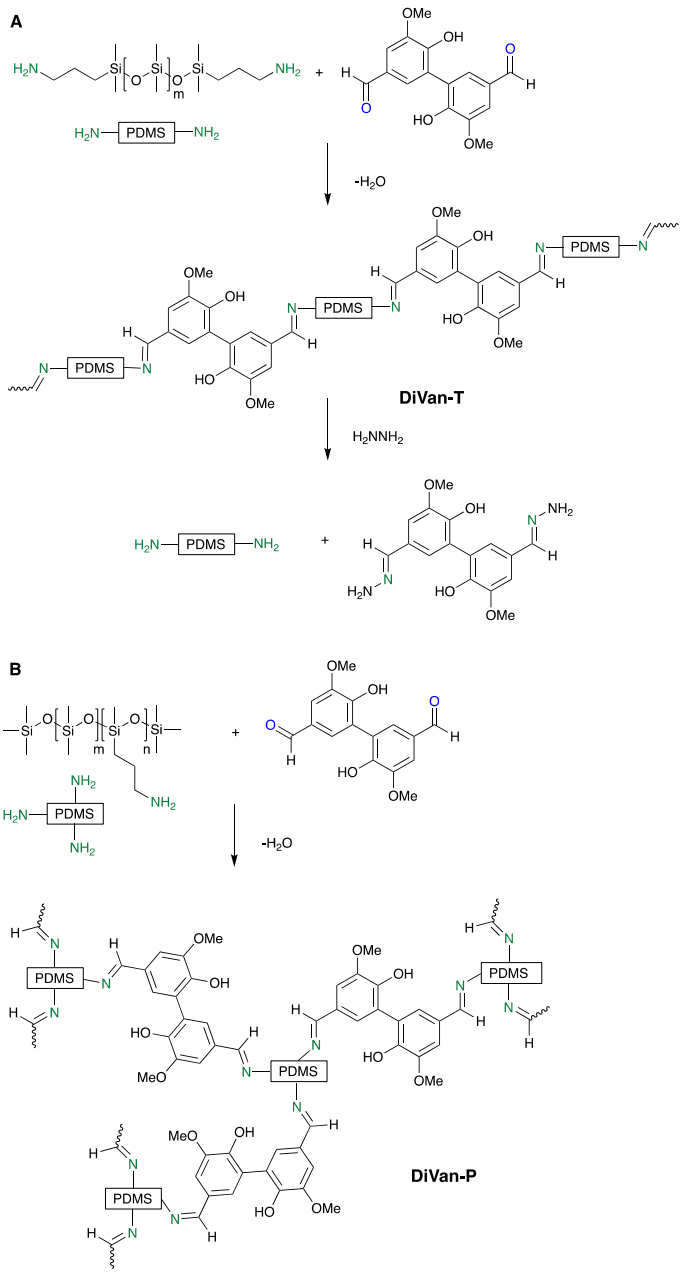

Figure 5.2. Crosslinking via with divanillin Schiff-base bonds of A) (3-aminopropyl)methylsiloxane-dimethylsiloxane copolymers to give **DiVan-T** and, B) α,ω-(3-aminopropyl)polydimethylsiloxanes to create **DiVan-P**, respectively.

dispersion of divanillin with the desired 3-aminopropylsilicone using a 1:1 ratio of $[amine]_0$: $[aldehyde]_0$ for 48 hours; the reactions were impractically slow at room temperature. The

synthesis of **DiVan-P** elastomers can be accelerated using an excess of amine, however, reaction times were still > 36 hours. As **DiVan** and 3-aminopropylsilicones reacted to form Schiff-base bonds, solutions of the newly formed **DiVan-T** and **DiVan-P** adducts turned a deep wine-red color. Elastomers were recovered upon removal of the solvents.

An alternative, greener synthesis that avoided solvents entirely was conducted with **DiVan-T** to produce similar materials. **DiVan** was dispersed in α,ω-(3-aminopropyl)polydimethyl-siloxanes using a starting ratio of 1:0.75 for $[amine]_0$ = $[aldehyde]_0$ and heated for 3 days with stirring at 160 °C to get partial cure; a viscous, but still tractable fluid, was produced. Then the remaining **DiVan** was added to the viscous polymer mixture that was heated for an additional 3 days at 160 °C. The elastomer rapidly hardened as it cooled to room temperature. Reaction progress was monitored by tracking the decreasing [amine] and [aldehyde] or the increasing [imine] signals with nuclear magnetic resonance or infrared spectroscopy (Figure S 23). This method was useful for **DiVan-T** but proved unsuitable for preparing **DiVan-P**, as the rapidly evolving viscosity build, and consequent issues with mixing, led to inconsistent crosslinking through the sample. We are exploring the use of green catalysts to speed up the reactions both with and without solvents.

5.4.3 Physical Properties of Divanillin-Silicone Elastomers

A series of **DiVan-P** elastomers was prepared using pendent aminoalkyl silicone polymers that possessed different fractions of amine monomers (Table S 6, **P-B**); in all cases, a slight excess of **DiVan** was added to ensure all amines were consumed. That is, the primary contributors to the physical properties of the elastomers were divanillin crosslinks, rather than excess amines (Figure 3). The physical properties of these polymers were

compared with analogous products **Tere-P** and **DiPhen-P** formed from the non-phenolic aryl aldehydes terephthaldehyde and 4,4'-biphenyldialdehyde, respectively (Figure 5.3A, Table S 6, ESI†). In all cases, the Young's moduli of these materials increased with crosslink density, but the presence of the OH and, to a lesser extent, -OMe groups on the **DiVan-P** elastomers led to much harder materials at the same crosslink density than those derived from simple aromatic aldehydes **DiPhen-P**. It is inferred this is due to secondary crosslinking provided by H-bonding of the phenols.

Table 5.1 Mechanical properties of all **DiVan-T**, **DiVan-P** elastomers and control samples (prepared from pendent aminosilicones using 4,4'-biphenyldialdehyde **DiPhen-**P).

DiVan-T-A Starting Material[a] **T-A**	Base Molar mass	YM[b] MPa	Shore A[c]	Tensile Stress MPa	Tensile Strain at Break (%)
T-19	0.9k	3.05	65	1.128	103
T-5	3k	1.38	35	0.430	176
T-3	5k	1.10	21	0.115	197
T-0.6	25k	0.483	54 (OO)	0.0218	220
T-0.3	50k	0.104	31 (OO)	0.0143	255
DiVan-P-B Starting Material[a] **P-B**	Base Molar mass	YM[b] MPa	Shore A[c]	Tensile Stress (MPa)	Tensile Strain at Break (%)
P-3	5.5k	1.44	54 (OO)	1.02	153
P-5	8k	2.98	52	1.97	118
P-7	4k	5.71	61	3.22	110
P-10	2.5k	8.43	75	5.21	108

a The number refers to the % amine-containing monomers in the starting aminosilicone polymer. The products are: **DiVan-T-A**, and **DiVan-P-B**. b YM Young's modulus. c Where indicated, Shore OO rather than Shore A hardness measurements were made on softer samples.

DiVan-T polymers, prepared analogously, unexpectedly presented as solid elastomeric materials even at very low [divanillin] (e.g., [divanillin] = 0.02 mM for **DiVan-T-0.3**, Table S 5, ESI†). Polymers synthesized using 900 g mol^{-1} **DiVan-T-19** or 3000 g mol^{-1} **DiVan-T-**

5 α,ω-(3-aminopropyl)polydimethylsiloxanes had Young's moduli of 3.05 or 1.32 MPa, respectively. This contrasted with the viscous fluids that result from analogous reactions with 4,4'-biphenyldialdehyde or terephthaldehyde.[5] This observation is consistent with the comment above about secondary curing via H-bonding that, unlike simple aromatic aldehydes, is available to **DiVan** derivatives (Figure 5.3A).

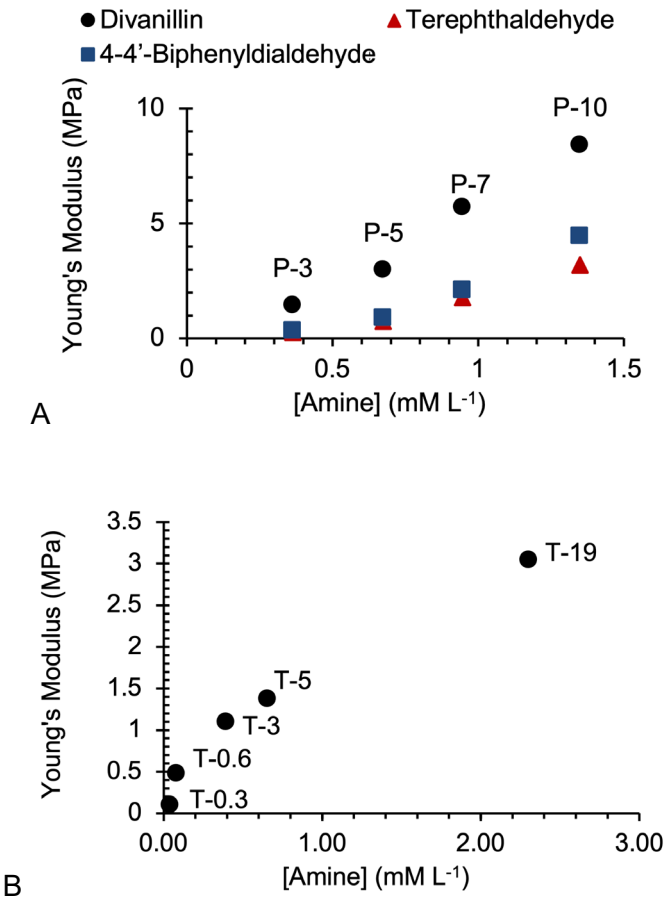

Figure 5.3. A) Young's moduli for elastomers formed from pendent (3-aminopropyl)methylsiloxane-dimethylsiloxane copolymers with different amine densities and **DiVan-P**, terephthaldehyde **Tere-P**, and 4,4'-biphenyldialdehyde **DiPhen-P**, respectively. B) Young's modulus measurements for a series of **DiVan-T** formed from different molecular weights of α,ω-(3-aminopropyl)polydimethylsiloxanes.

Note that, unlike **DiVan-P** materials that have a covalently crosslinked network structure, the **DiVan-T** materials are chain extended but not covalently crosslinked. Their physical properties are tuned by H-bonding that can be overcome at higher temperatures; they are thermoplastic elastomers.

Distinct differences in silicone networks derived from pendent or telechelic polymers were evident from their behaviors in solvents. After 12 hours, **DiVan-T** completely dissolved in toluene; after evaporation, the elastomer reformed in the shape of the vessel. By contrast, **DiVan-P** only swelled after soaking for 7 days. The **DiVan-T** elastomers can be reformed into their original shapes after evaporation of the solvent, allowing for recycling of the elastomer. The gel fraction of each elastomer sample was measured for 15-cycles of recycling (Figure S 25). Both elastomers maintained their Young's moduli after 15-cycles of recycling. The gel fraction of **DiVan-T** elastomers decreases after each cycle, while **DiVan-P** elastomers remained constant. If permanent, irreversible degradation of either elastomer type was desired, this could be invoked by use of phenylhydrazine in the toluene. The reaction led to recovery of the original aminosilicone oils, and **DiVan** dihydrazone (Figure 5.4, Figure S 25). The reaction and dissolution of **DiVan-T** with the hydrazine solution was much faster than the **DiVan-P** sample: 3 vs 48 hours. These data are consistent with dynamic imine exchange[5, 36, 37] being intercepted by phenylhydrazine to give hydrazones that are favored over imines in the equilibrium.

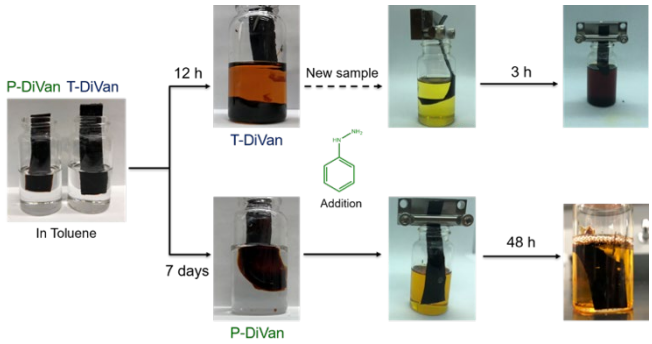

Figure 5.4. Solvent interactions of **DiVan-T** and **DiVan-P** elastomers with toluene, and an excess of phenylhydrazine in toluene.

5.4.4 Remouldability/Thermal Properties of DiVan-P and DiVan-P Elastomers

We reasoned that the dynamic crosslinks could be facilitated by thermal compression remolding as an alternative to the use of solvents. Pieces of cut **DiVan-T** elastomers were placed in a heat press (130 °C) using 2 ToF (tons of force) for 30 minutes. As can be seen, this was insufficient to completely reform the elastomer (Figure 5.5A); the elastomer pieces melted and coalesced into a single flat elastomer sheet without exhibiting cracks or edges from the original pieces after an additional 30 minutes cycle at 4 ToF for 30 minutes. Increasing the sample temperature, however, to 180 °C allowed for remolding by hand, obviating the need of a heat press (Figure 5.5B).

This double pressure/thermal treatment was insufficient to melt process the **DiVan-P** samples. The individual pieces retained their shape and exhibited only slight adherence between sites where one elastomer piece contacted another. One strategy to improve the processability of the **DiVan-P** elastomers involves the addition of an amine catalyst to promote bond exchange. A series of **DiVan-P** elastomers were made with different excesses of amine ([aminopropyl]$_{excess}$) at a constant crosslink density (**DiVan-PX-3CL**, Table S 7). For example, **DiVan-P5-3CL** elastomers were prepared by using a 5 mol %

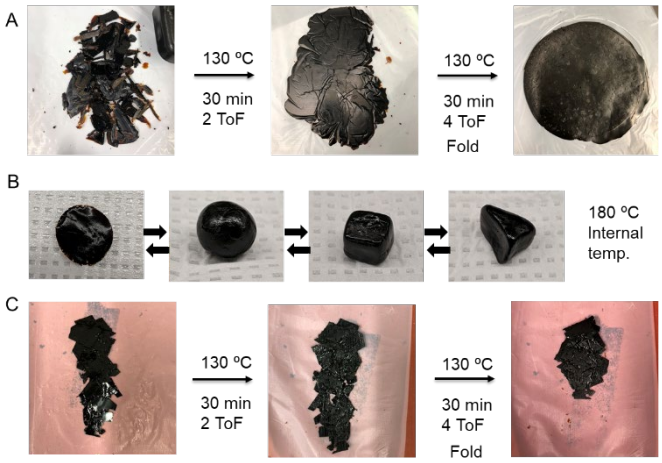

Figure 5.5. A) Thermal compression remolding of **DiVan-T-5**. B) Remolding of **DiVan-T-5** After heating at 180 °C for 5 min. C) **DiVan-P-7-3CL** elastomers over two cycles at 130 °C using 2 and 4 ToF, respectively.

(3-aminopropyl)methylsiloxane-dimethylsiloxane as the starting prepolymer, but then crosslinking only 3 mol% (1.92 mmol) of the available amine groups leaving 2% (1.45 mmol) of the amines unreacted. When the **DiVan-P-X-3CL** elastomers containing excess amine were heat pressed under the same conditions the materials rapidly self-adhered provided elastomer/elastomer contact existed between individual pieces. However, the pieces maintained their shape and didn't exhibit melt flow (Figure 5.5C). These samples required significantly longer contact times to initiate adhesion at polymer interfaces when compared to **DiVan-T** elastomers. Increasing the concentration of $[amine]_{excess}$ led to more rapid adhesion because they possess a greater surface concentration of amine groups that can initiate bond exchange (Figure 5.6A); **DiVan-P11-3CL**, initiated adhesion most rapidly, requiring only 3 h of heating to heal 90 % of its tensile strength. After 6 h of heating, all **DiVan-PX-CL** healed > 90 % of their original tensile strength (Figure 5.6B). The control sample, **DiVan-P3-3CL**, which possesses no excess amines, showed very little adhesion between elastomer pieces even after 6 hours of heating.

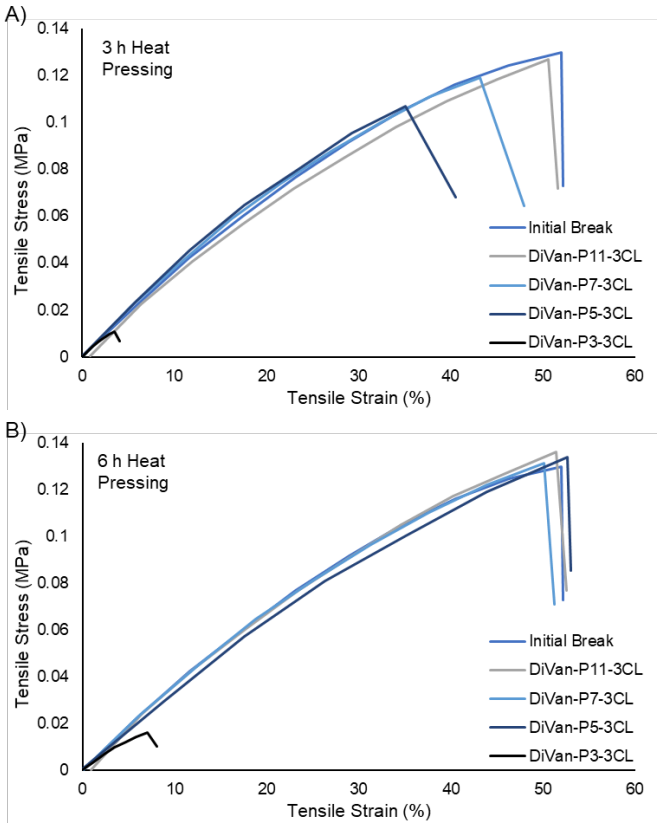

Figure 5.6. Tensile testing of self-adhered **DiVan-PX-3CL** elastomers after heat pressing at 130 ˚C for A) 3h and B) 6h showing the efficiency of healing by the recovered tensile strength when compared to the initial break of a **DiVan-P-3** sample.

The thermal stress-relaxation behavior was further examined using dynamic mechanical compression analysis. **DiVan-T** elastomer coupons were compressed under constant strain (10% strain) at constant elevated temperature (120-150 °C, Figure 5.7, and Figure S 26); controls were provided by **DiVan-T** at 25 °C, and a cured commercial thermoset silicone sample (Sylgard 184) at 150 °C. The room temperature **DiVan-T** control showed no significant relaxation after 1500 s, while the Sylgard 184 control relaxed to ~90% of its initial modulus after 1500 s at 150 °C.

Unsurprisingly, all materials relaxed more rapidly as the temperature increased. Furthermore, a decrease in the relaxation times was observed to correlate with a higher

fraction of silicone in the sample. The calculated Arrhenius activation energy for each molecular weight of α,ω-(3-aminopropyl)polydimethylsiloxane prepolymer was calculated by fitting the material relaxation to Equation S1 (Table S 8). The **DiVan-T** elastomer made from 5000 g mol^{-1} α,ω-(3-aminopropyl)polydimethylsiloxane prepolymer (**DiVan-T-3**) had an activation energy of 103.8 kJ mol^{-1} (Table S 8), a value that coincides with reported activation energies for transimination of Schiff-base bonds (96.2 kJ mol^{-1}).[36, 38] These results indicate that the material can be simply reprocessed or remolded with very little loss in energy. **DiVan-T** networks prepared from lower molecular weight α,ω-(3-aminopropyl)polydimethylsiloxane prepolymers such as **DiVan-T-19** exhibited longer relaxation times, resulting in a much larger activation energy of 206.03 kJ mol^{-1}, indicating that the dynamic bond exchange kinetics depend on the structure of the crosslinker and also the concentration of entities that can participate in noncovalent interactions. These observations are consistent with work done by Dichtel et al.,[38] that showed the rates of relaxation in a material depend on several factors that are not present in traditional solution-based chemistry.

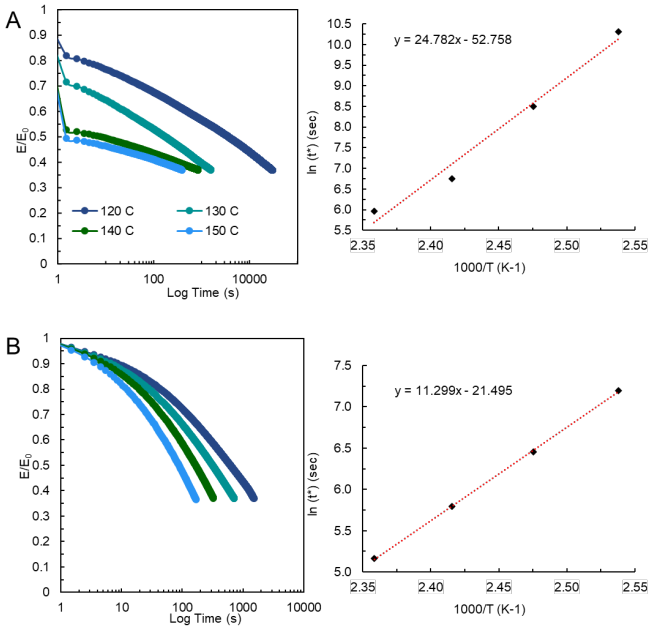

Figure 5.7. Dynamic mechanical analysis of A) **DiVan-T-19** and B) **DiVan-T-0.6** elastomers under constant strain (10%) from 120-150 °C and at 25 °C as a control. Showing the relaxation of the material from initial stress, to E/E_0 = 1/e (~0.37), and Arrhenius plot modelling the Maxwell viscoelastic relaxation. ToF = tons of force.

These results further support the dynamic nature of the Schiff-base crosslinks. The bond exchange is promoted by elevated temperatures likely by increasing the chain-mobility of the silicone, allowing for bonds to rearrange in response to the pressure exerted by the press. Upon cooling to room temperature, both types of elastomers **DiVan-T** and **DiVan-P** retained their original hardness and modulus. The differences in thermal response between the two types of materials can be explained by the relative chain-mobility in two types of materials. Covalent crosslinking in the **DiVan-P** elastomers restricts the mobility of the amine and imine groups, preventing the bulk flow of the material. Bond exchange therefore only occurs at the interface between **DiVan-P** elastomer pieces resulting in adhesion. At elevated temperatures, **DiVan-T** elastomers exhibit bulk flow, as the weaker noncovalent (H-bonding) interactions are broken, allowing for the linear **DiVan-T** polymer chains to flow. Even here, increased crosslink density inhibits the dynamic behavior and

higher temperatures were needed for samples with higher crosslink densities **DiVan-T-19** vs **DiVan-T-0.3** (Figure 5.7, Figure S 26). These observations are likely the result of a balance between increased bond concentration, which allows for greater contact between bonds to initiate bond exchange, with a reduction in mobility of the more highly crosslinked material that conversely reduces the ability for the groups to find each other.

Vanillin brings several benefits to dynamic silicone elastomers. In particular, it permits replacement of petroleum-derived materials with biomass derivatives. The **DiVan** linker is produced in a sustainable fashion, in water, with a cleanly produced, electrically generated persulfate oxidant. More interestingly, the presence of the phenolic OH groups in **DiVan** transforms the physical behaviors of elastomers derived from aminosilicones when compared to the petroleum-derived analogues 4,4'-diphenyldialdehyde or terephthaldehyde. In this process, neither catalyst nor solvent is required and the water byproduct spontaneously phase separates, facilitating isolation. Strong H-bonding from the OH groups lead to elastomers with much higher thermal stability. These could be overcome with both telechelic and pendant-derived elastomers by reaction with hydrazine, which irreversibly converted elastomer back to aminosilicone oil and divanillin dihydrazone. The pendent elastomer **DiVan-P** swelled slightly in solvent and only under pressure and heat exhibited slight dynamic adhesion at interfaces. By contrast, the telechelic analogue **DiVan-T** dissolved, eventually, in solvent, exhibited dynamic responses at interfaces and could conveniently be melt processed. The properties of the telechelic materials are readily tuned and, because of their dynamic properties, are readily converted into new elastomers – repurposed – using solvent or simply heat.

5.5 Conclusions

The natural product vanillin, after dimerization, serves as crosslinker for both telechelic and pendent (3-aminopropyl)polydimethylsiloxanes via dynamic Schiff-base bonds. The mechanical properties of these elastomers can be controlled with [amine] in the starting prepolymer. Pendent derived materials were thermosets that were difficult to reprocess. Products derived from telechelic silicones were thermoplastic materials and, in addition, dissolution in solvent led to analogous elastomers after solvent evaporation. Both types of polymers were readily converted back to the silicone starting materials by adding phenylhydrazine These materials improve the sustainability of silicone elastomers by the inclusion of a reagent derived from renewable biomass, decreasing the amount of silicone required in the material; and improving processability using the dynamic bond exchange mechanisms such that reuse of the elastomer is facilitated.

5.6 Acknowledgments

We gratefully acknowledge the financial support of the Natural Sciences and Engineering Research Council of Canada.

5.7 References

[1] Y. Chen, A. M. Kushner, G. A. Williams, Z. Guan, *Nat. Chem.*, **2012**, 4, 467-472.

[2] K. Yu, A. Xin, Z. Feng, K. H. Lee, Q. Wang, *J. Mech. Phys. Solids*, **2020**, 137, 103831.

[3] J. Huang, L. Cao, D. Yuan, Y. Chen, *ACS Appl. Mater. Interfaces*, **2018**, 10, 40996-41002.

[4] A. Fatona, J. Moran-Mirabal, M. A. Brook, *Polym. Chem.*, **2019**, 10, 219-227.

[5] R. Bui, M. A. Brook, *Polymer*, **2019**, 160, 282-290.

[6] J.-W. Kim, D. H. Lee, H.-J. Jeon, S. I. Jang, H. M. Cho, Y. Kim, *Appl. Surf. Sci.*, **2018**, 429, 128-133.

[7] M. A. Brook, L. Dodge, Y. Chen, F. Gonzaga, H. Amarne, *Chem. Commun.*, **2013**, 49, 1392-1394.

[8] M. E. Belowich, J. F. Stoddart, *Chem. Soc. Rev.*, **2012**, 41, 2003-2024.

[9] Y. Jin, Q. Wang, P. Taynton, W. Zhang, *Acc. Chem. Res.*, **2014**, 47, 1575-1586.

[10] S. P. Black, J. K. M. Sanders, A. R. Stefankiewicz, *Chem. Soc. Rev.*, **2014**, 43, 1861-1872.

[11] B. Zhang, P. Zhang, H. Zhang, C. Yan, Z. Zheng, B. Wu, Y. Yu, *Macromol. Rapid Comm.*, **2017**, 38, 1700110.

[12] Y. Miwa, J. Kurachi, Y. Kohbara, S. Kutsumizu, *Commun. Chem.*, **2018**, 1, 5.

[13] J. Liu, J. Liu, S. Wang, J. Huang, S. Wu, Z. Tang, B. Guo, L. Zhang, *J. Mater. Chem. A*, **2017**, 5, 25660-25671.

[14] Y. Peng, Y. Yang, Q. Wu, S. Wang, G. Huang, J. Wu, *Polymer*, **2018**, 157, 172-179.

[15] Y. Chen, Z. Tang, Y. Liu, S. Wu, B. Guo, *Macromolecules*, **2019**, 52, 3805-3812.

[16] H. A. Wittcoff, B. G. Reuben, J. S. Plotkin, in *Industrial Organic Chemicals*, Wiley, Hoboken NJ, 3rd edn., **2012**, 4, 93–138.

[17] Y. Liao, S.-F. Koelewijn, G. Van den Bossche, J. Van Aelst, S. Van den Bosch, T. Renders, K. Navare, T. Nicolaï, K. Van Aelst, M. Maesen, H. Matsushima, J. M. Thevelein, K. Van Acker, B. Lagrain, D. Verboekend, B. F. Sels, *Science*, **2020**, 367, 1385.

[18] K. Faiczak, M. A. Brook, A. Feinle, *Macromol. Rapid Comm.*, **2020**, 41, 2000161.

[19] S. E. Laengert, A. F. Schneider, E. Lovinger, Y. Chen, M. A. Brook, *Chem. Asian J.*, **2017**, 12, 1208-1212.

[20] J. Zhang, E. Fleury, Y. Chen, M. A. Brook, *RSC Adv.*, **2015**, 5, 103907-103914.

[21] A. Lusterio, M. Melendez-Zamudio, M. A. Brook, *Ind. Eng. Chem. Res.*, **2021**, 60, 3830-3838.

[22] J. Zhang, E. Fleury, M. A. Brook, *Green Chem.*, **2015**, 17, 4647-4656.

[23] I. A. Pearl, *J. Am. Chem. Soc.*, **1942**, 64, 1429-1431.

[24] J. D. P. Araújo, C. A. Grande, A. E. Rodrigues, *Chem. Eng. Res. Des.*, **2010**, 88, 1024-1032.

[25] G. Banerjee, P. Chattopadhyay, *J. Sci. Food Agric.*, **2019**, 99, 499-506.

[26] C. Fargues, Á. Mathias, A. Rodrigues, *Ind. Eng. Chem. Res.*, 1996, **35**, 28-36.

[27] A. S. Amarasekara, R. Garcia-Obergon, A. K. Thompson, *J. Appl. Polym. Sci.*, **2019**, 136, 47000.

[28] M. Fache, B. Boutevin, S. Caillol, *Eur. Polym. J.*, **2015**, 68, 488-502.

[29] R. Zhao, X. Yong, M. Pan, J. Deng, K. Pan, *Separ. Purif. Tech.*, **2020**, 246, 116916.

[30] J. F. Stanzione III, J. M. Sadler, J. J. La Scala, K. H. Reno, R. P. Wool, *Green Chem.*, **2012**, 14, 2346-2352.

[31] E. Savonnet, E. Grau, S. Grelier, B. Defoort, H. Cramail, *ACS Sus. Chem. Eng.*, **2018**, 6, 11008-11017.

[32] G. Garbay, L. Giraud, S. M. Gali, G. Hadziioannou, E. Grau, S. Grelier, E. Cloutet, H. Cramail, C. Brochon, *ACS Omega*, **2020**, 5, 5176-5181.

[33] J. Zhang, M. A. Brook, in *Mobilizing Chemistry Expertise To Solve Humanitarian Problems Volume 2*, American Chemical Society, **2017**, 1268, 6, 91-116.

[34] J. C. Sadler, S. Wallace, *Green Chem.*, **2021**, 23, 4665-4672.

[35] P. Jantaree, K. Lirdprapamongkol, W. Kaewsri, C. Thongsornkleeb, K. Choowongkomon, K. Atjanasuppat, S. Ruchirawat, J. Svasti, *J. Agric. Food Chem.*, **2017**, 65, 2299-2306.

[36] P. Taynton, C. Zhu, S. Loob, R. Shoemaker, J. Pritchard, Y. Jin, W. Zhang, *Polym. Chem.*, **2016**, 7, 7052-7056.

[37] M. Ciaccia, S. Di Stefano, *Org. Biomolec. Chem.*, **2015**, 13, 646-654.

[38] B. R. Elling, W. R. Dichtel, *ACS Central Science*, **2020**, 6, 1488-1496.

[39] Q. Wang, R. E. Smith, R. Luchtefeld, A. Y. Sun, A. Simonyi, R. Luo, G. Y. Sun, *Phytomedicine*, **2008**, 15, 496-503.

Chapter 6 : General Conclusions

Silicones have exceptional physical properties that are difficult to emulate with carbon-based polymers, leading to their widespread use in industrial applications. The chemical behaviour of silicone base polymers must be modified with organic functionality to permit utilization in specific applications. Reports of silicone materials crosslinked via novel organic bonds are limited, in part, by the need for appropriate organic functionalization and, in some cases, intolerance by silicones of the catalysts needed for crosslinking via organic functional groups. As discussed in this thesis, the utilization of amine-functionalized silicones – crosslinked through organic reactions – provides alternative organic crosslinking methods for silicone elastomers that exhibit different tolerances than classical crosslinking reactions. The resulting silicones possess unique physical and chemical properties that can be predicted by the crosslinking moieties used. The expansion of potential crosslinking reactions for silicones leads to further innovation in current use cases of silicone materials such as sealants, adhesives, and elastomeric materials as well as potential applications outside the current scope of silicone materials.

Chapter 2 reports on the investigation of crosslinking of aminopropylsilicones through various condensation reactions with aliphatic aldehydes; formaldehyde, glutaraldehyde, and glyoxal. It was shown that aqueous solutions of aliphatic aldehydes are readily with the amine-functionalized silicone despite their immiscibility. This high reactivity allows for rapid crosslinking at room temperature without the requirement of solvent or catalyst and leads to the release of water as the only byproduct. These properties give the reactions greater functional tolerance compared to classical crosslinking methods, as exemplified by the ability for these reactions to occur in the presence of water.

In Chapter 3, the crosslinking of aminopropylsilicones by polycondensation with glutaraldehyde discussed in Chapter 2 was explored as a printing material for an innovative droplet ejection and free space droplet merging 3-D printer. The rapid rate of crosslinking and relatively low vapour pressure of glutaraldehyde allowed for the use of low viscosity ink formulations, which is advantageous for droplet ejection, merging, and mixing and completely different – much more rapid – than traditional silicone crosslinking methodologies. Secondary condensation reactions that occur after the initial gelation of the aminosilicone-glutaraldehyde elastomer aid in adhesion between layers of printed material. The printer was able to print free-standing silicone elastomers with detailed features without the need of the support materials commonly used in other printing methods.

Chapter 4 examined the extension of aldehyde/amine reactions of aminopropylsilicones with aromatic aldehydes to polymers and elastomers formed using Schiff-base crosslinks that can undergo dynamic exchange reactions. The manipulation of these bonds with solvent, acid, or an amine catalyst after crosslinking gives chemoplastic properties, selective adhesion, and controlled degradation abilities to elastomers. The robustness of this crosslinking reaction and the facile reactivity with simple primary amines post-cure allows for the exploration of nucleophilic amine chemistry that was previously difficult to achieve in a silicone environment with previous curing methods.

In Chapter 5 of this thesis, the Schiff-base crosslinking scheme in Chapter 4 was used to create more sustainable silicone materials. This was accomplished through a two-pronged approach. First, crosslinking of aminopropylsilicones was achieved using divanillin, a product derived from renewable biomass. Second, the product elastomers contain remouldable Schiff-base bonds such that the product may be repurposed. The

combination of a larger π-system and phenolic groups, when compared to materials from Chapter 4, introduced additional noncovalent hydrogen bonding and π-interactions to the silicones. These noncovalent bonds behave as additional weak crosslinks that cause linear divanillin-crosslinked silicone polymers to become solids. These weaker bonds can be manipulated by heating, allowing the elastomers to be easily remoulded. The thermal properties of these elastomers were probed by dynamic mechanical analysis to determine the thermal energy required for remoulding at different crosslinker concentrations.

In conclusion, this thesis showed that two reactions well known in organic chemistry could be profitably used to crosslink functional-silicone elastomers through the reaction of aminopropylsilicones with organic aldehydes and further demonstrated their utility in various applications. These reactions contribute to the expansive catalogue of methods for crosslinking silicone materials by having unique functional tolerance allowing for the design of novel silicone materials previously hindered by classical curing technologies. The crosslinking with aliphatic aldehydes from Chapter 2 has unprecedented tolerance with aqueous solutions and would be suited for combining silicones with hydrophilic materials. The reaction with aromatic aldehydes examined in Chapter 5 to produce silicones crosslinked through dynamic bonds. The unique properties of these bonds can further the application of silicones in novel applications. In addition, silicones provide an advantageous medium for studying dynamic bonds because of their high chain mobility at room temperature. Future work will focus on the application of these two reactions with novel crosslinkers, which should lead to unique physical and chemical properties, as seen in the materials discussed. In addition, these studies could examine the synthesis of aldehyde-functionalized silicone fluids that can be crosslinked with novel organic amines through the same types of bonds.

Appendix

List of Supplementary Figures

Figure S 1: ATR-IR spectra of elastomers synthesized from the crosslinking of DMS-A15 (3000 g mol^{-1} telechelic aminopropylsilicone) with A) formaldehyde, B) glutaraldehyde, or C) glyoxal. 150

Figure S 2: NMR overlay of products from reaction the of 3-aminopropylpentamethyldisiloxane with formaldehyde 151

Figure S 3: NMR overlay of different products from reaction of 3-aminopropylpentamethyldisiloxane with glutaraldehyde in 1:1 and 1:2 [NH_2]:[CHO] ratios. 151

Figure S 4: NMR overlay of different products from reaction of 3-aminopropylpentamethyldisiloxane with glyoxal in 1:1, 2:1, and 2:3; [NH_2]:[CHO] ratios. 152

Figure S 5: Young's modulus of DMS-A15 (3000 g mol^{-1} telechelic aminopropylsilicone) elastomer cured with aldehyde; glutaraldehyde, glyoxal, formaldehyde, using different mole ratios [NH2]:[CHO]. 153

Figure S 6: Optical images of DMS-A21 (5000 g mol^{-1} telechelic aminopropylsilicone) cured with A) formaldehyde, B) glyoxal, or C) glutaraldehyde after initial gelation, and after complete cure and drying. 155

Figure S 7: Cure as determined by change in compressive Young's modulus for aldehydes with A: lower MW telechelic aminopropylsilicones and B: formaldehyde with a 50,000 MW aminopropylsilicones. 156

Figure S 8: Infrared spectra of DMS-A15 (3000 g mol-1 telechelic 3-aminopropyl-terminated polydimethylsiloxane) crosslinked A) with excess glutaraldehyde after drying in oven for 1 h, showing residual aldehyde groups (1708 cm-1) and B) after submerging in aqueous solution of lysine. C) With 1:1 stoichiometry [NH2]:[CHO] using formaldehyde; red curve after cure in air 1 hour, blue curve after 24 h in boiling water. 158

Figure S 9: SEM images elastomers cured in 50 wt% emulsions of 3000 g mol-1 telechelicaminopropylPDMS with 2-4 to give A) For-T, B) Gly-T, C) Glu-T. Scale bar – 100 µm. 160

Figure S 10: TGA of the degradation of AMS-152 (4-5% mol aminopropylmethylsiloxane, 7000-9000 g mol-1) crosslinked with A: formaldehyde, B: glyoxal, or C: glutaraldehyde. 163

Figure S 11: Long-term printing. The diameter of droplets of each material was stable and equal to 40.22 μm for silicone base, 32.78 μm for curing agent, and 50.57 μm for PDMS, with a small standard deviation of 0.52 μm, 0.69 μm, and 0.81 μm, respectively. The velocity also maintained a stable value, 1.04 m/s for silicone base, 1.05 m/s for curing agent and 0.82 m/s for PDSM, with the negligible variation of 0.02 m/s for each material. 166

Figure S 12: Impact of the electrostatic forces generated by the glass substrate on the droplet mixing stabilization. ***a)*** *Printing process – the distance between the merging point and the surface is equal to four centimeters. The droplets of 50% glutaraldehyde in water (left-hand side) were dispensed with the velocity of 0.83 m/s, and they were inclined at 30.25^{o} with respect to the vertical axis, while the droplet, made of DMS-A11, had a velocity of 0.84 m/s and the angle 30.28^{o}.* ***b)*** *The distance was reduced to 6mm. The trajectory and velocity of DMS-A11 were unchanged, however, drops of 50% glutaraldehyde in water exhibited a higher velocity, 0.93 m/s, and reduced angle, 28.72^{o}, which hindered the droplet merging process.* ***c)*** *Neutralization of the electrostatic forces by connecting the nozzles and the substrate electrically to the ground.****d)*** *Neutralization of the charging by polarizing the print bed through placing a silicon wafer below the glass substrate and using it as a gate electrode, which compensates the charges on the substrate (scale bar 100 μm).* 167

Figure S 13: Visualization of the mixing and deposition of the droplet on a non-uniform surface, made of 1 mm thick glass segments, which does not influence the stabilization of the mixing process (scale bar = 100 μm). 168

Figure S 14: Printing on demand. Stabilization of the mixing process in multiple start-stop cycles. During the unstable printing regime, which takes 94ms, the material loss was equal to 298.5 pL of DMS-A11, and 186 pL in case of the 50% glutaraldehyde in water. 169

Figure S 15: Dark polymerization of aminopropyl-terminated polydimethylsiloxane and glutaraldehyde solution 50% wt. in water. 170

Figure S 16: NMR of the product from the reaction between 3-aminopropylpentamethyldisiloxane and benzaldehyde. 172

Figure S 17: IR of TPA-PDMS elastomer at 5 mins and after full cure (3 hours) showing aledehyde and imine at 5 mins but only imine at full cure. 173

Figure S 18: Overlay of IR spectra from 2-10% crosslinked TPA-PDMS elastomers, and terephthaldehyde. 174

Figure S 19: Partial hydrolysis of pentamethyldisiloxane imine shows both aldehyde (9.95 ppm), imine (8.20 ppm), and water (1.56 ppm) after 20 minutes (complete hydrolysis required 30 minutes). 175

Figure S 20: NMR spectrum of the product from the degradation of a 5% crosslinked TPA-PDMS elastomer by dodecylamine solution. 175

Figure S 21: TGA of the decomposition of 7% crosslinked TPA-PDMS elastomer from 25-700 °C heating at a rate of 10 °C min-1 _____ *176*

Figure S 22: NMR spectrum of the ***DiVan*** *crosslinker dissolved in DMSO-d_6.* _____ *177*

Figure S 23: Infrared spectra from the reaction between divanillin and α,ω-(3-aminopropyl)polydimethylsiloxanes, showing the conversion of aldehydes to imines. 178

Figure S 24: Swelling and Young's Modulus of ***DiVan-T-5*** *and* ***DiVan-P-5*** *after multiple cycles of swelling crumbled elastomer and heat pressing to obtain new monolithic samples.* _____ *180*

Figure S 25: Infrared spectrum of the products from degrading DiVan-P elastomers with excess phenylhydrazine for 48 h. _____ *180*

Figure S 26: Arrhenius thermal stress-relaxation of A) DiVan-T-19, B) DiVan-T-5, C) DiVan-T-3 and D) DiVan-T-0.6 elastomers under constant strain (10%) from 120-150 °C and at 25 °C as a control. Showing the relaxion of the material from initial stress, to E/E0 = 1/e (~0.37), and Arrhenius plot modeling the Maxwell viscoelastic relaxation. _____ *182*

List of Supplementary Tables

Table S 1: Physical properties of aldehyde crosslinked silicone elastomers. _____ *157*

Table S 2: Young's modulus of DMS-A15 (3000 g mol-1 telechelic aminopropylsilicone) _____ *160*

Table S 3: Changes in Young's Modulus as a function of heating at 250 °C. _____ *162*

Table S 4: Crosslink densities for formaldehyde crosslinked elastomers calculated using Flory-Rehner equation. _____ *164*

*Table S 5: Formulations of **DiVan-T** elastomers using different molecular weights of α,ω-(3-aminopropyl)polydimethylsiloxanes and **DiVan-P** elastomers using pendent (3-aminopropyl)methylsiloxane-dimethylsiloxane copolymers in which the mol% aminopropyl mole groups varied in a 1:1, or 1:1.1 ratio; the latter being used exclusively for determining physical properties.* _____ *178*

Table S 6: Physical properties of DiPhen-P elastomers made using 4'4-diphenyldialdehye and pendent (3-aminopropyl)methylsiloxane-dimethylsiloxane copolymers in which the mol% aminopropyl differ _____ *179*

*Table S 7: Formulations of elastomers **DiVan-P-B-3CL** with the same crosslink density made from pendent (3-aminopropyl)methylsiloxane-dimethylsiloxane copolymers in which the mol% aminopropyl differ, but with the same amount of divanillin (leading to different excesses* _____ *181*

Table S 8: Calculated material relaxation activation energies of DiVan-T elastomers using different molecular weights of telechelic 3-(aminopropyl)-terminated _____ *183*

Appendix: 1. Catalyst Free Silicone Sealants That Cure Underwater - Supplementary Information

Appendix 1.1. Spectroscopic Analysis of Aliphatic Aldehyde Crosslinking

Model Studies of Aliphatic Aldehydes with 3-aminopropylpentamethyldisiloxane

Small scale reactions were completed using 3-aminopropylpentamethyldisiloxane with eachaldehyde crosslinker (formaldehyde, glutaraldehyde, and glyoxal).

Glutaraldehyde: In a vial 3-aminopropylpentamethyldisiloxane (0.0990 g, 0.447 mmol) was diluted with chloroform (1.20 mL), then glutaraldehyde solution (79 μL, 50wt%

glutaraldehyde in water, 0.442 mmol glutaraldehyde) was added to the solution, resulting in a dark red solution after shaking for 1 min. Sodium sulfate (0.100 g) was added as a desiccant, which made the solution turn a darker red. The solution was heated at 60 °C for 2 h withstirring, then filtered to remove the hydrated sodium sulfate. The solvent was removed by rotary evaporation, yielding a dark red material that was soluble in organic solvents such astoluene, dichloromethane, or chloroform (0.131 g, mass balance 92%).

IR (ATR-IR): ν = 3016, 2953, 2929, 2864, 1663, 1634, 1586, 1505, 1456, 1409, 1356, 1250,1175, 1119, 1045, 836, 797, 751, 686, 543 cm^{-1}. ^{1}H NMR (600 MHz, chloroform-*d*) δ 8.12 (s,1H, -CHN), 7.58 (s, 1H, CHN), 5.90 (m, 1H, HC=C), 3.59 (q, 2H, CH_2), 1.76 (p, 2H, CH_2),0.50 (t, 2H, Si-CH_2), 0.050 (s, 15H, Si-CH_3).

Glyoxal: The preceding procedure was used. 3-Aminopropylpentamethyldisiloxane (0.0990 g, 0.447 mmol); chloroform (1.20 mL), glyoxal solution (34 μL, 40 wt% glyoxal) in water, 0.299 mmol glyoxal) resulting in a pale-yellow solution; after 1 min of shaking sodium sulfate(0.100 g) was added to the solution as desiccant. The solvent was removed

by rotary evaporation yielding a dark orange oil (0.103 g, mass balance 89%). IR (ATR-IR): ν = 3005, 2955, 2897, 2867, 2834, 1675, 1631, 1559, 1464, 1349, 1251, 1174, 1149, 1117, 1048, 901, 837, 750, 704, 687, 664. ^{1}H NMR (600 MHz, chloroform-*d*) δ 8.11 (s, 1H, CHN), 4.27 (m, 2H, H_2CN), 3.78 (m, 2H, H_2CN), 3.50 (t, 2H, H_2CN), 1.47 (p, 6H, CH_2), 0.44 (t,6H, Si-CH_2), 0.050 (s, 45H, Si-CH_3).

Formaldehyde: The preceding procedure was used. 3-Aminopropylpentamethyldisiloxane (0.0960 g, 0.433 mmol); chloroform (0.200 mL); formalin solution (32 μL, 37wt% formaldehyde in water, 0.433 mmol H_2CO); the solution was further diluted with additional chloroform (1.00 mL). The addition of sodium sulfate (0.100 g) as a desiccant led to the opaque-white solution becoming transparent. After removal of the solvent was removed by rotary evaporation, a transparent oil was recovered (0.100 g, mass balance 90%). IR (ATR-IR): ν = 2954, 2929, 2798, 1538, 1455, 1408, 1366, 1307, 1250, 1215, 1175, 1127, 1039, 915, 836, 750, 685, 625 cm^{-1}. ^{1}H NMR (600 MHz, chloroform-*d*) δ 3.24(s, 2H, CH_2), 2.34 (t, 2H, CH_2), 1.43 (p, 2H; CH_2), 0.44 (t, 2H; Si-CH_2), 0.00 (s, 15H; Si-CH_3).

Appendix 1.2. Spectroscopic Analysis of Aliphatic Aldehyde Crosslinking

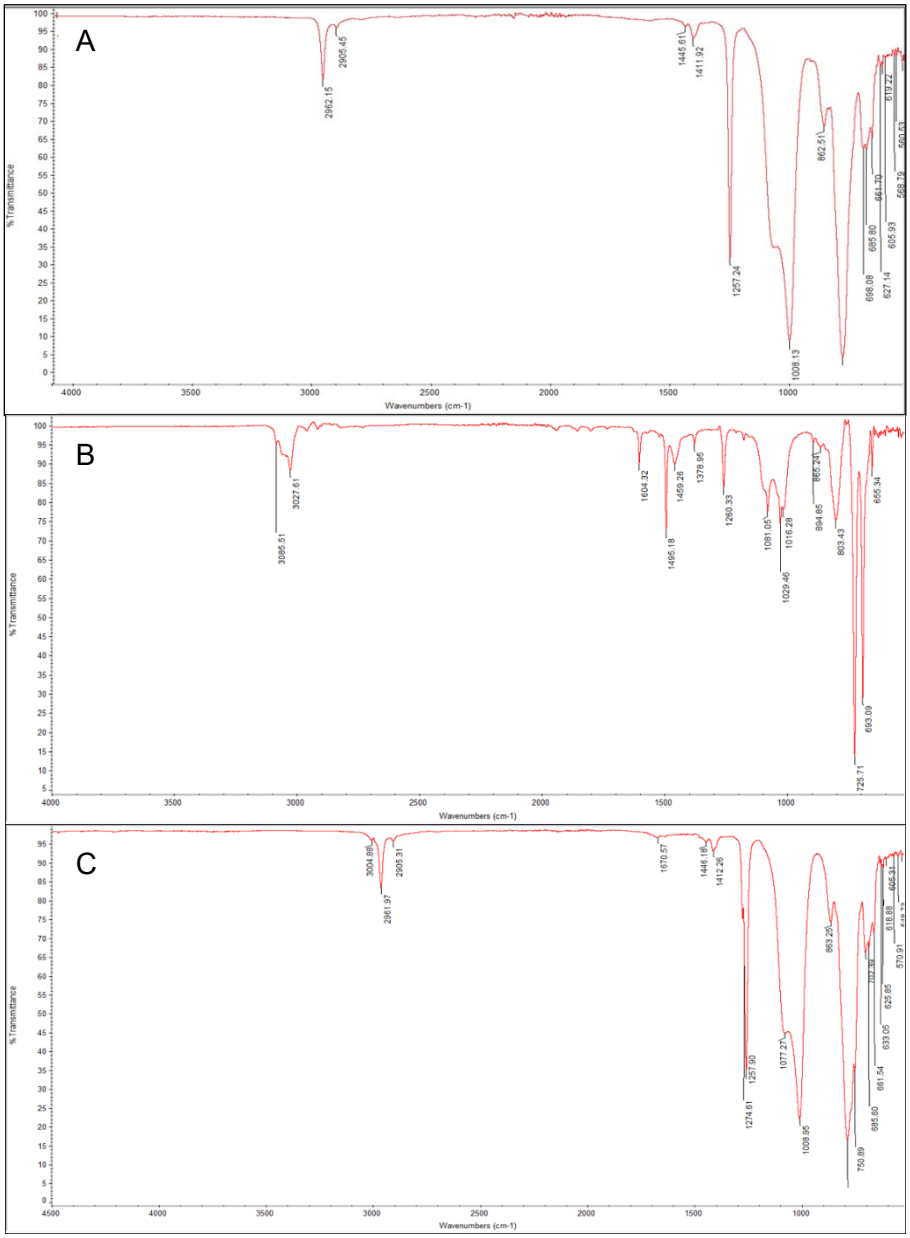

Figure S 1: ATR-IR spectra of elastomers synthesized from the crosslinking of DMS-A15 (3000 g mol^{-1} telechelic aminopropylsilicone) with A) formaldehyde, B) glutaraldehyde, or C) glyoxal.

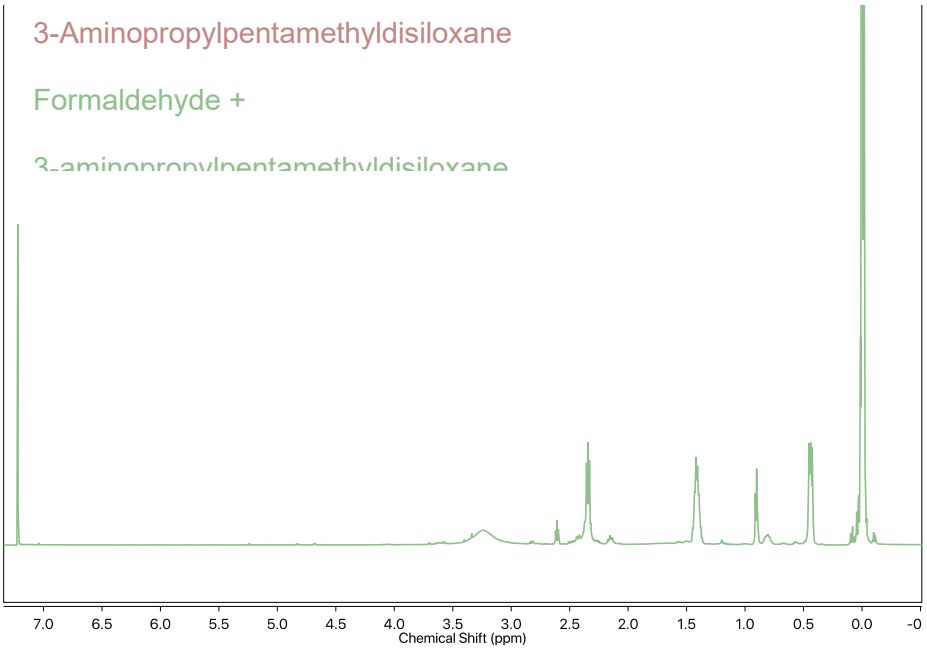

Figure S 2: NMR overlay of products from reaction the of 3-aminopropylpentamethyldisiloxane with formaldehyde

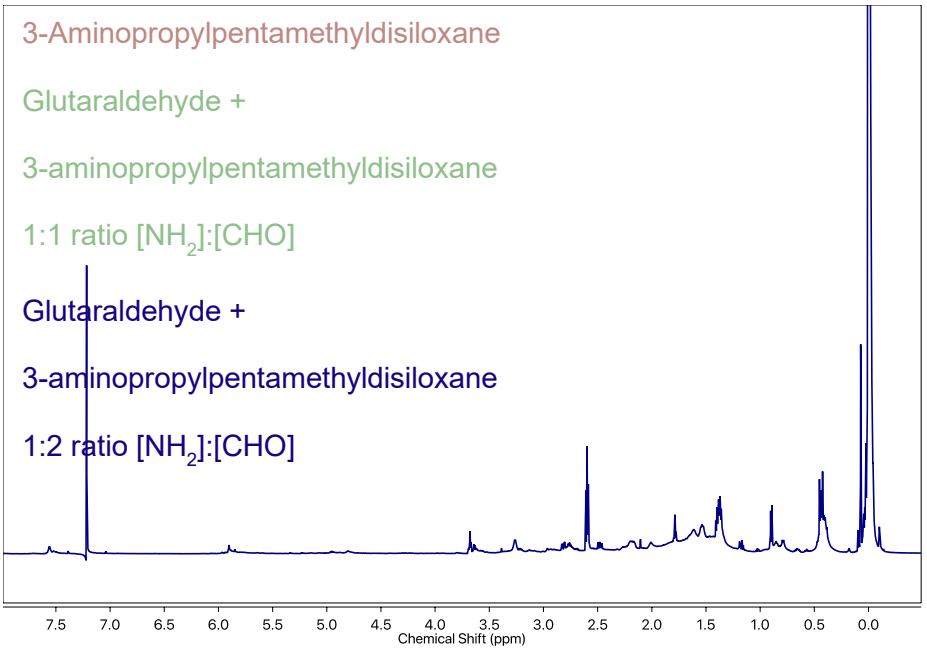

Figure S 3: NMR overlay of different products from reaction of 3-aminopropylpentamethyldisiloxane with glutaraldehyde in 1:1 and 1:2 [NH_2]:[CHO] ratios.

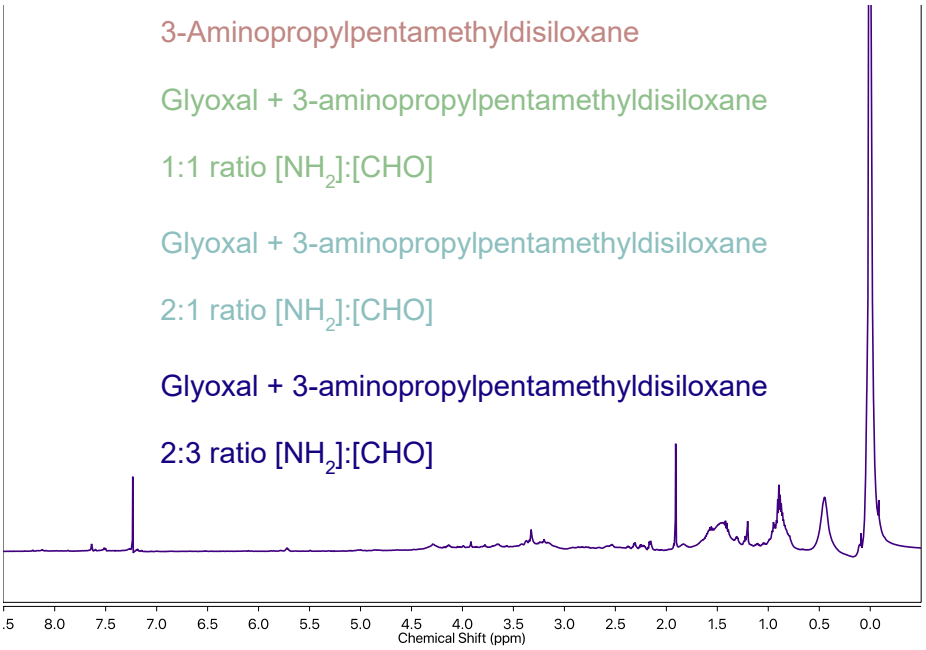

Figure S 4: NMR overlay of different products from reaction of 3-aminopropylpentamethyldisiloxane with glyoxal in 1:1, 2:1, and 2:3; $[NH_2]$:[CHO] ratios.

Appendix 1.3. Determination of Elastomer Stoichiometery

Elastomers were synthesized using a constant volume of DMS-A15 (1 mL, 0.983 g, 0.655 mmol, 3000 g mol^{-1} telechelic aminopropylsilicone) with each aqueous aldehyde solution in different mole ratios $[NH_2]$:[CHO] in a plastic vial. The elastomers were allowed to cure for 1.5 h, removed from the vial to dry in air for 24 h, then placed in a 45 ºC vacuum oven at 0.3 torr. The Young's modulus of the elastomers were measured in triplicate. The mole ratio that gives the highest Young's modulus for each aldehyde crosslinker was used for all elastomers in this work.

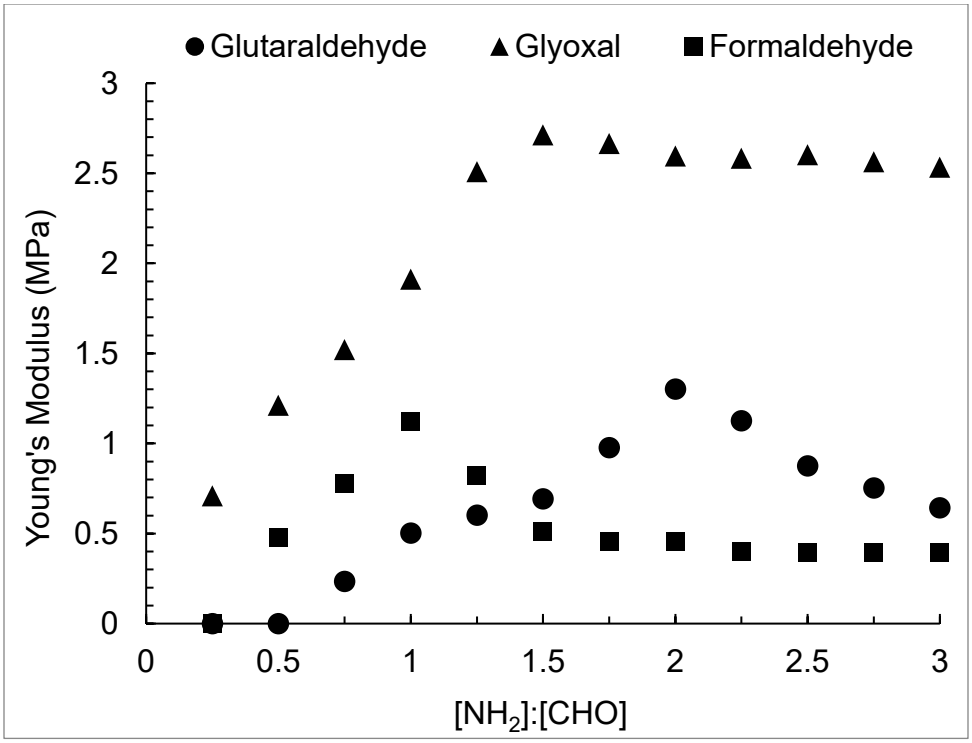

Figure S 5: Young's modulus of DMS-A15 (3000 g mol^{-1} telechelic aminopropylsilicone) elastomer cured with aldehyde; glutaraldehyde, glyoxal, formaldehyde, using different mole ratios [NH2]:[CHO].

Appendix 1.4. Preparation of Aliphatic Aldehyde Elastomers

Synthesis of Glyoxal-Crosslinked Silicone Elastomers

Gly-P (Glyoxal-Crosslinked Pendent- and Gly-T Telechelic- AminopropylPDMS Elastomers) were prepared using 3-(aminopropyl)methylsiloxane-dimethylsiloxane copolymers (@ 3, 5, 7, 10 % mol 3-(aminopropyl)methylsiloxane, respectively) or using telechelic 3-(aminopropyl)-terminated polydimethylsiloxanes (@ 900, 3000, 5000, 25000, 50000 g mol^{-1}) using a 2:3 ratio of NH_2: HCO (Table S1). For example, AMS-152 (0.923 g, 5% mol aminopropylmethylsiloxane 8500 g mol^{-1}, 0.624 mmol NH_2) was combined with glyoxal solution (26.5 μL, 40%wt glyoxal in water, 0.234 mmol, 0.468 mmol HCO) in a vial and stirred until homogenously white, then poured into a glass spot plate. The mixture slowly increased in viscosity until it gelled (15 s) and then converted to a pale-yellow

elastomer over 3 h at room temperature. The elastomer turned from pale yellow to light red after dehydrating for 12 h in a 60 °C vacuum oven at 0.3 torr.

IR (ATR-IR): v = 3005, 2962, 2905, 1670, 1446, 1412, 1274, 1257, 1077, 1009, 863, 785, 750, 661, 633 cm^{-1}.

Synthesis of Glutaraldehyde Crosslinked Silicone Elastomers

Glu-P and Glu-T elastomers were prepared using a similar procedures, using glutaraldehyde to crosslink pendent 3-(aminopropyl)methylsiloxane-dimethylsiloxane copolymers (@ 3, 5, 7, 10 % mol 3-(aminopropyl)methylsiloxane) or telechelic α,ω-(3-aminopropyl)PDMS (@ 900, 3000, 5000, 25000, and 50000 g mol^{-1}), using a 1:2 ratio of NH_2: HCO (Table S1). In a typical preparation, DMS-A11 (0.965 g, 900 g mol^{-1} telechelic 3-aminopropylpolydimethylsiloxane, 1.07 mmol, 2.14 mmol NH_2) was mixed with aqueous glutaraldehyde (0.380 μL, 5.65 M, 2.15 mmol, 4.32 mmol CHO) was added to the vial and the contents were vigorously mixed until homogenous. The mixture quickly gelled (<30 s) into an opaque pale-orange elastomer, which was allowed to cure for 3 h at room temperature to yield a dark red elastomer. The elastomer was placed in a 60 °C vacuum oven at 0.3 torr for 3 h. Physical tests on the elastomer were conducted after dehydration.

IR (ATR-IR): ν = 3085, 3027, 2961, 1654, 1523, 1495, 1459, 1379, 1260, 1081, 1029, 1016, 803, 725, 693, 655 cm^{-1}.

Appendix 1.5. Aliphatic Aldehyde Elastomer Images

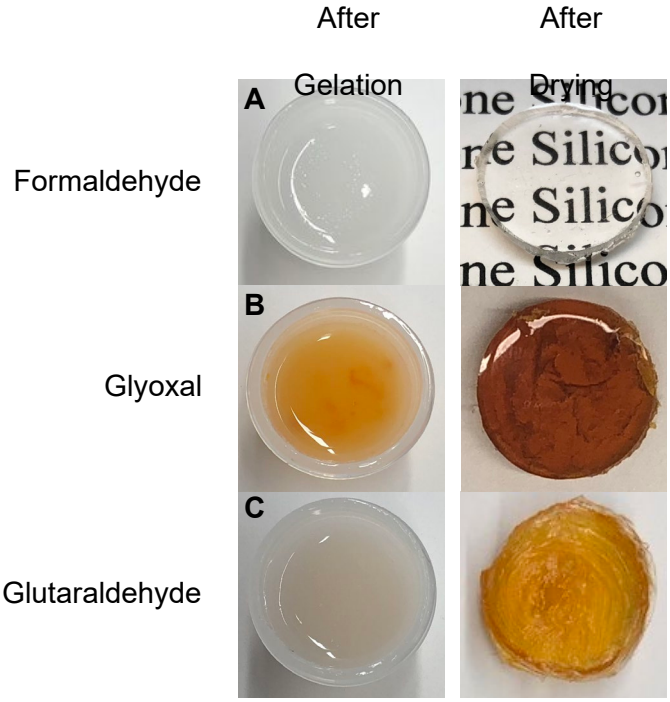

Figure S 6: Optical images of DMS-A21 (5000 g mol^{-1} telechelic aminopropylsilicone) cured with A) formaldehyde, B) glyoxal, or C) glutaraldehyde after initial gelation, and after complete cure and drying.

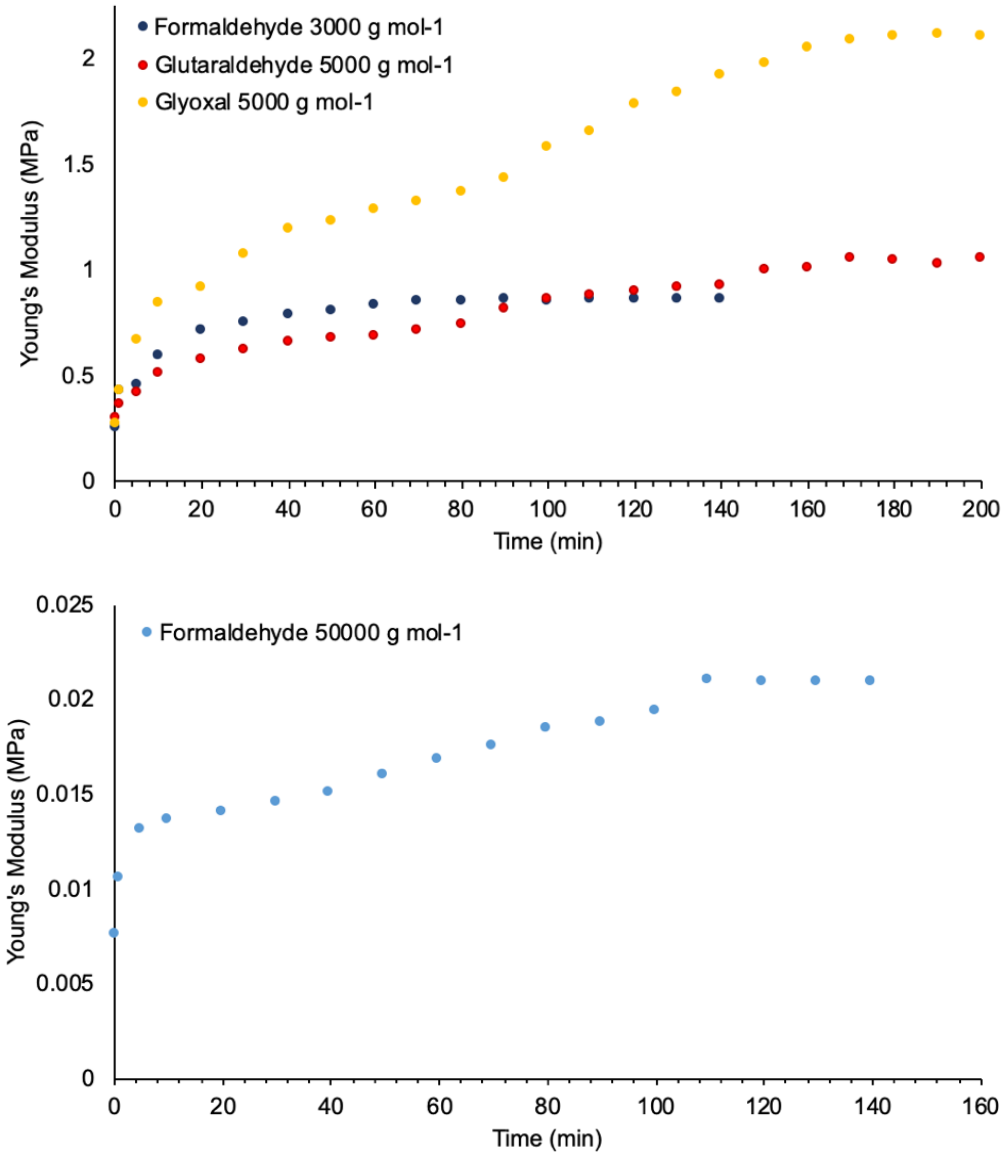

Figure S 7*:* Cure as determined by change in compressive Young's modulus for aldehydes with A: lower MW telechelic aminopropylsilicones and B: formaldehyde with a 50,000 MW aminopropylsilicones.

Table S 1: Physical properties of aldehyde crosslinked silicone elastomers.

Entry	% mol aminopropyl	M_n (g mol^{-1})[a)]	[Amine] (mol L^{-1})	Shore hardness (OO)	Young's modulus (MPa)[b,c)]	Stress at break (MPa)[b,c)]	Strain at break (%)[c)]
Telechelic-Modified AminopropylPDMS and Glyoxal (**Gly-T**)							
11		900	2.30	25(A)	5.09±0.02	0.491	119
12		3000	0.653	55	2.16±0.02	0.36	146
13		5000	0.392	43	1.15±0.03	0.205	176
14		25000	0.0784	35	0.0673±0.0004	0.114	258
15		50000	0.0392	18	0.0427±0.0003	0.0675	324
Pendent-Modified AminopropylPDMS and Glyoxal (**Gly-P**)							
16	3%	5500	0.258	13	0.241±0.004	0.258	160
17	5%	8000	0.675	58	1.81±0.03	0.349	133
18	7%	4000	0.946	65	3.23±0.01	0.442	125
19	10%	2500	1.35	10(A)	4.45±0.04	0.521	116
20	25%	2000	3.38	32(A)	6.03±0.05	0.702	108
Telechelic-modified aminopropylPDMS and Glutaraldehyde (**Glu-T**)							
21		900	2.30	74	1.14±0.02	0.660	135
22		3000	0.653	54	1.00±0.04	0.410	155
23		5000	0.392	47	0.434±0.005	0.341	165
24		25000	0.0784	33	0.0471±0.0003	0.172	220
25		50000	0.0392	28	0.0298±0.0005	0.121	250
Pendent-modified aminopropylPDMS and Glutaraldehyde (**Glu-P**)							
26	3%	5500	0.258	25	0.886±0.005	0.181	175
27	5%	8000	0.675	46	1.38±0.03	0.277	145
28	7%	4000	0.946	59	1.69±0.01	0.364	140
29	10%	2500	1.35	71	2.07±0.02	0.592	120
30	25%	2000	3.38	20(A)	3.29±0.03	0.88	115

Entry	Crosslinker	Ratio pendent to telechelic aminopropylsilicone	[Amine] (M)	Shore hardness (OO)	Young's modulus (MPa)	Stress at break (MPa)	Strain at break (%)
31	**2**	90:10	0.588	42	0.691±0.003	0.241	151
32	**2**	50:50	0.343	29	0.375±0.002	0.180	186
33	**3**	90:10	0.588	47	1.25±0.01	0.325	140
34	**3**	50:50	0.343	31	0.657±0.006	0.112	177
35	**4**	90:10	0.588	38	0.605±0.002	0.284	142
36	**4**	50:50	0.343	25	0.468±0.004	0.120	213

[a)] Manufacturer's specification, not measured. Since each amine can participate in 1 crosslink, this value constitutes the resulting crosslink density of the elastomer.

[b)] Mean value from triplicate measurements, with the standard deviation reported as error.

[c)] Moduli were determined using compression measurements, while Stress and Strain at break were determined with dogbones in tensile measurements.

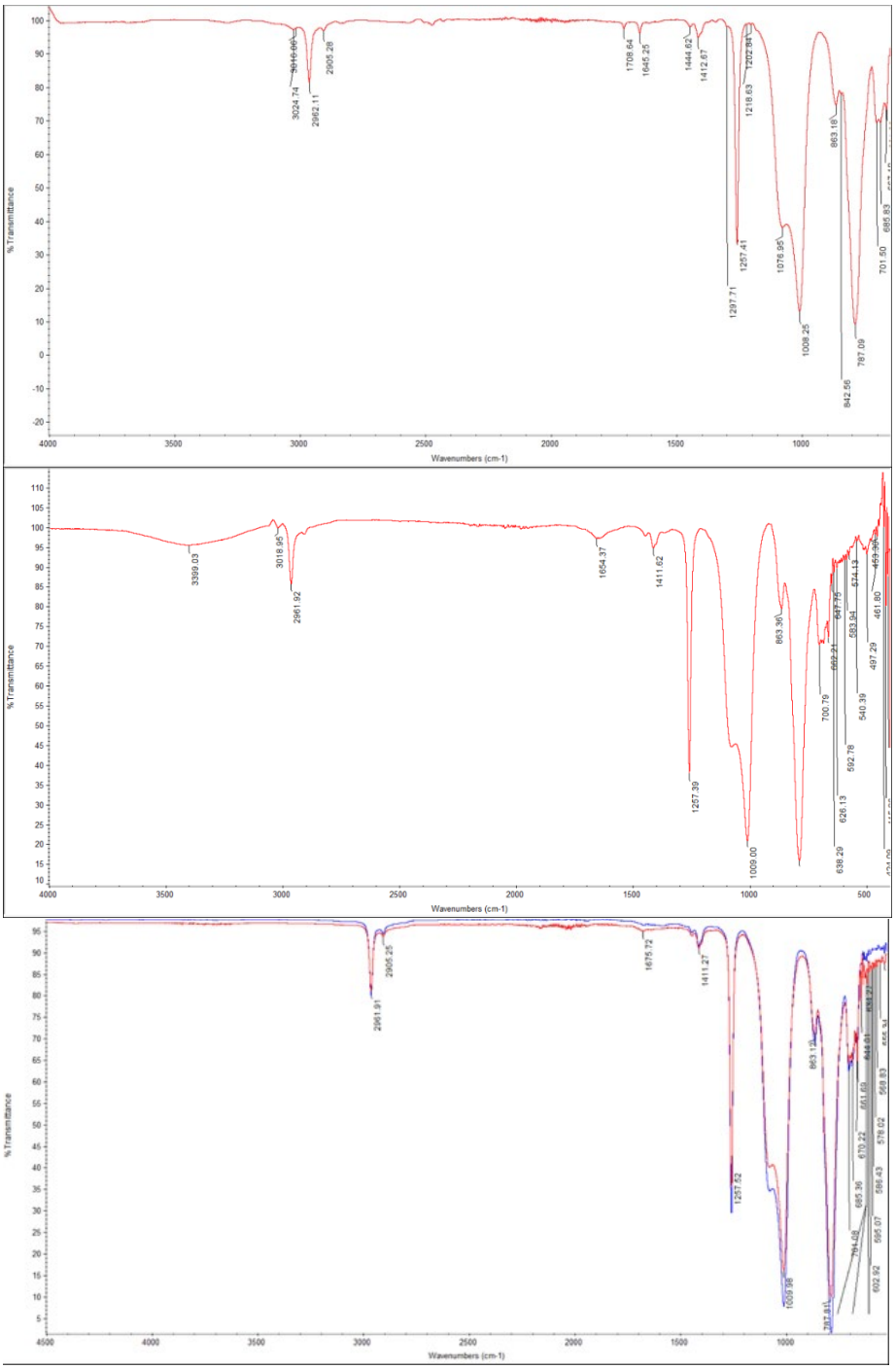

Figure S 8*:* Infrared spectra of DMS-A15 (3000 g mol-1 telechelic 3-aminopropyl-terminated polydimethylsiloxane) crosslinked A) with excess glutaraldehyde after drying in oven for 1 h, showing residual aldehyde groups (1708 cm-1) and B) after submerging in aqueous solution of lysine. C) With 1:1 stoichiometry [NH2]:[CHO] using formaldehyde; red curve after cure in air 1 hour, blue curve after 24 h in boiling water.

Appendix 1.6. Physical Properties of Elastomers Cured in Air and Water

A consequence of having large excesses of water, as with elastomers from the aminopropylPDMS-water emulsions, is that phase separation occurs during cure producing voids in the material that persist even after drying the elastomers at 50 °C in a vacuum oven (Figure S6 A-C). The quantity and size of the voids were greatest in the formaldehyde-cured elastomer because of the fast gelation time, which prevented diffusion of water out of the material, leading to an even dispersion of 5-30 μm voids throughout the material. In contrast, the slower gelation time of glyoxal cured elastomers allowed water to phase separate from the material prior to gelation, leaving very few voids in the material. It is interesting to note that despite the presence of voids in the material, the emulsified samples had similar Young's modulus as samples prepared neat after complete cure in water.

Table S 2: Young's modulus of DMS-A15 (3000 g mol-1 telechelic aminopropylsilicone) elastomers cured in air and as 50 wt% emulsion with water after complete cure and after drying in a vacuum oven for 12 h.

Young's Modulus (MPa)		Formaldehyde	Glyoxal	Glutaraldehyde
Cured in Air RT	Average	0.891	2.22	1.05
Cured in Air RT	Sample 1	0.890	2.20	1.09
	Sample 2	0.891	2.24	1.01
	Sample 3	0.892	2.21	1.07
Cured in Water RT	Sample 1	0.616	1.67	0.728
	Sample 2	0.636	1.58	0.711
	Sample 3	0.609	1.77	0.768
After Drying under reduced pressure[b)]	Sample 1	0.952	2.55	1.13
	Sample 2	0.931	2.71	0.989
	Sample 3	0.969	2.50	1.17
Δ Modulus		15%	7%	11%

[a)] This series only was measured at room temperature to compare the impact of crosslink density. [b)] 0.3 torr, 45 °C.

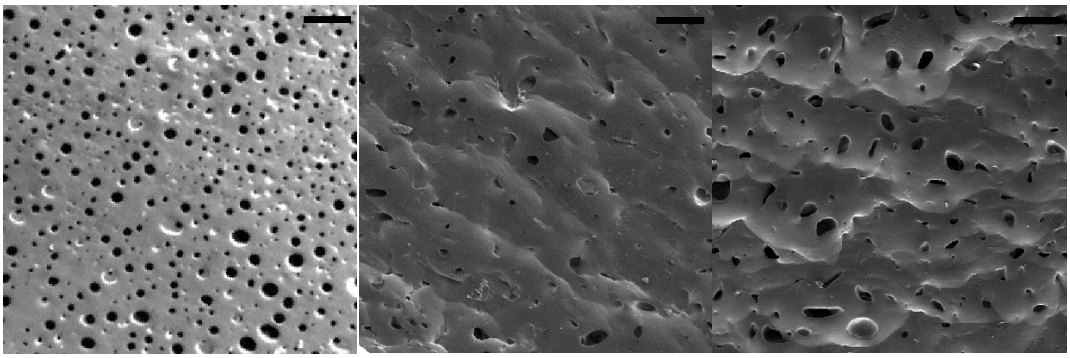

Figure S 9: SEM images elastomers cured in 50 wt% emulsions of 3000 g mol-1 telechelicaminopropylPDMS with 2-4 to give A) For-T, B) Gly-T, C) Glu-T. Scale bar – 100 µm.

Appendix 1.7. Hydrolytic and Thermal Elastomer Stability

Stability in Boiling Water

In order to test the hydrolytic stability of the aldehyde crosslinked elastomers, 1g samples of AMS-152 (4-5% mol aminopropylmethylsiloxane, 7000-9000 g mol^{-1}) were cured using formaldehyde, glutaraldehyde, or glyoxal in a polypropylene 24-well plate to create ~3 mm thick disks. Each elastomer disk was carefully dried using a vacuum oven, weighed, then the Young's modulus was measured. Then, the elastomers were placed into separate round bottom flasks containing 30 mL of distilled water and stirred to gently to keep the elastomer submerged. The flasks were heated to reflux for 24 h. The elastomers were removed from the solution and dried by placing on Kimwipes to remove excess water from the surface of the elastomers. The elastomers were weighed a second time, to measure the weight loss; none of the elastomers showed any weight loss. The Young's modulus of the elastomers was once again measured and compared to the starting modulus. All three types of aldehyde-crosslinked materials showed similar decreases in Young's modulus of 7, 7, and 5% for glutaraldehyde-, glyoxal-, and formaldehyde-derived elastomers, respectively, after submerging for 24 h in boiling distilled water (no changes were observed in the IR of the materials, Figure S8C). These moduli recovered after drying in air for 3 h. Thus, although both imine and aminal bonds can undergo hydrolysis, degradation of the elastomers was not observed in water, including boiling water, over 24 h, despite the known reversibility of aminal/aldehyde equilibria in the presence of water. It is likely that the hydrophobicity of the silicone helps to reduce the efficacy of water infiltration, thus preventing hydrolysis of the crosslinks.

Thermal Stability

To test the thermal stability of these elastomers, samples derived from 5% aminopropylsilicone cured with each aldehyde were prepared according to the procedure

outlined in section 2.2. These elastomers were placed in a 250 °C oven for 72 h. The Young's moduli of these elastomers were measured and compared to untreated samples of elastomer.

Table S 3: Changes in Young's Modulus as a function of heating at 250 °C.

Young's Modulus (MPa)	before heating	after 72 h @ 250 °C	percent change (%)
For-P	0.879	0.882	0.5
Glu-P	1.02	1.08	6
Gly-P	2.18	2.10	4

Appendix 1.8. Thermogravimetric Analysis of Silicone Elastomers Crosslinked with Aliphatic aldehydes

All three aldehyde-crosslinked silicone elastomers had similar thermal stability, as determined by TGA of 5% crosslinked elastomers using a heating ramp rate of 10 ºC min-1 (Figure S10). Each elastomer exhibited ~3 wt% loss starting at 100 °C, likely from the evaporation of residual water. All elastomers have good thermal stability, with significant (>10%) degradation occurring at temperatures >400 ºC.

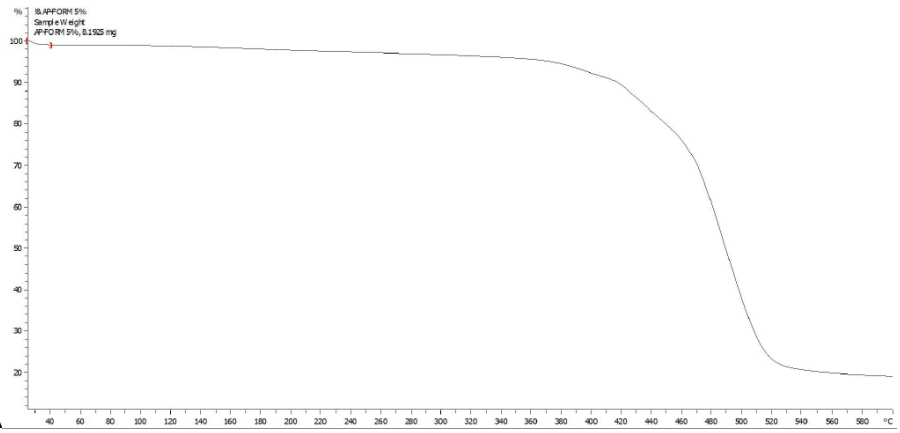

A

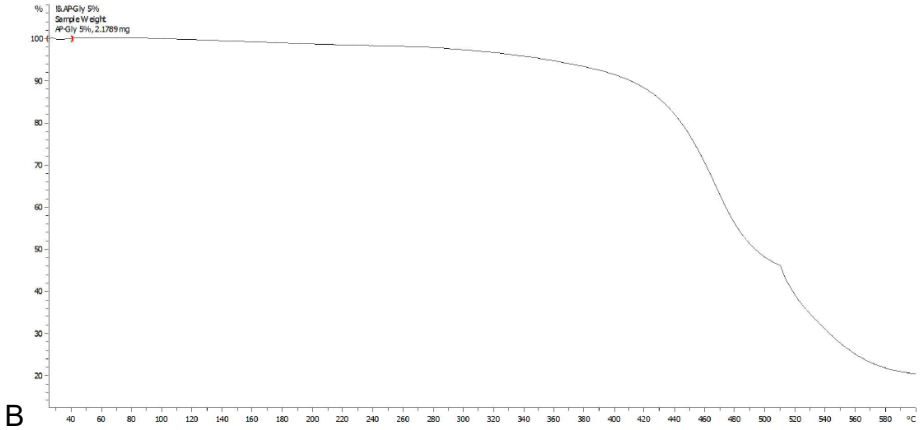

B

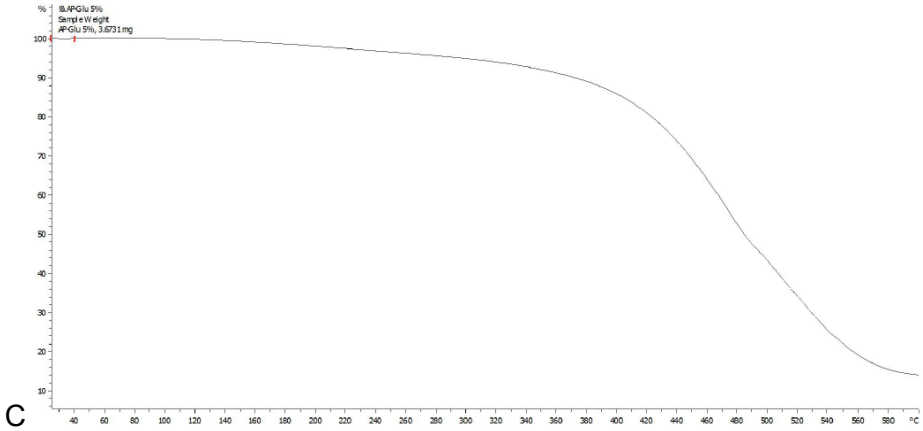

C

Figure S 10: TGA of the degradation of AMS-152 (4-5% mol aminopropylmethylsiloxane, 7000-9000 g mol-1) crosslinked with A: formaldehyde, B: glyoxal, or C: glutaraldehyde.

Appendix 1.9. Equilibrium Swell Test - Flory-Rehner

The crosslink densities of **Form-PDMS** elastomers was determined by a swelling test. In this experiment, cured elastomers were cut into congruent shapes (cubic) and weighed using an analytical balance (~ 1.1 g). The elastomer samples were placed into separate vials containing 30 mL of toluene. The elastomers were submerged and allowed to swell in the dark for 48 h until no further weight changes were observed. The elastomers were removed and blotted with a paper towel to remove excess solvent. The swollen elastomers

were weighed for their swollen mass, then the solvent was removed under vacuum to obtain the dry mass. The crosslink density of the elastomer was calculated (Table S4).[21]

Table S 4: Crosslink densities for formaldehyde crosslinked elastomers calculated using Flory-Rehner equation.

Entry	% mol amino-propyl	M_n (g mol^{-1})	[Amine] (mol L^{-1})	Crosslink Density (mol L^{-1})
Telechelic-modified aminopropylsilicones and Formaldehyde (**For-T**)				
1		900	2.30	2.14
2		3000	0.653	0.665
3		5000	0.392	0.355
4		25000	0.0784	0.0738
5		50000	0.0392	0.0286
Pendent-modified aminopropylsilicones and Formaldehyde (**For-P**)				
6	3%	5500	0.258	0.445
7	5%	8000	0.675	0.695
8	7%	4000	0.946	0.943
9	10%	2500	1.35	1.17
10	25%	2000	3.38	3.93

Appendix: 2. 3-D Printing of Highly Reactive Silicones Using Inkjet Type Droplet Ejection and Free Space Droplet Merging and Reaction

The 3D printer, presented in Figure 3.1a, consists of a printhead, positioner, electronic control system, chambers, and vacuum pressure system. The printhead includes the dispensing devices (MJ-AB- 80 from the MicroFab company) and holder, and its key role is to dispense materials and to facilitate the droplet mixing in free space. However, the deposition of the droplets is completely dependent on the positioner, which is adapted from a commercial and inexpensive 3D printer, The Micro+ from the M3D company, that is able to impose movement in all three directions on the print bed. Since the droplets are very sensitive to external factors, three sides of the positioner are protected against air flow by transparent plastic sheets and, in addition, the positioner is attached to vibration damping rubber to minimize the impact of vibrations. For the same reason, the printhead and the positioning device are not connected to each other. The electrical impulses regulating the parameters of ejected droplets are generated by an electronic control system, Jet Drive™, controlled via a computer using the JetServer software. Two reactive components are kept in separate barrel syringes (Nordson EFD), which are connected from the bottom to the dispensers via a chemically resistive tubing, and to the vacuum pressure system from the top. This system balances the capillary and hydrostatic pressure of the ink at the orifice and stabilizes the meniscus during the printing.

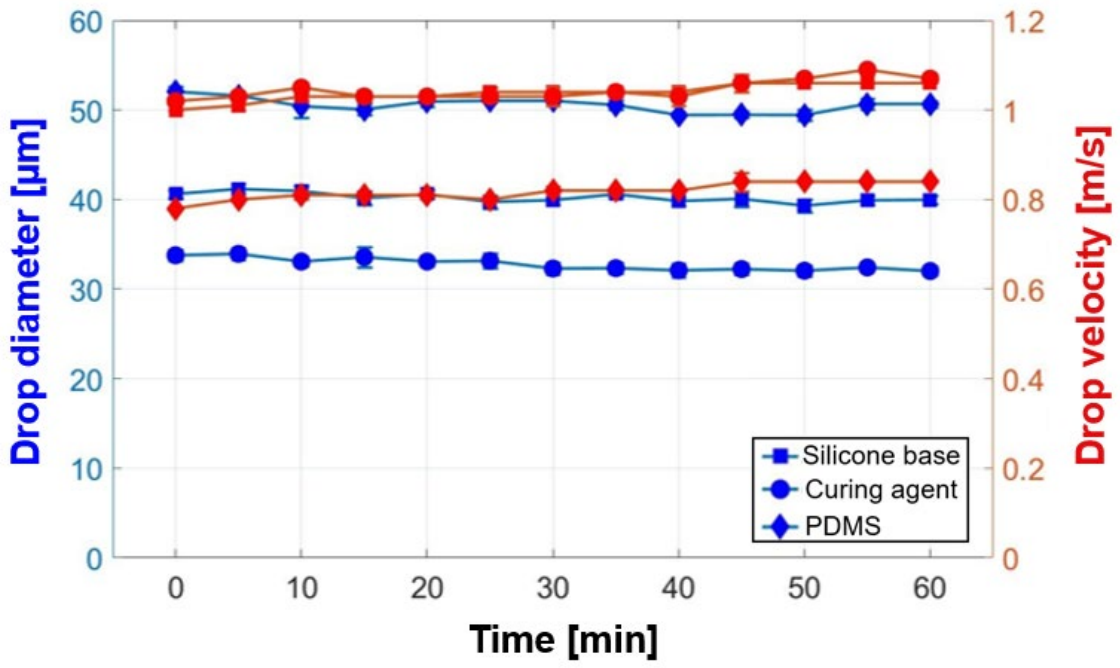

Figure S 11: Long-term printing. The diameter of droplets of each material was stable and equal to 40.22 µm for silicone base, 32.78 µm for curing agent, and 50.57 µm for PDMS, with a small standard deviation of 0.52 µm, 0.69 µm, and 0.81 µm, respectively. The velocity also maintained a stable value, 1.04 m/s for silicone base, 1.05 m/s for curing agent and 0.82 m/s for PDSM, with the negligible variation of 0.02 m/s for each material.

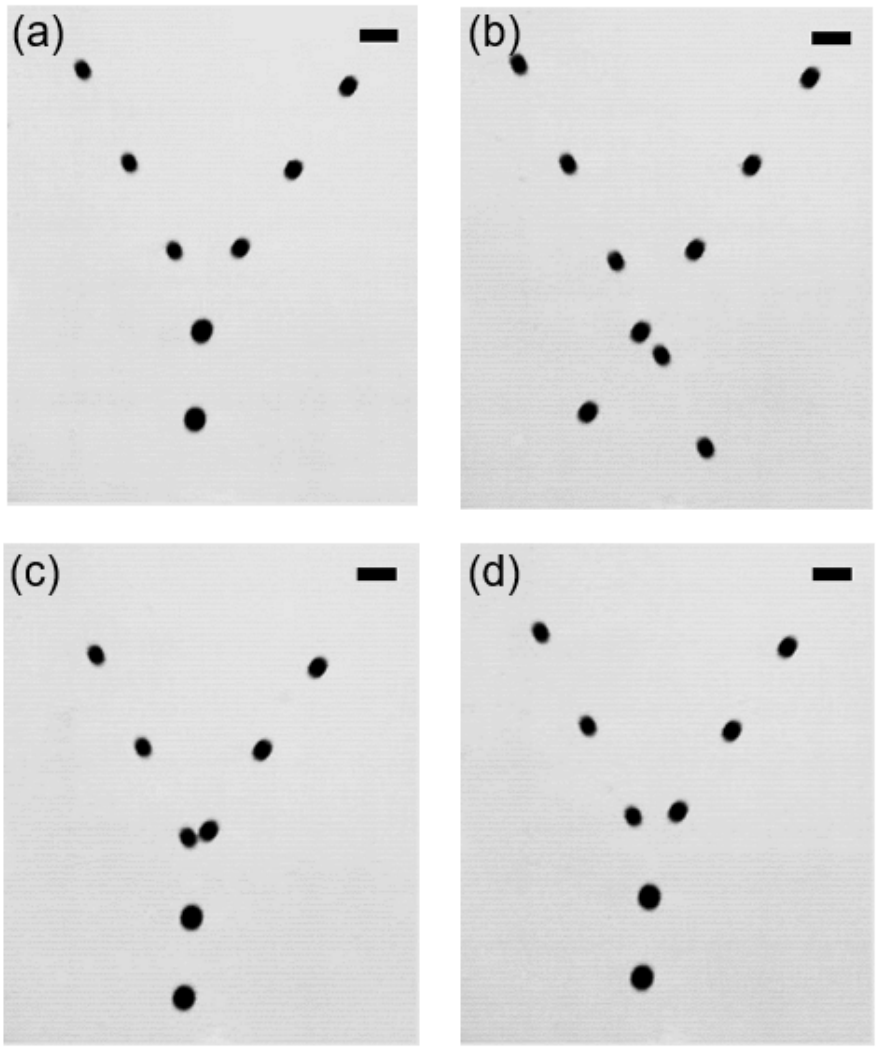

Figure S 12: Impact of the electrostatic forces generated by the glass substrate on the droplet mixing stabilization. **a)** Printing process – the distance between the merging point and the surface is equal to four centimeters. The droplets of 50% glutaraldehyde in water (left-hand side) were dispensed with the velocity of 0.83 m/s, and they were inclined at 30.25° with respect to the vertical axis, while the droplet, made of DMS-A11, had a velocity of 0.84 m/s and the angle 30.28°. **b)** The distance was reduced to 6mm. The trajectory and velocity of DMS-A11 were unchanged, however, drops of 50% glutaraldehyde in water exhibited a higher velocity, 0.93 m/s, and reduced angle, 28.72°, which hindered the droplet merging process. **c)** Neutralization of the electrostatic forces by connecting the nozzles and the substrate electrically to the ground.**d)** Neutralization of the charging by polarizing the print bed through placing a silicon wafer below the glass substrate and using it as a gate electrode, which compensates the charges on the substrate (scale bar 100 µm).

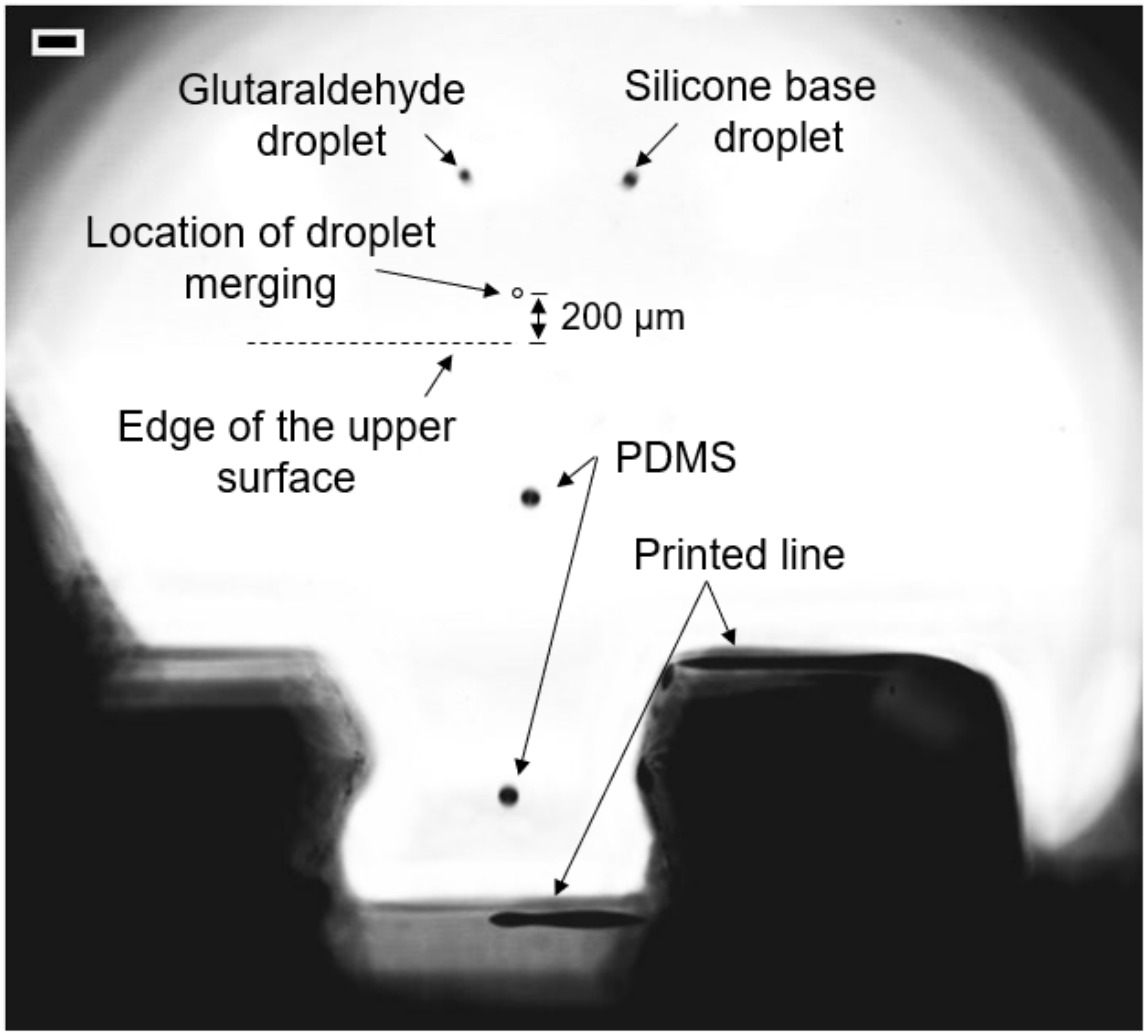

Figure S 13: Visualization of the mixing and deposition of the droplet on a non-uniform surface, made of 1 mm thick glass segments, which does not influence the stabilization of the mixing process (scale bar = 100 µm).

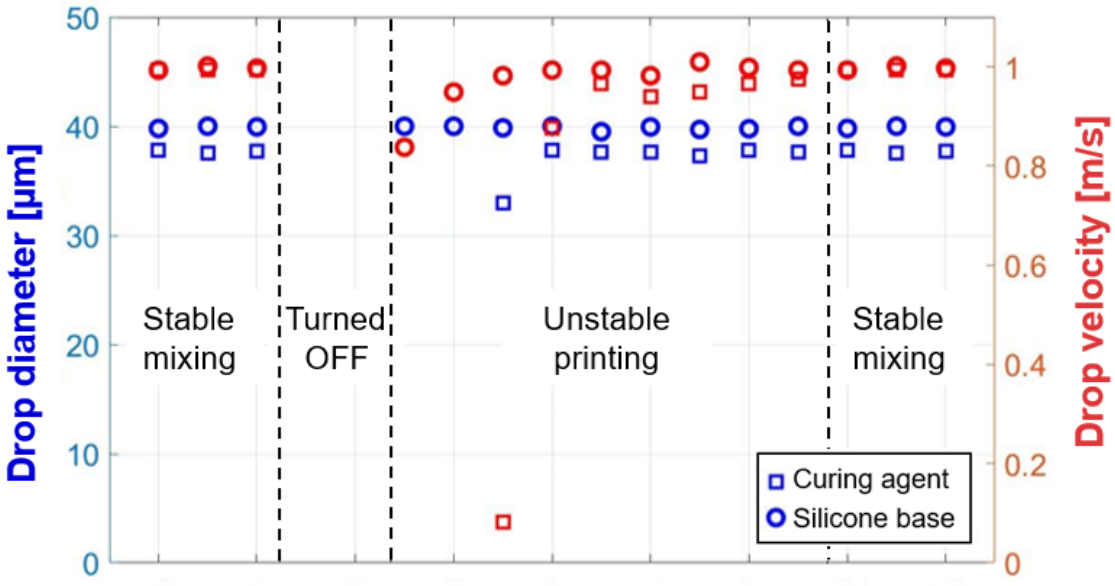

Figure S 14: Printing on demand. Stabilization of the mixing process in multiple start-stop cycles. During the unstable printing regime, which takes 94ms, the material loss was equal to 298.5 pL of DMS-A11, and 186 pL in case of the 50% glutaraldehyde in water.

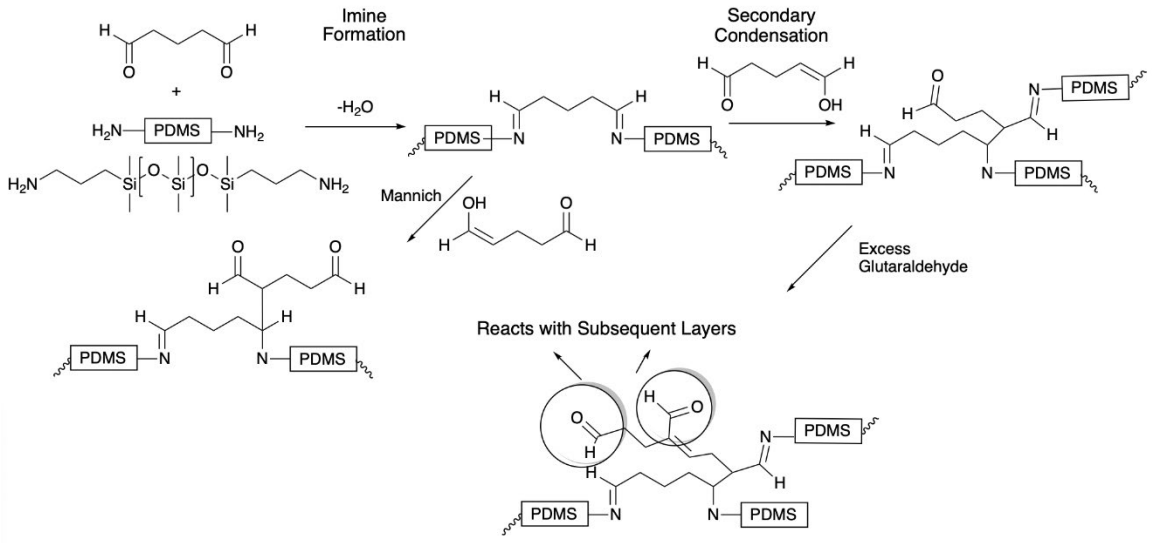

Figure S 15: Dark polymerization of aminopropyl-terminated polydimethylsiloxane and glutaraldehyde solution 50% wt. in water.

Low viscosity and highly reactive PDMS components cross-link almost immediately in a direct (dark) chemical reaction. Glutaraldehyde is widely used as a crosslinking agent for amine-bearing compounds such as proteins. Aqueous solutions of glutaraldehyde are prone to auto condensation to form poly glutaraldehyde, which reacts with amines to create crosslinks and can promote further autocondensation reactions. The materials for this study were made from the crosslinking of telechelic 3-(aminopropyl)polydimethylsiloxane using an aqueous solution of glutaraldehyde. Initial attack of the aldehyde by an amine forms an imine, expelling water as a byproduct. Subsequent reactions can occur with another amine to form a second imine, condensation with another glutaraldehyde molecule through aldol condensation, Mannich reaction or hemiacetal formation (Figure S5). Despite the incompatibility of the hydrophobic silicone and the aqueous glutaraldehyde, the high reactivity of the components causes the droplets react on contact to rapidly form the organosilicone composite materials. Typically, the use

of difunctional monomers should yield an extended linear polymer chain, but the presence of polyglutaraldehyde allows for crosslinking of the silicone. This is advantageous because it allows for use of lower viscosity telechelic-aminopropyl silicone oils instead of viscous pendent-aminopropyl silicone oils. Although the material is composed of a mixture of condensation products, all functional groups are reactive with each other allowing for adhesion between deposited layers.

Appendix: 3. Dynamic Covalent Schiff-Base Silicone Polymers and Elastomers

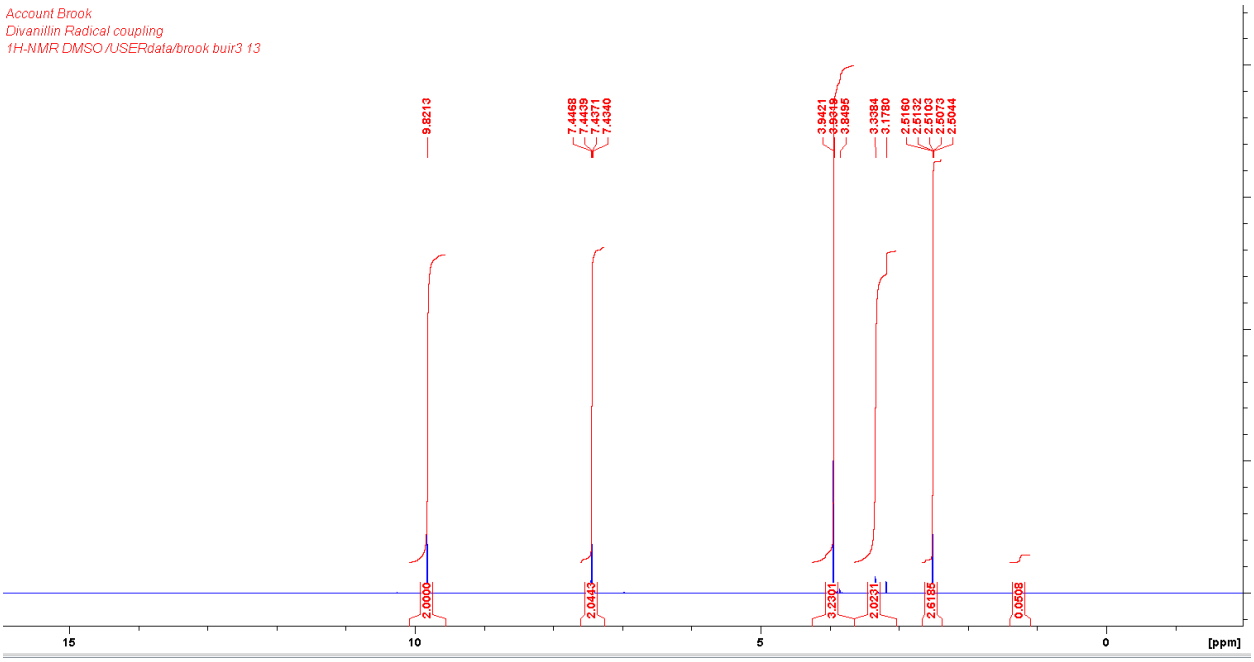

Figure S 16: NMR of the product from the reaction between 3-aminopropylpentamethyldisiloxane and benzaldehyde.

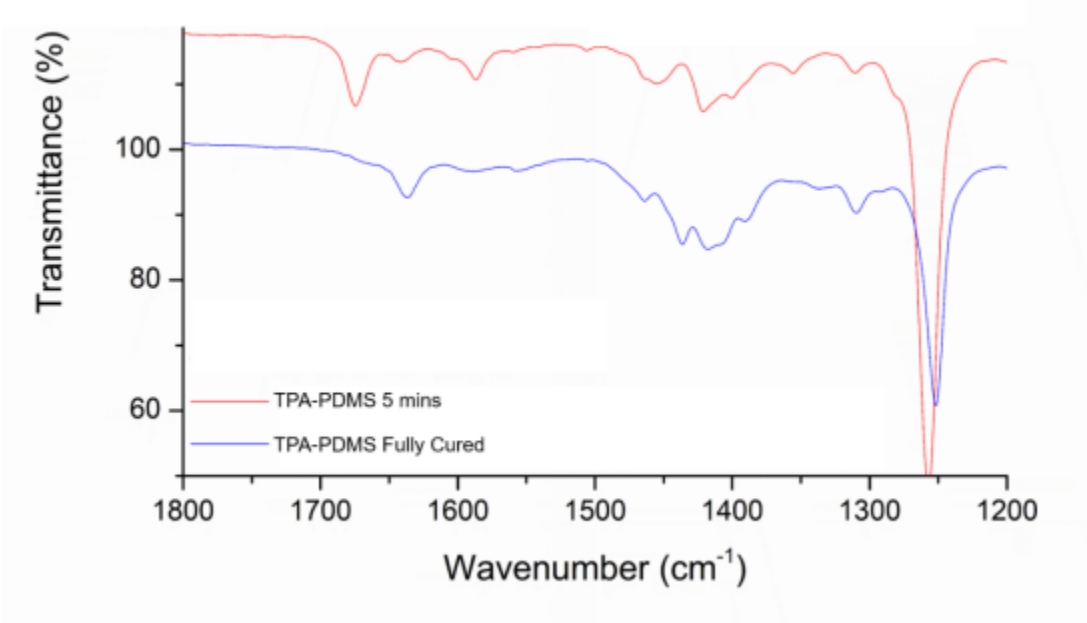

Figure S 17: IR of TPA-PDMS elastomer at 5 mins and after full cure (3 hours) showing aledehyde and imine at 5 mins but only imine at full cure.

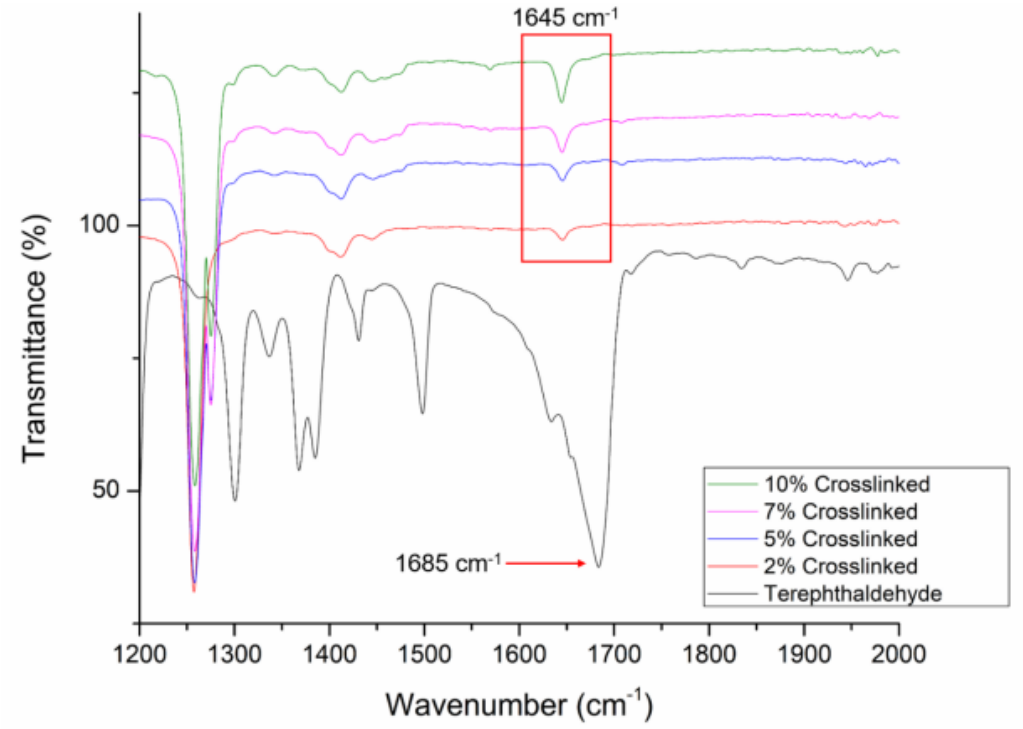

Figure S 18: Overlay of IR spectra from 2-10% crosslinked TPA-PDMS elastomers, and terephthaldehyde.

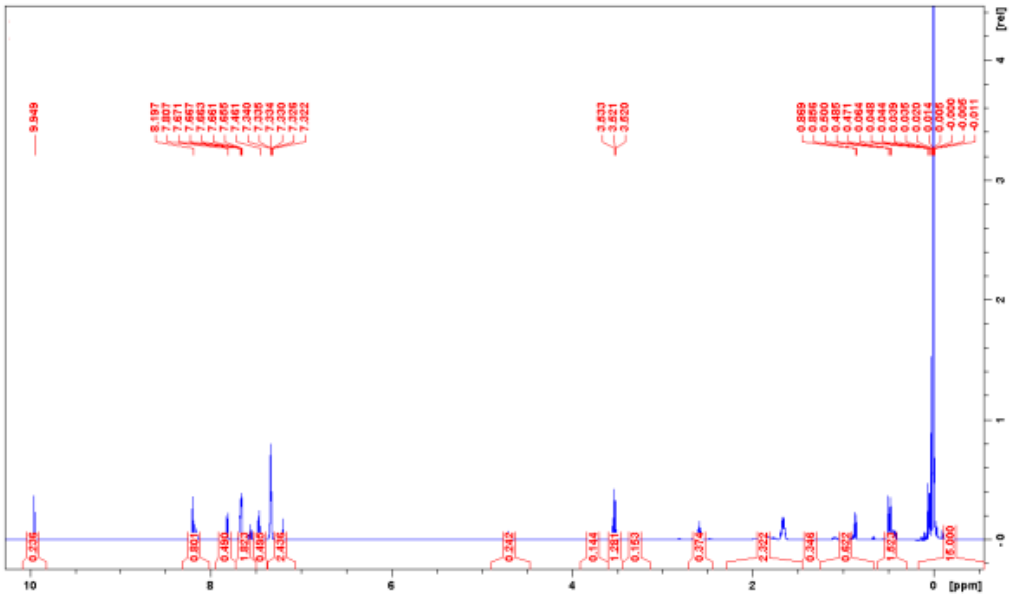

Figure S 19: Partial hydrolysis of pentamethyldisiloxane imine shows both aldehyde (9.95 ppm), imine (8.20 ppm), and water (1.56 ppm) after 20 minutes (complete hydrolysis required 30 minutes).

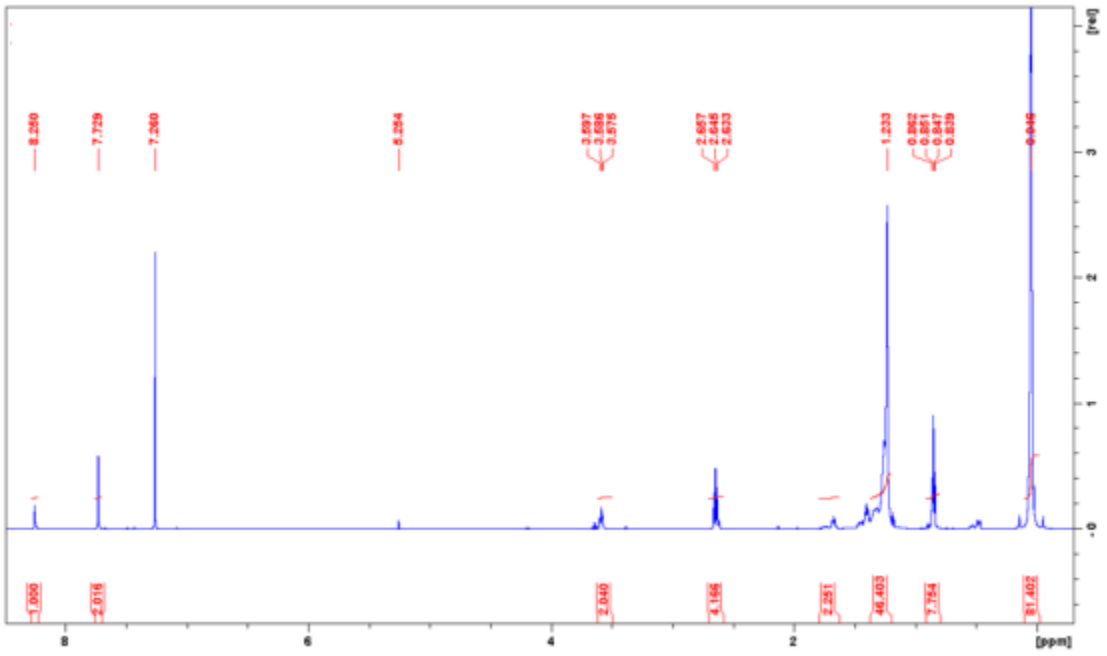

Figure S 20: NMR spectrum of the product from the degradation of a 5% crosslinked TPA-PDMS elastomer by dodecylamine solution.

Thermal Stability of TPA-PDMS Elastomers

The TPA-PDMS elastomers did not creep over one year sitting on the bench – cut edges and corners remained sharp. Heating for up to one week at temperatures between 25-150 °C similarly led to no dimentsional changes. When two elastomers were placed in contact with one another, and heated at 150 °C for 3 h, they formed a bond. However, it was extremely weak, falling apart simply during handling. Thus, heat alone was insufficient to significantly effect the dynamic processes that occurred in the presence of solvents, acids, aldehyde or amines catalysts. TGA of the materials demonstrates that the materials have excellent thermal stability; organic crosslinks degrade at 440 °C and the silicone backbone at 550 °C.

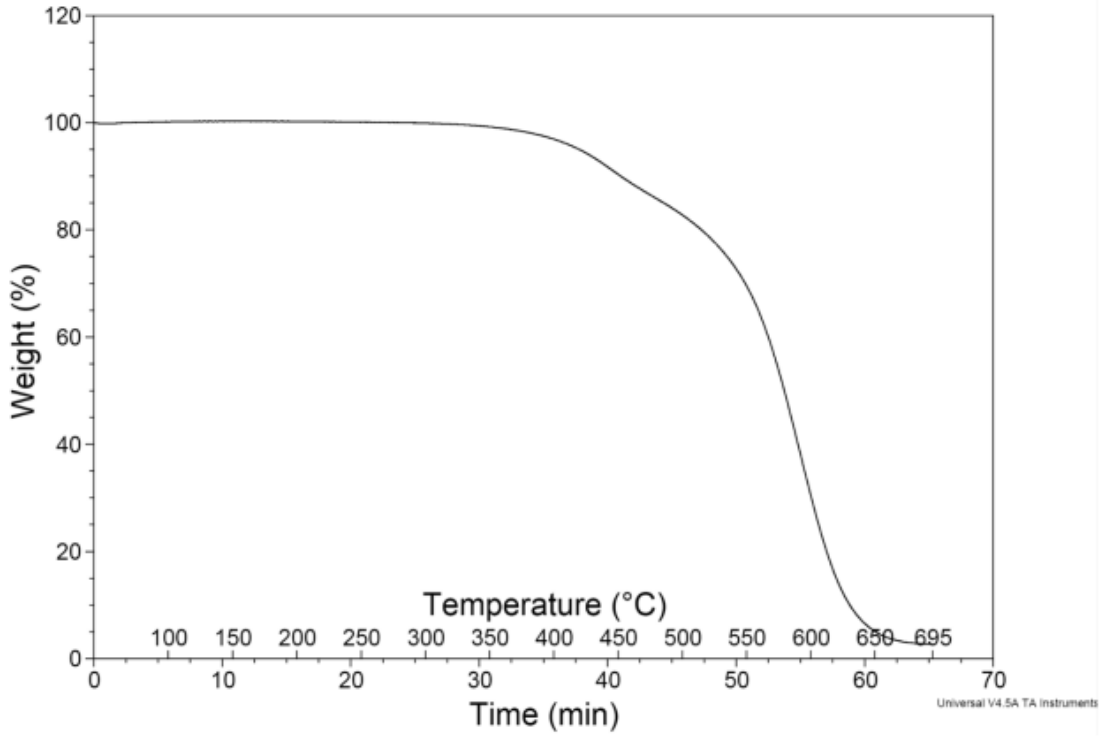

Figure S 21: TGA of the decomposition of 7% crosslinked TPA-PDMS elastomer from 25-700 °C heating at a rate of 10 °C min-1

Appendix: 4. Thermoplastic Silicone Elastomers from Divanillin Crosslinkers in a Catalyst-Free Process

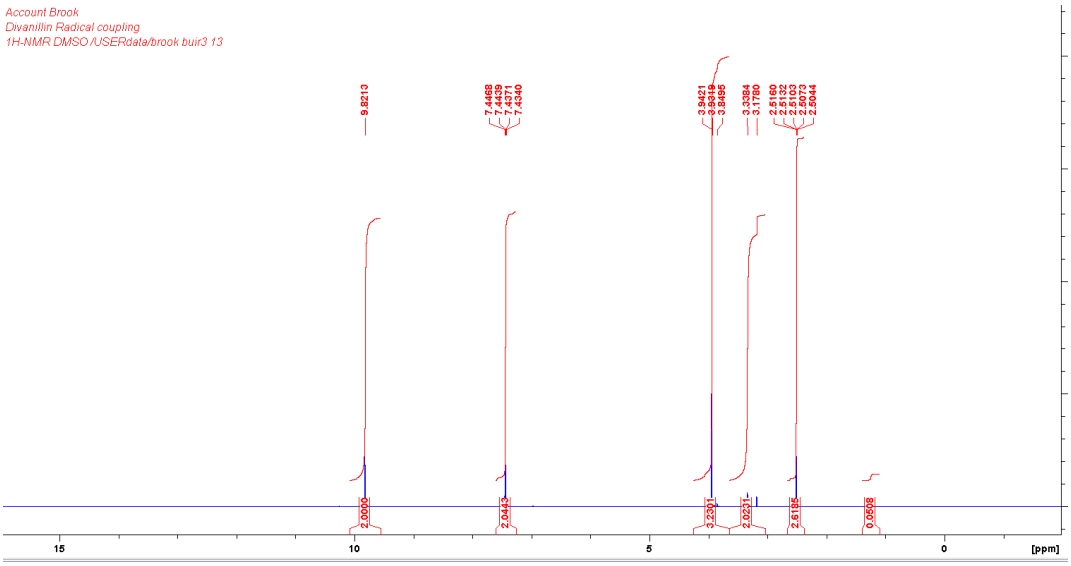

Figure S 22: NMR spectrum of the **DiVan** crosslinker dissolved in DMSO-d_6.

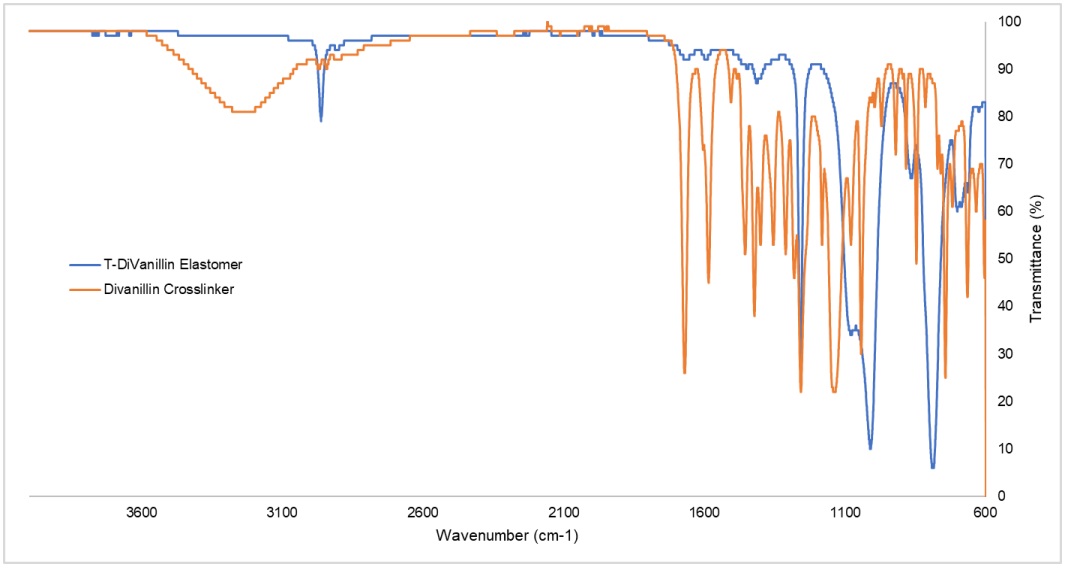

Figure S 23: Infrared spectra from the reaction between divanillin and α,ω-(3-aminopropyl)polydimethylsiloxanes, showing the conversion of aldehydes to imines.

Preparation of Terephthaldehyde Crosslinked Elastomers and DiPhen-P Controls

Terephthaldehyde and 4,4'-diphenyldialdehyde crosslinked elastomers with various functional group concentrations were fabricated as a comparison of viscoelastic properties with divanillin crosslinked elastomers. Elastomer were only formed using (3-aminopropyl)methylsiloxane-dimethylsiloxane copolymers, while α,ω-(3-aminopropyl)-polydimethylsiloxanes resulting in viscous fluids instead of elastomers.

In a typical preparation, terephthaldehyde (41.77 mg, 0.311 mmol) was first dissolved in chloroform (1 mL); there were no significant differences in the outcomes as a function of solvent), then added to a vial containing AMS-152 (5% mol aminopropylmethylsiloxane, 8500 g mol^{-1}, 0.923 g, 0.115 mmol), and rapidly stirred until homogenous. The mixture was then poured into the desired mold, or cast as a thin film. Similarly, 4,4'-diphenyldialdehyde (67.27 mg ,0.320 mmol) was dissolved in chloroform (0.8 mL), then added to a vial containing AMS-152 (5% mol aminopropylmethylsiloxane, 8500 g mol^{-1}, 0.923 g, 0.115 mmol), and stirred. The mixture was cast as a thin film or into the desired mold for tensile testing.

Table S 5: Formulations of **DiVan-T** elastomers using different molecular weights of α,ω-(3-aminopropyl)polydimethylsiloxanes and **DiVan-P** elastomers using pendent (3-aminopropyl)methylsiloxane-dimethylsiloxane copolymers in which the mol% aminopropyl mole groups varied in a 1:1, or 1:1.1 ratio; the latter being used exclusively for determining physical properties.

Telechelic Divanillin Elastomers (**DiVan-T**)	Molar mass (Da)	% Amine Functionality	[Amine] (M)	Mass of Aminosilicone (g)	[Amine] (mmol)	Mass DiVanillin	Silicone to Divanillin Mass Ratio
T-19	0.9k	Telechelic	2.17	5.102	11.3	1.714	25.1%

T-5	3k	Telechelic	0.653	5.052	3.36	0.509	9.2%
T-3	5k	Telechelic	0.392	5.082	2.03	0.307	5.7%
T-0.6	25k	Telechelic	0.0784	5.009	0.401	0.061	1.2%
T-0.3	50k	Telechelic	0.0392	5.074	0.203	0.031	0.6%
Pendent Divanillin Elastomers (**DiVan-P**)							
P-3	5.5k	3	0.387	5.066	2.01	0.302	5.6%
P-5	8k	5	0.675	5.017	3.45	0.522	9.4%
P-7	4k	7	0.946	5.101	4.92	0.744	12.7%
P-11	2.5k	11	1.35	5.038	6.94	1.049	17.2%

Table S 6: Physical properties of DiPhen-P elastomers made using 4'4-diphenyldialdehye and pendent (3-aminopropyl)methylsiloxane-dimethylsiloxane copolymers in which the mol% aminopropyl differ

DiPhen-P Starting Material[a] **P-B**	Molar mass (kDa)	YM[b] MPa	Shore A[c]	Tensile Stress (Mpa)	Tensile Strain at Break (%)
P-3	5.5k	0.36	30 (OO)	0.764	165
P-5	8k	0.881	55 (OO)	1.11	132
P-7	4k	2.1	13	2.54	118
P-11	2.5k	4.47	20	3.93	112

a The number refers to the % amine-containing monomers in the starting aminosilicone polymer. b YM Young's modulus. c Where indicated, Shore OO Hardness measurements were made on softer samples.

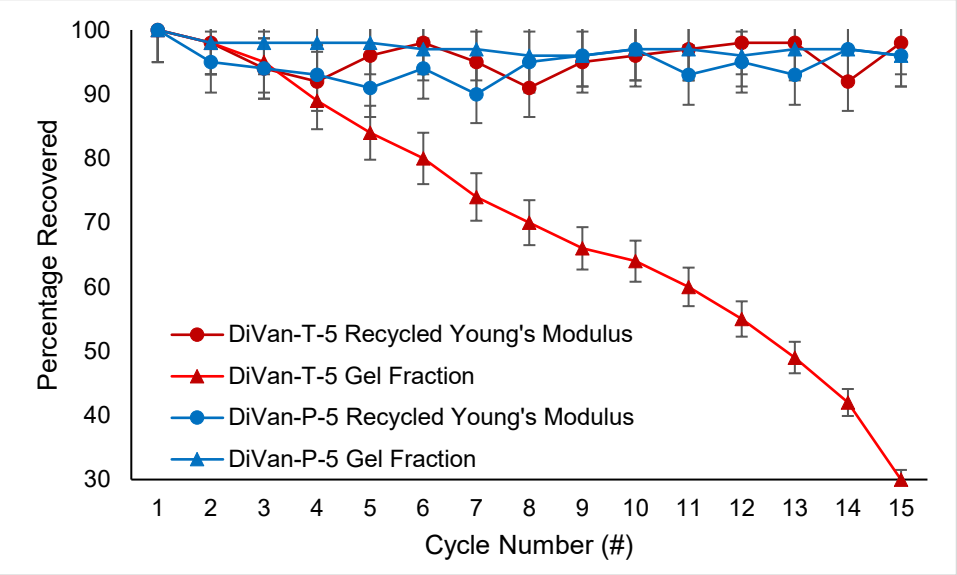

Figure S 24: Swelling and Young's Modulus of **DiVan-T-5** and **DiVan-P-5** after multiple cycles of swelling crumbled elastomer and heat pressing to obtain new monolithic samples.

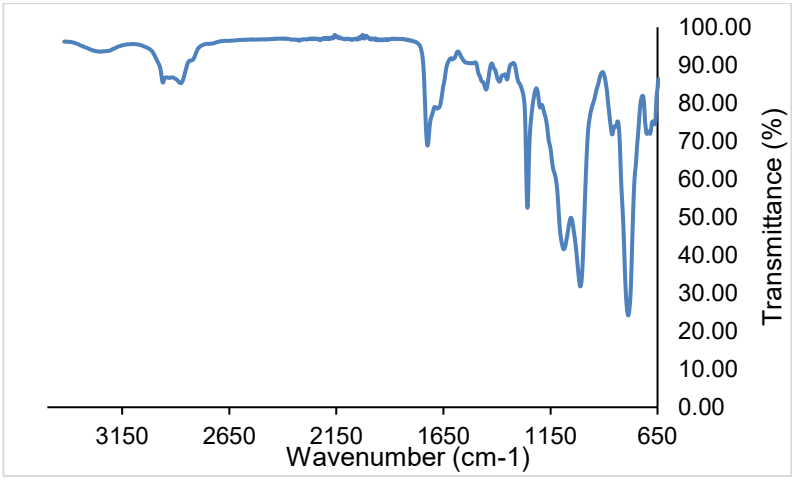

Figure S 25: Infrared spectrum of the products from degrading DiVan-P elastomers with excess phenylhydrazine for 48 h.

Table S 7: Formulations of elastomers **DiVan-P-B-3CL** with the same crosslink density made from pendent (3-aminopropyl)methylsiloxane-dimethylsiloxane copolymers in which the mol% aminopropyl differ, but with the same amount of divanillin (leading to different excesses

Pendent Divanillin Elastomers for Self-Healing	Molar Mass (kDa)	% Amine Functionality	[Amine] (M)	Mass of Amino-silicone	mmols Amine	Amine to Aldehyde Ratio	Mass DiVanillin	mmol DiVanillin	Amine Excess (mmol)	[Amine] Excess (M)
P-3-3CL	5.5k	3	0.387	5.062	1.92	1:1	0.291	0.959	0.00	0.00
P-5-3CL	8k	5	0.675	5.088	3.37	5:3	0.293	0.966	1.43	0.287
P-7-3CL	4k	7	0.946	5.011	4.65	7:3	0.297	0.979	2.69	0.537
P-11-3CL	2.5k	11	1.35	4.992	6.60	11:3	0.290	0.956	4.70	0.938

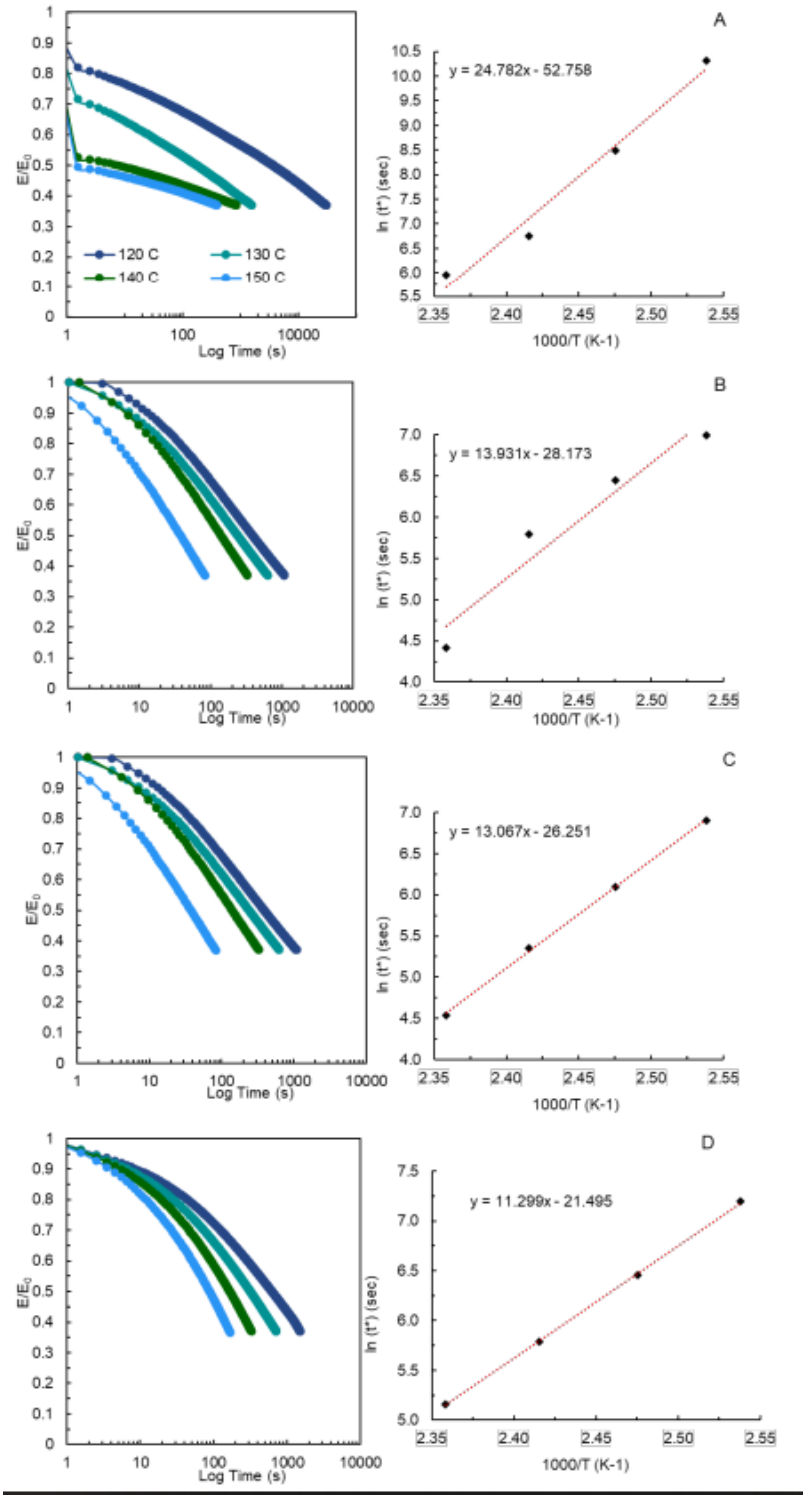

Figure S 26: Arrhenius thermal stress-relaxation of A) DiVan-T-19, B) DiVan-T-5, C) DiVan-T-3 and D) DiVan-T-0.6 elastomers under constant strain (10%) from 120-150 °C

and at 25 °C as a control. Showing the relaxion of the material from initial stress, to E/E0 = 1/e (~0.37), and Arrhenius plot modeling the Maxwell viscoelastic relaxation.

Table S 8: Calculated material relaxation activation energies of DiVan-T elastomers using different molecular weights of telechelic 3-(aminopropyl)-terminated polydimethylsiloxanes determined using DMTA

Sample Name	[Amine] (M)	Slope	Averaged Calculated Activation Energy of Relaxation (kJ mol^{-1})
DiVan-T-19	900	24.782	206.03
DiVan-T-5	3000	13.931	115.82
DiVan-T-0.6	5000	13.067	108.64
DiVan-T-0.3	25000	11.299	93.94

Equation S 1: Arrhenius model of elastomer relaxation where t_R is the relaxation time, E_a is activation energy, R is the Boltzmann's constant, and T is temperature

$$t_R = Ae^{\frac{-E_a}{RT}}$$

$$\ln(t_R) = \ln(A) + \frac{-E_a}{RT}$$